

Mutation-induced remodeling of BfmRS two-component system in *Pseudomonas aeruginosa*

Authors: Qiao Cao^{1,2}, Nana Yang², Yanhui Wang², Chenchen Xu², Xue Zhang², Ke Fan², Feifei Chen^{1,2}, Haihua Liang¹, Yingchao Zhang³, Xin Deng³, Youjun Feng⁴, Cai-Guang Yang², Min Wu⁵, Taeok Bae⁶, Lefu Lan^{1,2*}

Affiliations:

¹College of Life Science, Northwest University, Xi'an, 710127, China;

²State Key Laboratory of Drug Research, Shanghai Institute of Materia Medica, Chinese Academy of Sciences, Shanghai, 201203, China;

³Department of Biomedical Sciences, City University of Hong Kong, Kowloon Tong, Hong Kong, 999077, China;

⁴School of Medicine, Zhejiang University, Hangzhou, 310058, China;

⁵Department of Biomedical Sciences, University of North Dakota, Grand Forks, North Dakota, 58203-9037, USA;

⁶Department of Microbiology and Immunology, Indiana University School of Medicine-Northwest, Gary, Indiana, 46408, USA.

⁷NMPA Key Laboratory for Testing Technology of Pharmaceutical Microbiology, Shanghai Institute for Food and Drug Control, Shanghai, China.

*To whom correspondence should be addressed: llan@simm.ac.cn

One Sentence Summary: Spontaneous mutations induce remodeling of TCSs

Abstract: Genetic mutations are a primary driving force behind the adaptive evolution of bacterial pathogens. Here, we show that in *Pseudomonas aeruginosa*, an important human pathogen, the naturally evolved L181P/E376Q missense mutations in the two-component sensor BfmS gene increases the phosphorylation level and thus the regulatory activity of its cognate response regulator BfmR, which in turn directs this pathogen toward a chronic infection state. The elevated phosphorylation of BfmR appears at least in part due to the reduced phosphatase activity of BfmS, which also allows the cross-phosphorylation of BfmR by GtrS, a non-cognate sensor kinase. We documented that not only the L181P/E376Q but also other spontaneous missense mutations in *bfmS*, such as A42E/G347D, T242R, and R393H, cause a similar

remodeling of the BfmRS two-component system in *P. aeruginosa*. This study thus exemplifies the plasticity of two-component systems mediated by spontaneous mutations, also suggesting that mutation-induced activation of BfmRS may contribute to the host adaptation of *P. aeruginosa* during chronic infections.

Key words: *Pseudomonas aeruginosa*, spontaneous mutation, two-component system, gene expression, adaptation

Introduction

Pseudomonas aeruginosa is a Gram-negative opportunistic pathogen and frequently causes life-threatening infections in humans (1, 2). This pathogen is a leading cause of chronic pulmonary infections and high mortality in cystic fibrosis (CF) patients (2, 3). Once establishing a chronic infection, *P. aeruginosa* is nearly impossible to eradicate with current antibiotic regimens (3, 4). In order to design better strategies for clinical intervention, we need to improve our understanding of the evolution and adaptation of *P. aeruginosa* during infections (5-7).

During chronic infections, *P. aeruginosa* undergoes numerous genetic changes, leading to the development of mutants with altered phenotypes such as conversion to the mucoid colony, reduced production of acute infection-associated virulence factors, a transition to a biofilm-associated lifestyle, and enhanced antibiotic resistance (5, 6). Genome sequencing analyses have revealed recurrent patterns of mutations in CF isolates of *P. aeruginosa*. In particular, mutations are commonly found in the genes encoding global regulators such as MucA and LasR (5-13), indicating that, in *P. aeruginosa*, transcriptional reprogramming may be a key element of adaptation to the CF airway.

The survival of *P. aeruginosa* in the CF airways depends, at least in part, on its ability to sense and respond to changes in its environment. In fact, in the CF isolates of *P. aeruginosa*, genetic alterations are often found in genes, such as *pmrB*, *bfmS*, *retS*, *amgR*, *amgS*, *parS*, and *cbrB*, encoding proteins of two-component systems (TCS) (9, 11-16) that serve as a common bacterial mechanism for sensing and responding to the extracellular environment. The canonical TCS system consists of a sensor histidine kinase (SK) and a cognate response regulator (RR) (17, 18). Upon stimulus detection, the SK phosphorylates its conserved histidine residue and subsequently transfers the phosphoryl group to the conserved aspartate residue in RR. Then the phosphorylated RR coordinates changes in bacterial behavior, often through its activity as a transcriptional regulator (17, 18). Many SK proteins have both kinase and phosphatase activities (17, 18). Depending on the status of those activities, SK can behave as a net kinase (kinase activity > phosphatase activity) or a net phosphatase (phosphatase activity > kinase activity) (17, 18). Cross-regulation

between different TCSs is rare (17); however, in a few cases, it does occur, and many more examples of cross-regulation have been seen in genetically perturbed organisms (17, 19-21).

In various clonal types of *P. aeruginosa*, the SK BfmS gene is a frequent target of adaptive mutations (9, 12, 13, 16). It is also worthy to note that in MPAO1, a laboratory strain of *P. aeruginosa*, the wild-type BfmS negatively controls its cognate RR BfmR, which is a positively auto-regulated transcription factor and plays important roles in biofilm maturation (22, 23), *rhl* quorum sensing (24), and acute bacterial infections (24) in *P. aeruginosa*. Inspired by these observations, we decide to examine the effect of spontaneous missense mutations in *bfmS* on the physiology of *P. aeruginosa* and the underlying mechanisms.

Results

L181P/E376Q missense mutations in *bfmS* enhance the regulatory functions of BfmR

In our previous study, although the wild-type (WT) *bfmS* allele inhibited the regulatory activity of BfmR, the *bfmS* mutant alleles, *bfmS*^{L181P} and *bfmS*^{L181P/E376Q}, activated it (24). In the study, the *bfmS* alleles were provided by a multi-copy plasmid. To exclude the plasmid-copy number effect and to further assess the consequences of the *bfmS* missense mutations, we generated a *bfmS*^{L181P/E376Q} mutant allele at the native *bfmS* site in the chromosome of the laboratory strain MPAO1. As compared with its isogenic parent strain MPAO1, the resulting mutant, *bfmS*^{DK2}, exhibited much higher expression levels of *bfmR-lux* (Fig. 1A, fig. S1), an indicator for the transcriptional regulatory activity BfmR (24), demonstrating that the mutant allele can activate BfmR regardless of the copy number. The *bfmR-lux* reporter exhibited an activation surge in either WT MPAO1 or *bfmS*^{DK2} mutant that is following the growth curve. This is in line with the observation that BfmRS is auto-regulated (24) and indicates that the induction of the BfmRS system is growth-dependent.

Introduction of a plasmid-borne WT *bfmS* into the *bfmS*^{DK2} mutant reduced the *bfmR-lux* expression to a WT level (Fig. 1A and fig. S1), confirming the inhibitory role of the WT BfmS on BfmR. A similar effect was observed with the chromosomal *pa4103-lux* transcriptional reporter fusion (fig. S2A), another indicator of BfmR transcriptional regulatory activity (24). In a Western blot analysis, the *bfmS*^{DK2} mutant produced a much higher amount of BfmS proteins than the WT MPAO1 strain (Fig. 1B), which can be explained by the fact that *bfmR* and *bfmS* forms an operon (Fig. S2B). We also obtained consistent results in Western blot analysis in which the inner membrane fractions were analysed by immunoblotting (Fig. 1B), and this is in line with the prediction that BfmS is an inner membrane protein (1). Collectively, these

results suggest that the missense mutation (L181P/E376Q) in *bfmS* enhances the transcriptional regulatory activity of BfmR in *P. aeruginosa* MPAO1.

Since the function of BfmR is activated by phosphorylation (24), we next tested if the phosphorylation status of BfmR is affected by the *bfmS* missense mutation. With a plasmid (pAK1900-*bfmR-flag*, table S1), Flag-tagged BfmR was expressed in WT and the *bfmS* L181/E376 missense mutant (*bfmS*^{DK2}) of MPAO1 strain; then, the total bacterial proteins were resolved on SDS-PAGE gels containing Phos-tagTM acrylamide (25) and subjected to Western blotting with an anti-FLAG antibody. In the WT strain, only the non-phosphorylated BfmR-flag was observed, whereas, in the *bfmS*^{DK2} mutant, a large amount of phosphorylated BfmR-flag (P~BfmR-flag) was also detected (Fig. 1C), suggesting that the phosphorylation level of BfmR is elevated by the L181P/E376Q missense mutations in *bfmS*. The phosphorylation level of BfmR-flag in the *bfmS*^{DK2} mutant was reduced to the WT level by introduction of a WT *bfmS* with an integration-proficient vector (mini-*bfmS*, table S1) (Fig. 1C), confirming an inhibitory role of the WT BfmS in the phosphorylation of BfmR.

As compared with the WT MPAO1 strain, the *bfmS* L181/E376 missense mutant (*bfmS*^{DK2}) exhibited lesser production of quorum-sensing (QS) signal molecules N-butanoyl-l-homoserine lactone (C4-HSL) (Fig. 1D), reduced virulence in either lettuce leaf (Fig. 1E) or *Drosophila melanogaster* model (Fig. 1F), and increased biofilm formation (Fig. 1 G and H). Each of these phenotypes could be restored to the WT level by *in trans* expression of a plasmid-borne WT *bfmS* (Fig. 1D-G). These observations indicate that the naturally evolved missense mutations (L181P/E376Q) in *bfmS* may confer multiple important phenotypes relevant to the adaptation of *P. aeruginosa* to CF patients (5, 6). Moreover, deletion of *bfmR* totally suppressed all the observed phenotypes caused by the *bfmS* L181P/E376Q missense mutations (fig. S2 C-G), indicating that the functional activation of BfmR has an important role in directing *P. aeruginosa* toward enhanced adaptive performance.

BfmR is highly activated in the CF-adapted isolates of *P. aeruginosa* DK2 lineage

As aforementioned, BfmR is activated upon *bfmS* L181P/E376Q missense mutations (Fig. 1). In DK2 isolates from the long-term-infected CF patients (CF-adapted isolates, sampled between 1979 and 2008), *pa4107* (*efhp*), an BfmR-dependent gene (24), is the most abundant mRNA transcript, and also the most increased gene (with a >256-fold increase), as compared with the non-CF-adapted isolate PAO1 (26). In light of these observations, we compared the transcriptome of 12 CF-adapted isolates of DK2 with that of three DK2 isolates from an early infection (non-adapted isolates, sampled in 1973) (9, 12). The comparison identified that the CF-adapted DK2 isolates share common gene expression profiles, where the expression of 78 genes were increased, whereas the expression of 49 genes were decreased (Sheet 1 of Data file 1). To our surprise, genes activated by BfmR including *bfmR* itself, *pa4102* (*bfmS*),

pa4103, *pa4104*, *pa4105*, *pa4106*, and *pa4107* were found among the most increased genes in the CF-adapted DK2 isolates (Fig. 2A, Sheet 1 of Data file 1), indicating that BfmR is highly activated in the CF-adapted isolates of *P. aeruginosa* DK2 lineage. Similar results were seen in the microarray expression dataset GSE62970, which contains the gene expression profiles of two CF-adapted isolates (DK2-91 and DK2-07) and a non-adapted isolate (DK2-WT) of DK2 lineage (Sheet 2 of Data file 1).

To confirm that the increased transcriptional regulatory activity of BfmR in the CF-adapted clinical isolates is due to the L181P/E376Q mutation in BfmS, we replaced the *bfmS*^{L181P/E376Q} allele of the *P. aeruginosa* DK2 strain (27) with the WT *bfmS* by allelic exchange. When compared to its isogenic parent DK2 strain, the resulting mutant *bfmS*^{PAO1} exhibited phenotypes indicative of reduced BfmR activity, such as enhanced production of QS signal C4-HSL and virulence factor pyocyanin (Fig. 2 B and C), and decreased biofilm formation (Fig. 2D). The Phos-tag mobility shift assay showed that the *bfmS*^{PAO1} mutant produces a much smaller amount of the P~BfmR-flag, as compared with the WT DK2 strain (Fig. 2E). As expected, in both *bfmS*^{PAO1} and $\Delta bfmRS$ mutants, the activity of *pa4103-lux* was much lower than that of the WT DK2 strain (Fig. 2F). Thus, in the CF-adapted clinical isolates of the DK2 lineage, an activation of BfmR and the resulting adaptive changes (such as virulence-associated traits and gene expression) are due, at least in part, to the L181P/E376Q missense mutations in *bfmS*.

gtrS* is essential for the transcriptional regulatory activity of BfmR in the absence of *bfmS

It appears that increased regulatory activity of BfmR, which resulted from L181P/E376Q missense mutations of *bfmS*, may be critical for the pathogenesis of *P. aeruginosa* DK2 in CF patients (Fig. 2). To further identify whether or not BfmS is the only regulator controlling the regulatory activity of BfmR, we performed a suppressor screening using a transposon mutant library of $\Delta bfmS$. In the screening, the activity of BfmR was measured by the *bfmR* promoter-*lacZ* reporter fusion (table S1). On M8-glutamate minimal agar medium supplemented with glucose and 5-bromo-4-chloro-3-indolyl- β -D-galactoside (X-gal), the reporter fusion brings about intense blue colonies (indicative of high activity of BfmR) in the $\Delta bfmS$ mutant; however, in the WT MPAO1 strain, it causes very weak blue colonies (indicative of low BfmR activity). From a library of ~30,000 $\Delta bfmS$ transposon mutants, we identified 12 weak blue colonies. Of the 12 mutants, 10 had a transposon insertion in either the promoter or coding region of *bfmR*. The other two had a transposon insertion in *pa3190* (*gltB*) and *pa3191* (*gtrS*), respectively. The *gltB* gene encodes a periplasmic binding protein GltB involved in glucose transport (28), whereas the *gtrS* gene encodes the sensor kinase GtrS that forms a TCS with the glucose uptake response regulator GltR (29-31) (fig. S3A).

To verify the role of GltB in the transcriptional regulatory activity of BfmR, we deleted *gltB* in the *bfmS* deletion mutant ($\Delta bfmS$) background. Like the original transposon mutant, the resulting *bfmS-gltB* double deletion mutant ($\Delta bfmS\Delta gltB$) showed a WT level of low *bfmR* promoter activity (fig. S3B). Ectopic expression of *gltB* in the $\Delta bfmS\Delta gltB$ mutant strain significantly increased the activity of *bfmR* promoter to a level similar to that of the *bfmS* single deletion mutant ($\Delta bfmS$) (fig. S3B), demonstrating that GltB is a potent activator of BfmR in the $\Delta bfmS$ mutant. Likewise, we verified that, in $\Delta bfmS$, *gtrS* is also crucial for the transcriptional regulatory activity of BfmR, as evidenced by the facts that deletion of both *gltR* and *gtrS* decreases the *bfmR-lux* activity of the $\Delta bfmS$ mutant to a level of the WT MPAO1 strain (Fig. 3A), while the introduction of a plasmid containing *gtrS* (p-*gtrS*) into the $\Delta bfmS\Delta gltR-gtrS$ triple mutant increases the *bfmR-lux* activity to the high level seen in the $\Delta bfmS$ mutant (Fig. 3A). These results also suggest that the increased transcriptional regulatory activity of BfmR by GtrS does not require GltR. On the other hand, ectopic expression of *gtrS* failed to induce the level of *pa4103-lux* activity when *bfmR* was further deleted ($\Delta bfmRS\Delta gltR-gtrS$) (Fig. 3B), supporting the idea that the activation of *pa4103-lux* expression by GtrS requires BfmR. Taken together, these results suggest that GltB and GtrS are critical in the regulatory activity of BfmR in the *bfmS* deletion mutant ($\Delta bfmS$). Also, we found that GtrS can increase the regulatory activity of BfmR independently of GltB, but not vice versa (fig. S3C). These observations prompted us to investigate the molecular pathway(s) that links GtrS to the functional activation of BfmR.

Glucose signals the transcriptional regulatory activity of BfmR through GtrS in the $\Delta bfmS$ mutant

In GtrS, the conserved H280 residue is predicted to be autophosphorylated (<http://www.pseudomonas.com/>). In order to examine the functional importance of this His residue, we examined the ability of the GtrS^{H280A} protein to activate the expression of *pa4103-lux*. The H280A amino acid substituent had no obvious effect on the expression/stability of the GtrS protein (fig. S3D). However, unlike the WT GtrS, the GtrS^{H280A} failed to promote the expression of *pa4103-lux* in a *bfmS-gtrS* double deletion mutant strain ($\Delta bfmS\Delta gtrS$) (fig. S3E), indicating that the autokinase activity is required for GtrS in order to activate BfmR.

Since the uptake of glucose in *P. aeruginosa* is likely regulated by GtrS (32), we next sought to examine the effects of glucose on the expression of the *pa4103-lux* reporter in WT MPAO1 strain, *bfmS* deletion mutant ($\Delta bfmS$), and the $\Delta bfmS$ mutant complemented with p-*bfmS*, in order to further examine the role of GtrS in the transcriptional regulatory activity of BfmR. Although the following 16 carbohydrates failed to induce the promoter activity of *pa4103* in all strain backgrounds: glycerol, D-mannitol, D-fructose, D-(+)-trehalose, succinate, pyruvate, citrate, sucrose, α -ketoglutarate, maltose, D-gluconate, DL-malate, D-Glucose-6-Phosphate, 5-Keto-d-

gluconic acid, and D-(+)-xylose, the addition of glucose promoted *pa4103-lux* expression in the *bfmS* deletion mutant strain ($\Delta bfmS$) but not in either the WT MPAO1 strain or the complemented strain of $\Delta bfmS$ (fig. S4A). In $\Delta bfmS$, glucose can induce the *pa4103-lux* activity in a concentration-dependent manner, even at low micromolar levels (fig. S4B); however, in the $\Delta bfmS\Delta gtrS$ double mutant, it gave no effect (fig. S4C), indicating that, in the $\Delta bfmS$ mutant, the glucose-mediated activation of BfmR requires GtrS.

Additionally, we observed that glucose induces the promoter activity of *gltB* (*gltB-lux*) in a GtrS- and concentration-dependent manner (fig. S4 D and E), consistent with the notion that the high-affinity glucose transport system of *P. aeruginosa* is induced by glucose and the GtrS-GltR TCS (32). Deletion of *gltB* in *P. aeruginosa* MPAO1 was associated with lower expression of *gltB-lux*, indicative of reduced GtrS-GltR TCS activity (fig. S4F). The introduction of p-*gltR-gtrS*, but not p-*gtrS*, into the $\Delta gltB$ strain was able to enhance the activity of *gltB-lux* (fig. S4F). These results suggest that GltB may activate GtrS-GltR TCS by a hitherto unknown mechanism.

GtrS forms a TCS with BfmR in *P. aeruginosa* mutant deficient in *bfmS*

Since GtrS is a SK, most likely, it activates BfmR through phosphorylation. To examine this possibility, BfmR-flag was expressed, and the phosphorylation of the BfmR protein was analyzed by Phos-tag assay in WT MPAO1, $\Delta bfmRS$ double mutant, and the $\Delta bfmRS\Delta gltR-gtrS$ tetra mutant. As expected, only non-phosphorylated BfmR was detected in the WT MPAO1 strain (lane 6 in Fig. 3C), whereas both phosphorylated and non-phosphorylated forms of BfmR were detected in the $\Delta bfmRS$ double mutant (lane 1). In the $\Delta bfmRS\Delta gltR-gtrS$ tetra mutant, however, only a slight amount of phosphorylated BfmR was detected (lane 2). The level of P~BfmR was restored by the introduction of either *gltR-gtrS* (lane 3) or *gtrS* (lane 5), but not *gltR* alone (lane 4). Thus, GtrS has a substantially positive effect on the phosphorylation of BfmR in *P. aeruginosa* deficient in *bfmS*.

When BfmR-flag was expressed in the $\Delta bfmRS$ double mutant, a high amount of phosphorylated BfmR was observed only in the presence of glucose (fig. S5A, lane 2 and 6). A similar result was obtained with the $\Delta bfmRS\Delta pta-ackA$ mutant (fig. S5A, lanes 3 and 7), indicating that the acetyl phosphate does not play a major role in the phosphorylation of BfmR under the experimental condition employed. The *in vivo* phosphorylation of BfmR was eliminated by substituting the predicted phosphorylation site Asp55 with alanine (fig. S5A, lane 4), confirming that BfmR is phosphorylated at Asp55 (24).

To examine whether GtrS directly interacts with BfmR, we performed co-immunoprecipitation (co-IP) experiments. Both HA-tagged GtrS (GtrS-HA) and Flag-

tagged BfmR (BfmR-flag) were expressed in the *bfmS* deletion mutant ($\Delta bfmS$). After GtrS-HA was immunoprecipitated with an anti-HA antibody, the co-precipitation of BfmR-flag was examined with anti-Flag antibody. BfmR-flag was detected only when GtrS was co-expressed (lane 6 in Fig. 3D). Conversely, the immunoprecipitation of BfmR-flag with anti-Flag antibody was also able to bring down HA-tagged GtrS (GtrS-HA) (fig. S5B, lane 5), indicating that GtrS directly interacts with BfmR in vivo.

Next, to investigate whether GtrS can directly phosphorylate BfmR, we purified the N-terminally 6His-tagged cytosolic fragment GtrS (hereafter referred to as His₆-GtrSc) and examined whether it can phosphorylate the His₆-BfmR. In the presence of ATP, His₆-GtrSc was autophosphorylated (Fig. 3E). When the His₆-BfmR was further added, the phosphoryl group was transferred from His₆-GtrSc to BfmR (Fig. 3E). His₆-BfmR alone was unable to autophosphorylate (fig. S5C, see also in lane 1 in Fig. 5B). Heating the sample converted all P~His₆-BfmR to His₆-BfmR (fig. S5D, lane 3), consistent with the heat-liability of aspartyl-phosphate bonds (17, 18). His₆-BfmR^{D55A} was not phosphorylated by GtrSc (fig. S5D), however, indicating that the phosphorylation of BfmR by GtrS depends on the phosphorylation residue (Asp55). Using Pro-Q Diamond stain as an indicator of phosphorylation, we also observed that His₆-BfmR can be phosphorylated by His₆-GtrSc (Fig. 3F). Taken together, these results support that, in $\Delta bfmS$, GtrS forms a TCS with BfmR.

GtrS and BfmR still forms a TCS in the presence of BfmS^{L181P/E376Q}

We next sought to examine whether GtrS contributes to the activation of BfmR in the *bfmS*^{DK2} mutant background. We deleted *gtrS* in the *bfmS*^{DK2} and measured the *pa4103-lux* expression. In the presence of glucose, the expression of *pa4103-lux* was high in *bfmS*^{DK2}; however, it was obviously, although not completely, reduced (~ 75% reduction) by the deletion of *gtrS* (+ Glucose in Fig. 4A). The reduced expression of *pa4103-lux* was restored upon introduction of *gtrS* with a plasmid (Fig. 4A). In contrast to the glucose-replete condition, however, in the absence of glucose, the expression of *pa4103-lux* was lower, and it was not obviously affected by the *gtrS* deletion (- Glucose in Fig. 4A). Similar results were obtained when the expression level of BfmS was used as an indicator of the BfmR regulatory activity (Fig. 4B). These results suggest that GtrS is an important contributor to the highly active status of BfmR in the *bfmS*^{DK2} mutant, and, for the contribution, glucose is essential. Such a notion was further supported by the fact that the *gtrS* deletion suppressed the phenotypes conferred by the *bfmS* L181P/E376Q missense mutations, including reduced production of C4-HSL, reduced virulence against either lettuce leaf or *D. melanogaster*, and increased biofilm formation (Fig. 4C-F).

When co-expressed with BfmR-flag in the *bfmS*^{DK2} mutant, GtrS-HA co-immunoprecipitated with BfmR-flag (Fig. 4G), indicating the direct interaction

between GtrS and BfmR in the presence of BfmS^{L181P/E376Q}. A similar result was obtained when the use of a bacterial two-hybrid system to study the interactions of GtrS and BfmR in *Escherichia coli* (fig. S6). These results are consistent the fact that in *P. aeruginosa* MPAO1, GtrS is the closest homolog of BfmS with 38.5% sequence identity. What is more, 85.7% (6 out of 7) of the partner specificity-determining residues, which inferred from studies on EnvZ (33) and HK853 (34), are completely conserved in BfmS and GtrS (fig. S7). Thus, the interacting interfaces of BfmS and GtrS may share common features that enable similar protein-protein interactions with the BfmR. Additionally, we observed that exogenously applied glucose, even at low micromolar concentrations, could induce the expression of *pa4103-lux* in *bfmS*^{DK2} mutant, but fail to do this in the WT MPAO1 (Fig. 4H). Thus, GtrS and BfmR still form a functional TCS in the presence of BfmS^{L181P/E376Q}.

To further explore whether the GtrS-mediated activation of BfmR also occurs in the clinical isolate DK2 strain, we repeated the *pa4103-lux* activity assay for the WT DK2 strain and its isogenic *gtrS* deletion mutant (DK2- Δ *gtrS*). Because the DK2 strain grows poorly in minimal medium, in this assay, bacterial cells were grown in PB medium. As with the MPAO1 strain background, in the DK2 background, the *pa4103-lux* activity was lower in the absence of glucose (PB versus PB + Glucose in Fig. 4I). The deletion of *gtrS* significantly decreased the *pa4103-lux* activity (~70%) when glucose was present in the growth medium (PB + Glucose in Fig. 4I). Similar results were also observed in the Western blot analysis of BfmS (Fig. 4J and K). These data verify that the functional GtrS-BfmR interaction in the presence of BfmS^{L181P/E376Q} is not limited to the genetic background of MPAO1.

L181P/E376Q substitutions promote the autophosphorylation level of BfmS in vivo

When grown without glucose, *bfmS*^{DK2} mutant exhibited a much higher *pa4103-lux* activity than the Δ *bfmS* mutant (fig. S8A). The *bfmS*^{DK2} Δ *gtrS* mutant also displayed much higher *pa4103-lux* activity than Δ *bfmS* Δ *gtrS* strain regardless of the presence of glucose (fig. S8A). These results indicate that, although the BfmS protein inhibits the transcriptional regulatory activity of BfmR, the BfmS^{L181P/E376Q} mutant protein can activate it in a GtrS-independent manner. Indeed, the co-IP experiment showed that BfmS^{L181P/E376Q} directly interacts with BfmR in vivo (Fig. 5A). The purified N-terminal His₆/GST-double tagged cytosolic fragment of BfmS^{L181P/E376Q} (hereafter referred to as BfmSc^{DK2}) protein was able to autophosphorylate (Fig. 5B, lane 3; fig. S8B) and, subsequently, phosphorylated His₆-BfmR (Fig. 5B, lane 5; fig. S8B). As expected, BfmR^{D55A} was not phosphorylated by BfmSc^{DK2} (Fig. 5B, lane 6). In accordance with the previous report (24), the BfmS inhibited the regulatory function of BfmR in various growth media such as minimal medium (Fig. 3 A and B), LB medium, and PB medium (fig. S8D). However, like BfmSc^{DK2}, the cytosolic fragment of BfmS (BfmSc) was able to autophosphorylate and, subsequently, phosphorylated

BfmR *in vitro* (fig. S8C), indicating that BfmS have the potential ability to activate BfmR under certain conditions.

BfmS is predicted to autophosphorylate the His238 residue (<http://www.pseudomonas.com/>). Following the prediction, the purified cytosolic fragment BfmS^{DK2 H238A} protein (that is, the BfmSc^{DK2} protein with H238A substitution) was unable to autophosphorylate (Fig. 5B, lane 4). Moreover, in the MPAO1 strain background, the H238A substitution completely abolished the ability of BfmS^{L181P/E376Q} to induce the expression of *pa4103-lux* (Fig. 5C), to reduce the bacterial virulence in either *D. melanogaster* (Fig. 5D) or lettuce leaf (Fig. 5E), and to enhance biofilm formation (Fig. 5F), indicating that the autophosphorylation at His238 is essential for mediating the molecular and cellular effects of BfmS^{L181P/E376Q}. Although non-detectable levels of P~BfmS was observed in WT MPAO1, a very high level of P~BfmS^{DK2} was seen in the *bfmS*^{DK2} mutant (Fig. 5G). Similar results were obtained in the DK2 strain background as well (Fig. 5H). In addition, we observed that BfmSc^{DK2} and SUMO-BfmSc^{DK2} proteins (N-terminal His₆-SUMO tagged cytosolic segment of BfmS^{DK2}) purified from *E. coli*, respectively, display much higher level of autophosphorylation compared with BfmSc and SUMO-BfmSc (N-terminal His₆-SUMO tagged cytosolic segment of BfmS) (fig. S9 A and B), and as expected, higher level of phosphorylation of BfmR by SUMO-BfmSc^{DK2} was also seen (fig. S9C). These results suggest that the L181P/E376Q amino acid substitutions caused elevated phosphorylation of BfmS at His238 and thus provide a more significant number of phosphoryl groups for the transfer to BfmR, thereby contributing to the increased regulatory activity of BfmR.

L181P/E376Q substitutions compromises the phosphatase activity of BfmS

It is known that the phosphatase activity of a HK is a key mechanism of preventing cross-talk between two-component systems (17). We therefore examined the effect of L181P/E376Q amino acid substitutions on the phosphatase activity of BfmS by using *in vitro* assays with the truncated form of recombinant BfmS (SUMO-BfmSc), given that BfmS is a membrane protein (Fig. 1B) and is thus difficult to overexpress and purify. When transphosphorylation reactions were performed at a 1:6 (SUMO-BfmSc/His₆-BfmR) molar ratio and then ATP was removed from the assays, P~His₆-BfmR showed a half-life more than 30 min (Fig. 5I). When SUMO-BfmSc was added after ATP removal to reach a 4:1 (SUMO-BfmSc/His₆-BfmR) molar ratio, the half-life of P~His₆-BfmR decreased to 2 min, with a full reduction of phosphorylation of within 30 min (Fig. 5J). These results suggest that BfmS has significant phosphatase activity for P~BfmR, and are consistent with the previous observation that BfmS is a negative regulator of BfmR *in vivo* (24). However, when SUMO-BfmSc^{DK2} was added, the half-life of P~His₆-BfmR was more than 5 min, a 2.5-fold higher than that in the presence of SUMO-BfmSc (Fig. 5J). These results indicate that L181P/E376Q amino acid substitutions may reduce the phosphatase activity of BfmS. Moreover, the

BfmR phosphorylation wanes over times (Fig. 5J), indicating that BfmS^{DK2} not only acts as a kinase (fig. S8) but also acts as a phosphatase against BfmR. Using surface plasmon resonance assay, we observed that SUMO-BfmSc and SUMO-BfmSc^{DK2} display similar binding activity to the His₆-BfmR (fig. S9 D and E), which suggests that L181P/E376Q amino acid substitutions may have no significant effect on the ability of BfmS to sequester BfmR from GtrS. Additionally, using Pro-Q Diamond stain, we found that the kinetics of the phosphorylation of His₆-BfmR by SUMO-BfmSc and SUMO-BfmSc^{DK2} are similar, indicating that L181P/E376Q amino acid substitutions have no significant effect on the ability of SUMO-BfmSc to transfers its phosphoryl group to His₆-BfmR (figS9 F and G).

GtrS mediates changes in gene expression profile of *P. aeruginosa* evoked by *bfmS* mutations

To further investigate the roles of *gtrS* in $\Delta bfmS$ and *bfmS*^{DK2} mutants, we performed RNA-seq analysis on WT, $\Delta bfmS$ mutant, $\Delta bfmS\Delta gtrS$ mutant, *bfmS*^{DK2} mutant, *bfmS*^{DK2} $\Delta gtrS$ mutant, and the $\Delta bfmRS$ mutant strain of MPAO1. Deletion of *bfmS* in MPAO1 decreased the transcript levels of 490 genes (designated as *bfmS*-activated genes, Sheet 3 in Data file 2), while it increased the expression of 201 genes (designated as *bfmS*-repressed genes, Sheet 4 in Data file 2) (Fig. 6A). Of note, deletion of *gtrS* in the *bfmS* deletion mutant ($\Delta bfmS$) background increased the transcript levels of 60.2% (295 out of 490) of the *bfmS*-activated genes, while it decreased the transcript levels of 75% (151 out of 201) of the *bfmS*-repressed genes (Fig. 6A and Sheet 3-4 in Data file 2). These results indicate that GtrS can has an opposite role to BfmS in regulating the expression of a number of *P. aeruginosa* genes, which also suggest that a functional *gtrS* is key in determining the alterations in gene expression levels caused by *bfmS* deletion, and this is well in line with our biochemical data (Fig. 3).

By comparing the transcriptome of *bfmS*^{DK2} mutant to that of WT PAO1, we identified 887 L181P/E376Q-induced genes and 1350 L181P/E376Q-reduced genes (Fig. 6B, Sheet 5-6 in Data file 2). These genes represent approximately 39.3% of the total number of annotated genes in the *P. aeruginosa* PAO1 genome. We found that the expression of 27.2% (241 out of 887) of the L181P/E376Q-induced genes was decreased in the *bfmS*^{DK2} mutant due to the deletion of *gtrS*, whereas the transcript levels of 17.5% (236 out of 1350) of the L181P/E376Q-reduced genes were increased (Fig. 6B, Sheet 5-6 in Data file 2). These results suggest that GtrS contributes to the L181P/E376Q-induced alterations of gene expression in *P. aeruginosa* MPAO1, albeit to a lesser extent than it does in the *bfmS* deletion mutant strain ($\Delta bfmS$).

We identified 417 BfmR-activated genes and 409 BfmR-repressed genes, by comparing the transcriptome of $\Delta bfmS$ to that of $\Delta bfmRS$ (Sheet 7 in Data file 2). As expected, the transcript levels of most, if not all, of the BfmR-activated and -repressed genes in the $\Delta bfmS$ mutant were either decreased or induced by the deletion of *gtrS*,

respectively (Fig. 6C, lane 3; Sheet 7 in Data file 2), supporting the notion that GtrS has an essential role for the transcriptional regulatory activity of BfmR in the $\Delta bfmS$ mutant. We also found that deletion of *gtrS* in the *bfmS*^{DK2} mutant has a similar effect on the expression of some BfmR-activated and -repressed genes (Fig. 6C, genes in clusters I and II; Sheet 7 in Data file 2). For instance, the transcript levels of genes directly activated by BfmR, including *pa4103*, *pa4104*, *pa4105*, *pa4106*, and *pa4107*, were significantly decreased by more than 65% in the *bfmS*^{DK2} mutant upon the deletion of *gtrS*, and a ~84% decrease was observed for the mRNA level of *pa4107* (Fig. 6C, Sheet 7 in Data file 2).

Additionally, in both $\Delta bfmS$ and *bfmS*^{DK2} mutants, like in the CF-adapted isolates, the most abundant mRNA transcript was the BfmR-dependent gene *pa4107*, which was also the most up-regulated gene (with a >2000-fold increase) in these two mutants as compared with the WT MPAO1 strain (Sheet 1-2 in Data file 2). Thus, it is very likely that BfmR is highly activated in these two mutant strain. In all, these transcriptome data support the conclusion that BfmR can be activated by GtrS in either $\Delta bfmS$ or *bfmS*^{DK2} mutant.

Activation of BfmR by missense mutations in *bfmS* is not limited to L181P/E376Q

Not only *bfmS*^{L181P/E376Q} but also other *bfmS* missense variants exist in the *P. aeruginosa* CF isolates (table S3). To examine whether those missense mutations in *bfmS* affect the activity of BfmR, we generated 22 missense variants of *bfmS* and introduced them with the pAK1900 plasmid into the $\Delta bfmS$ strain. Of these 22, the following 10 *bfmS* missense variants have a more than 2-fold increase in the expression of *pa4103-lux*: L181Q, A42E/G347D, F31L, F31L/D295N, T242R, T120K/L164F/G179D/Y280H, A4T/R393H, L168-L, Q92E/L184P, and T120K/L164F/A281T, as compared to the wild type *bfmS* (Fig. 6D). Along with the 10 *bfmS* missense variants, the L181P, L181P/E376Q, and R393H also significantly increased the *pa4103-lux* activity in the $\Delta bfmS$ strain (Fig. 6D), this is consistent with the result of our previous study where the BfmR activity was measured by *bfmR-lux* (24). All of these 13 *bfmS* variants only have a slight effect (<1.2-fold) on the expression of *pa4103-lux* in the $\Delta bfmRS$ mutant (fig. S10A), indicating that those BfmS variant proteins require BfmR in order to activate the expression of *pa4103-lux*. Those variants bear amino acid substituent at different domains of the BfmS (Fig. 6E), implying that the regulatory activity of BfmS can be modulated by diverse mechanisms.

Among the 25 *bfmS* alleles tested, *bfmS*^{A42E/G347D} (found in AU15431 and AU7032 isolates) (35) was most potent in increasing the *pa4103-lux* activity (>300-fold increase) (Fig. 6D). However, a single A42E missense mutation alone has a much weaker effect (< 3-fold increase) than the A42E/G347D missense mutation, while the

G347D missense mutation alone has no obvious effect (fig. S10B). These observations suggest that the combination of these two amino acid substituents (A42E and G347D) synergistically enhances the regulatory functions of BfmS. Similar results were observed for the L181P/E376Q missense mutations (Fig. 6D, Fig. S10B) and the A4T/R393H missense mutations (Fig. 6D), indicating that the interaction of point mutations in *bfmS* can manifest in positive epistasis. Together, these results indicate that *bfmS* mutation-induced activation of BfmR is not limited to either DK2 lineage or the certain types of amino acid changes.

A42E/G347D, T242R, and R393H substituents promote the activation of BfmR by GtrS

In the AU15431 isolate, a high amount of P~BfmR-flag was detected, whereas no P~BfmR-flag was detected in the AU15431::*bfmS*^{PAO1} (in which the WT *bfmS* replaced the *bfmS*^{A42E/G347D}) (fig. S10C). The AU15431::*bfmS*^{PAO1} mutant strain also exhibited a much lower *pa4103-lux* activity, as compared with its isogenic parent AU15431 (fig. S10D). Moreover, the deletion of *gtrS* in AU15431 reduced the expression of both *pa4103-lux* (fig. S10D) and the BfmS protein (fig. S10E). These results suggest that, as with the L181P/E376Q missense mutations in DK2 strain, the A42E/G347D missense mutations in *bfmS* induces an GtrS-mediated activation of BfmR in the AU15431 isolate.

Like L181P/E376Q, the A42E/G347D amino acid substituents also caused an elevated autophosphorylation levels of BfmS in *P. aeruginosa* (fig. S10 F and G). Similar results were observed for the T242R missense mutation of *bfmS* (fig. S10F), which is the second potent mutation in increasing the regulatory activity of BfmR (Fig. 6D). Although glucose did not increase the expression of *pa4103-lux* in the presence of WT *bfmS* or *bfmS*^{DK2 H238A} allele, it did so with either a *bfmS*^{A42E/G347D} (fig. S10H), a *bfmS*^{A42E/G347D/H238A} (fig. S10H), a *bfmS*^{T242R} (fig. S10I), or a *bfmS*^{T242R/H238A} allele (fig. S10I). These results suggest that A42E/G347D and T242R amino acid substituents in BfmS, respectively, enables bacteria to modulate the activity of BfmR in response to glucose. When *gtrS* was further deleted in Δ *bfmS* carrying either *bfmS*^{A42E/G347D/H238A} (fig. S10H) or *bfmS*^{T242R/H238A} (fig. S10I), glucose fails to induce the expression of *pa4103-lux*. Thus, as with the L181P/E376Q missense mutations, other missense mutations in *bfmS* can enable the activation of BfmR by GtrS. This notion is further supported by the observation that *gtrS* is required for the ability of the *bfmS*^{R393H} mutant of MPAO1 (in which the *bfmS*^{R393H} replaced the wild type *bfmS* allele, table S1) to increase the expression of *pa4103-lux* in response to glucose (fig. S10J).

Using Pro-Q Diamond stain, we showed that the T242R substitution nearly completely abolish the phosphatase activity of BfmSc against the phosphorylated BfmR (fig. S11A and B). This is in line with the fact that Thr242 is at a known

location required for phosphatase activity of the HisKA subfamily of bacterial SKs (37). In addition, like the L181P/E376Q amino acid substitutions, R393H substitution caused a decrease in the phosphatase activity of BfmSc as well (fig. S11A and B). These results suggest *bfmS* mutation-induced cross-phosphorylation of BfmR by GtrS is not limited to the L181P/E376Q (Fig. 6F).

Discussions

In this study, we showed that *bfmS* spontaneous mutations induce remodeling of TCSs and allow *P. aeruginosa* to integrate information from multiple sources to activate BfmR, which in turn directs this bacterium toward a chronic infection state (Fig. 6F). Like many TCSs, the WT BfmRS TCS is auto-regulated (24). We observed that the mutated BfmRS TCS (BfmR-BfmS^{DK2}) is auto-regulated as well and responds to certain factor(s) during bacterial growth, as evidenced by the fact that the *bfmR-lux* reporter exhibited an activation surge in the *bfmS*^{DK2} mutant grown in different media (Fig. 1A, fig. S1). The change in the opposing biochemical activities (kinase and phosphatase) of BfmS^{DK2} (Fig. 5J, fig. S8B) may result in such an effect. Additionally, autoregulation may affect the BfmR-BfmS^{DK2} system by controlling the relative concentrations of BfmR and BfmS^{DK2}, and thus provide a threshold for gene regulation, as it did for some other TCS systems (36).

It is worthy to note that during adaptation to the CF lung environment, L181P and E376Q missense mutations in *bfmS* were fixed in the *P. aeruginosa* DK2 lineage, which is a dominating clone in Denmark (9, 12, 37). However, *bfmS* mutant alleles were also found in more than three hundred *P. aeruginosa* CF isolates from different continents and countries, in addition to at least 50 DK2 CF-adapted isolates (table S3). Of note, *bfmS* mutant alleles encoding BfmS variants that bear amino acid substituent at position 181 (L181Q), which causes an increase in the regulatory activity of BfmR (Fig. 6D), was also observed in all 26 isolates belong to the M3L7 sub-lineage emerged in Australia (16). These would suggest that, the prevalence of *bfmS* mutations is not limited to the DK2 CF-adapted isolates and may be higher than we have found.

Mutations in regulatory genes are important in the adaptation process (5, 37). When mutations affect global regulatory genes, considerable phenotypic divergence can be rapidly achieved, thereby setting the scene for adaptive radiations (5-7). The evolution of a new trait has been proposed to occur in three-steps: potentiation, actualization, and refinement (38). We showed that naturally evolved mutations in *bfmS* are sufficient to direct *P. aeruginosa* toward a chronic state (decreased QS-signal production, attenuation of bacterial acute virulence, and enhanced biofilm formation), by activating a single protein (BfmR) (Fig. 1, Fig. 2, fig. S2, and Fig. 6F). The functional activation of BfmR can also explain some adaptive gene expression changes in the DK2 lineage (Fig. 2A, Fig. 6C). Therefore, it is possible that

L181P/E376Q (or L181P) represents an actualizing mutation, producing various origins and diversity in phenotypes and gene expression of the DK2 isolates. Given these, mutation in *bfmS*, and/or its combination with mutations in other global regulatory genes such as *pmrB*, *rpoN*, *mucA*, and *lasR* (9, 12, 37), may have a critical role in directing *P. aeruginosa* DK2 toward increased adaptive performance, and thus resulting in lineages that are highly successful in the CF lungs and have the capacity to be transmitted among individuals with CF.

We showed that L181P/E376Q, A42E/G347D, T242R, or R393H missense mutations in *bfmS* can enable *P. aeruginosa* to exploit the cross-regulation between GtrS and BfmR in order to alter its response to glucose (Fig. 6F), although TCSs typically insulated from one another (17). Moreover, L181P/E376Q, T242R, and R393H substituents respectively decreased the phosphatase activity of SUMO-BfmSc (Fig. S11). Therefore, it is not a far-fetched idea that the phosphatase activity of BfmS may be a key mechanism of preventing the phosphorylation of BfmR by GtrS. This notion is further supported by the fact that when *bfmS* is absent, both the phosphorylation level and the regulatory activity of BfmR are largely dependent on the *gtrS* (Fig. 3C, Fig. 6 A and C).

In airway surface liquid (ASL), glucose concentrations (~ 0.4 mM) are about 12 times lower than that in the blood (39), which might be a homeostatic mechanism inhibiting bacterial proliferation by depriving the bacteria of an essential nutrient (39, 40). Indeed, from studies in animals and patients with either chronic obstructive pulmonary disease (COPD) or cystic fibrosis, an association has been reported between airway glucose concentrations and increased susceptibility to bacterial infection (39-42). Given these, the functional interaction between GtrS and BfmR, which contributes to the transcriptional regulatory activity of BfmR, may be physiologically relevant. Since BfmR is highly activated in a number of CF-isolates grown both *in vitro* and *in vivo* (GDS2869, GDS2870, GDS4249, GSE62970, and GSE31227) and has a crucial function in biofilm formation (22-24) (fig. S2 F and G), targeting BfmR function might be of particular interest.

In conclusion, in this study, we have provided evidence that, during chronic infections, the *P. aeruginosa* can remodel its signaling cascades to integrate different signals to regulate a major lifestyle switch (between virulence and biofilm formation) (Fig. 6C). Our data also suggest that, in addition to *cis*- and *trans*-regulatory changes (43-46), mutation-induced remodeling of signaling cascades may also contribute to changes in gene expression during the evolution (Fig. Data files 1-2, Fig. 6C). More in-depth knowledge about the adaptive changes in signaling pathways will provide clues to the selective forces driving pathogen evolution in the host environment and help to improve the treatment of the infection.

Materials and Methods

Bacterial strains, plasmids, and culture conditions

The bacterial strains and plasmids used in this study are listed in table S1. Unless noted otherwise, *P. aeruginosa* MPAO1 and its derivatives were grown in Luria-Bertani (LB) medium, Pyocyanin production broth (PB medium) (20 g peptone, 1.4 g MgCl₂, 10 g K₂SO₄, 20 ml glycerol per liter; pH 7.0), or M8-glutamate minimal medium (6 g Na₂HPO₄, 3 g KH₂PO₄, 0.5 g NaCl, 0.24 g MgSO₄, 0.5 g glutamate per liter; pH 7.4) supplemented with or without glucose (2 mM), as indicated. DK2 and AU15431 and their derivatives were grown in PB medium. *E. coli* were grown in LB medium. All cultures were incubated at 37°C with shaking (250 rpm) unless noted otherwise. For plasmid maintenance in *P. aeruginosa*, the medium was supplemented with 100 µg/ml carbenicillin, 50 µg/ml tetracycline, or 100 µg/ml kanamycin when required. For plasmid maintenance in *E. coli*, the medium was supplemented with 100 µg/ml carbenicillin, 50 µg/ml kanamycin, 10 µg/ml tetracycline, or 10 µg/ml gentamicin, as appropriate. For marker selection in *P. aeruginosa* DK2 and AU15431 isolates, 500 µg/ml gentamicin and 150 µg/ml tetracycline were used when required.

Transposon mutagenesis

The $\Delta bfmS::bfmR-lacZ$ mutant strain was subjected to transposon mutagenesis using the mariner transposon vector pBT20 (47). To construct the strains $\Delta bfmS::bfmR-lacZ$, the *bfmR* promoter region (-995 to +20 of the start codon) was amplified by PCR using the primers pro-bfmR-F (with *Xho*I site) and pro-bfmR-R (with *Bam*HI site) (table S2) and cloned into the *Xho*I and *Bam*HI sites of the integration-proficient mini-CTX-*lacZ* (48) in order to generate mini-CTX-*bfmR-lacZ* (mini-*bfmR-lacZ*). The resulting plasmid was conjugated into $\Delta bfmS$ and the construct was integrated into the *attB* site through a diparental mating using *E. coli* S17 λ -pir as the donor, following excision of the mini-CTX backbone from the chromosome using a flippase (FLP) recombinase encoded on the pFLP2 plasmid (49).

For transposon mutagenesis, the transposon in pBT20 was conjugally transferred by biparental mating into the $\Delta bfmS::bfmR-lacZ$ mutant, following a protocol previously described (50). Briefly, the donor strain (*E. coli* SM10- λ pir) containing the pBT20 and the recipient $\Delta bfmS::bfmR-lacZ$ strain were scraped from overnight plates and suspended in 1 ml of M8-glutamate minimal medium. Concentrations of the bacteria in the suspensions were adjusted to OD₆₀₀ of 40 for the donor and OD₆₀₀ of 20 for the recipient. Next, each donor and recipient were mixed together and spotted on a LB agar plate and incubated at 37°C for 7 h. Mating mixtures were scraped and resuspended in 1 ml of M8-glutamate minimal medium. Transposon-mutagenized bacteria were selected by plating on PIA plates containing gentamicin at 150 µg/ml. A sterile tip was used to pick up individual colonies and dip them into the M8-glutamate minimal agar plates (supplying 1.5% agar and 2 mM glucose) with 20 µg/ml X-gal. Approximately 30,000 colonies were screened for the appearance of

blue color. The localization of the Mariner transposon with respect to the *P. aeruginosa* genome was determined using an established protocol (47).

Plasmid construction for the constitutive expression of *P. aeruginosa* genes

All the primers used for plasmid construction are listed in table S2. To construct the plasmid for constitutive expression of *gtrS*, a ~1.5 kb PCR product covering 72 bp of the *gtrS* upstream region, the *gtrS* gene, and 9 bp downstream of *gtrS* was amplified from MPAO1 genomic DNA using primers *gtrS*-comp-F (with *Hind*III site) and *gtrS*-comp-R (with *Bam*HI site). For generating pAK1900-*gltR* (p-*gltR*), a ~0.77 kb PCR product covering 38 bp of the *gltR* upstream region, the *gltR* gene, and 7 bp downstream of *gltR* was amplified MPAO1 genomic DNA using primers *gltR*-comp-F (with *Hind*III site) and *gltR*-comp-R (with *Kpn*I site). For generating pAK1900-*gltR-gtrS* (p-*gltR-gtrS*), a ~2.3 kb PCR product covering 38 bp of the *gltR* upstream region, the *gltR* and *gtrS* genes, and 9 bp downstream of *gtrS* was amplified MPAO1 genomic DNA using primers *gltR*-comp-F (with *Hind*III site) and *gtrS*-comp-R (with *Bam*HI site). For generating pAK1900-*gltB* (p-*gltB*), a ~1.3 kb PCR product covering 40 bp of the *gltB* upstream region, the *gltB* gene, and 15 bp downstream of *gltB* was amplified MPAO1 genomic DNA using primers pa3190-comp-F (with *Hind*III site) and pa3190-comp-R (with *Kpn*I site). All the products were digested with the indicated enzymes and cloned into pAK1900 (51), and the direction of transcription of the cloned genes is in the same orientation as *lac* on pAK1900.

In order to generate pRK415-*bfmS*, a ~1.4 kb PCR product covering 20 bp of the *bfmS* upstream region, the *bfmS* gene, and 15 bp downstream of *bfmS* was amplified from MPAO1 genomic DNA using primer pair *bfmS*-comp-F/*bfmS*-comp-R (*Hind*III/*Bam*HI sites). For generating pRK415-*gtrS*, the primer pair *gtrS*-comp-F/*gtrS*-comp-R and MPAO1 genomic DNA were used. All the PCR products were cloned into pRK415 (52), and the direction of transcription of the cloned genes was in the same orientation as the *lac* promoter on pRK415.

For generating mini-*bfmS*, mini-*gltR-gtrS*, mini-*gltR*, and mini-*gtrS*, primers pAK1900-mini-F (with *Xho*I site) and pAK1900-mini-R (with *Xba*I site) were used. Briefly, a ~1.7 kb PCR product covering the *lac* promoter of pAK1900 plasmid and the *bfmS* was amplified from p-*bfmS* plasmid (table S1) DNA, and the PCR products were cloned into integrated mini-CTX-*lacZ* vector. For generating mini-*gltR-gtrS*, a ~2.5 kb PCR product covering the *lac* promoter of pAK1900 plasmid and the *gltR-gtrS* was amplified from p-*gltR-gtrS* plasmid (table S1) DNA. For generating mini-*gltR*, a ~1 kb PCR product covering the *lac* promoter of the pAK1900 and the *gltR* was amplified from p-*gltR* plasmid (table S1). For generating mini-*gtrS*, a ~1.8 kb PCR product covering the *lac* promoter of the pAK1900 and the *gtrS* was amplified from p-*gtrS* plasmid DNA (table S1). The PCR products were cloned into integrated mini-CTX-*lacZ* vector (48).

All constructs were sequenced to ensure that no unwanted mutations resulted.

Plasmid construction for the expression of FLAG- or HA-tagged genes

For generating pAK1900-*bfmR*-flag (p-*bfmR*-flag), a ~0.8 kb PCR product covering the region from 15 bp upstream and the *bfmR* gene (not including the stop codon) was generated from MPAO1 genomic DNA with primers *bfmR*-comp-F (with *Hind*III site) and *bfmR*-flag-R (with *Bam*HI site) (table S2). The *Hind*III and *Bam*HI digested PCR product was cloned into pAK1900 to generate pAK1900-*bfmR*-flag (p-*bfmR*-flag). The pAK1900-*bfmR*^{D55A}-flag (p-*bfmR*^{D55A}-flag, the aspartate 55 of BfmR was replaced by alanine) was obtained by using the primer pair BfmR(D55A)-F/BfmR(D55A)-R and a QuikChange II site-directed mutagenesis kit (Stratagene, Catalog#: 200518). For generating pRK415-*bfmR*-flag, primers *bfmR*-comp-F and *bfmR*-flag-R were used again, and the PCR product was cloned into pRK415 plasmid. For generating pAK1900-*gtrS*-HA, primers *gtrS*-comp-F (with *Hind*III site) and *gtrS*-HA-R (with *Bam*HI site) (table S2) were used to perform PCR of the *GtrS* gene that was meant to fuse with a C-terminal HA-tag, and a ~1.55 kb PCR product covering the region from 72 bp upstream and the *GtrS* gene (not including the stop codon) was generated from MPAO1 genomic DNA and cloned into the pAK1900. For generating pAK1900-*gtrS*^{H280A}-HA, the primer pair *GtrS*(H280A)-F/*GtrS*(H280A)-R and a QuikChange II site-directed mutagenesis kit (Stratagene, Catalog#:200518) were used. All constructs were sequenced to ensure that no unwanted mutations resulted.

Construction of gene deletion mutant strains of *P. aeruginosa* MPAO1

For gene replacement, a *SacB*-based strategy was employed as previously described (49). To construct the *gltB* null mutant (Δ *gltB*), polymerase chain reactions (PCRs) were performed in order to amplify sequences upstream (~1.2 kb) and downstream (~1.3 kb) of the intended deletion. The upstream fragment was amplified from MPAO1 genomic DNA using primers D-pa3190-up-F (with *Eco*RI site) and D-pa3190-up-R (with *Kpn*I site), while the downstream fragment was amplified with primers D-pa3190-down-F (with *Kpn*I site) and D-pa3190-down-R (with *Hind*III site). These two PCR products were digested and then cloned into the *Eco*RI/*Hind*III digested gene replacement vector pEX18Ap, yielding pEX18Ap::*pa3190UD*. A 1.8 kb gentamicin resistance cassette was cut from pPS858 with *Kpn*I and then cloned into pEX18Ap::*pa3190UD*. The resultant plasmid, pEX18Ap::*pa3190UGD*, was electroporated into MPAO1 with selection for gentamicin resistance. Colonies were screened for gentamicin sensitivity and loss of sucrose (5%) sensitivity, which typically indicates a double-cross-over event and thus marks the occurrence of gene replacement.

A similar strategy was used to construct the $\Delta gtrS$, $\Delta gltR-gtrS$, and $\Delta bfmR$ as described above. Briefly, for the construction of $\Delta gtrS$, the upstream fragment (~ 1 kb) of the intended deletion was amplified with primers D-gtrS-up-F (with *EcoRI* site) and D-gtrS-up-R (with *BamHI* site), and the downstream fragment (~ 1 kb) was amplified with primers D-gtrS-down-F (with *BamHI* site) and D-gtrS-down-R (with *HindIII* site). For the construction of $\Delta gltR-gtrS$, the upstream fragment (~ 1.3 kb) of the intended deletion was amplified with primer pair D-gltR-up-F/D-gltR-up-R (*EcoRI/BamHI* sites) and the downstream fragment (~1 kb) was amplified with primer pair D-gtrS-down-F/D-gtrS-down-R (*BamHI/HindIII*). For the construction of $\Delta bfmR$, the upstream fragment (~ 1 kb) of the intended deletion was amplified with primer pair D-bfmR-up-F/D-bfmR-up-R (*EcoRI/BamHI* sites) while the downstream fragment (~1.2 kb) was amplified with primer pair D-bfmR-down-F/D-bfmR-down-R (*BamHI/HindIII*). A 1.8 kb gentamicin resistance cassette was cut from pPS858 with *BamHI* and then cloned into the pEX18Ap::*gtrS*UD, pEX18Ap::*gltR-gtrS*UD, and pEX18Ap::*bfmR*UD, yielding pEX18Ap::*gtrS*UGD, pEX18Ap::*gltR-gtrS*UGD, and pEX18Ap::*bfmR*UGD, respectively, as described above.

For the construction of $\Delta bfmS\Delta gltB$, the gentamicin resistance cassette of $\Delta gltB$ was excised by using the plasmid pFLP2 that encoded Flp recombinase, and then the pEX18Ap::*bfmS*UGD plasmid (table S1) was electroporated into the $\Delta gltB$ (without gentamicin resistance cassette) in order to generate $\Delta bfmS\Delta gltB$. The same strategy was used to construct the $\Delta bfmS\Delta gtrS$ and $\Delta bfmS\Delta gltR-gtrS$ mutants. For generating $\Delta bfmRS\Delta pta-ackA$ mutant, pEX18Ap::*ackA-pta*UTD (24) was electroporated into the $\Delta bfmRS$. For the construction of $\Delta bfmRS\Delta gltR-gtrS$, the gentamicin resistance cassette of $\Delta gltR-gtrS$ was excised by using the plasmid pFLP2 that encoded Flp recombinase, and the pEX18Ap::*bfmRS*UGD (table S1) was electroporated into the $\Delta gltR-gtrS$ (without gentamicin resistance cassette) in order to generate $\Delta bfmRS\Delta gltR-gtrS$.

The primers used for PCRs are listed in table S2, and all the mutant strains were confirmed by PCR.

Construction of gene deletion mutants of *P. aeruginosa* clinical isolates

For construction of $\Delta gtrS$ mutant of DK2 strain and AU15431 isolate, pEX18Ap::*gtrS*UGD plasmid (table S1) was electroporated into DK2 and AU15431, respectively, and the transformants were screened on an LB plate containing 500 μ g/ml gentamicin and 5 % sucrose. For the construction of $\Delta bfmRS$ in DK2, a similar strategy as described above and pEX18Ap::*bfmRS*UGD plasmid (table S1) were used. For the construction of $\Delta bfmS$ mutant strain of either DK2 strain or AU15431 isolate, pEX18Ap::*bfmS*UGD plasmid (table S1) was used. All the mutant strains were confirmed by PCR and DNA sequencing.

Construction of allelic exchange mutants

To construct the *bfmS*^{DK2} (MPAO1-*bfmS*^{DK2}) allelic exchange mutant, a ~3.3 kb PCR product covering ~1 kb upstream of *bfmS*, the *bfmS* gene, and ~0.95 kb downstream of *bfmS* was amplified from *P. aeruginosa* DK2 genomic DNA using primers *bfmS*-allelic-DK2-F (with *EcoRI* site) and *bfmS*-allelic-DK2-R (with *HindIII* site). The fragments were subsequently digested and cloned into *EcoRI/HindIII* digested gene replacement vector pEX18Tc (table S1). The resultant plasmid, pEX18Tc-For-*bfmS*^{DK2} were electroporated into the Δ *bfmS* mutant (with gentamicin resistance cassette) (table S1) with selection for both tetracycline and gentamicin resistance, which typically indicates a single-cross-over event. Colonies were further screening for tetracycline and gentamicin sensitivity, and loss of sucrose (5%) sensitivity, which typically indicates a double-cross-over event thus marks the occurrence of gene replacement. The *bfmS*^{DK2} mutant was further confirmed by PCR and DNA sequencing. For generating MPAO1-*bfmS*^{DK2 H238A}, plasmid pEX18Tc-For-*bfmS*^{DK2 H238A} was constructed by using the primer pair BfmS(H238A)-F/BfmS(H238A)-R, a QuikChange II site-directed mutagenesis kit (Stratagene, Catalog#: 200518), and MPAO1-*bfmS*^{DK2 H238A} plasmid DNA.

To construct the *bfmS*^{R393H} (MPAO1-*bfmS*^{R393H}) allelic exchange mutant, PCR product was amplified from *P. aeruginosa* MPAO1 genomic DNA using primers *bfmS*-allelic-DK2-F (with *EcoRI* site) and *bfmS*-allelic-DK2-R (with *HindIII* site) and then cloned into pEX18Tc, yielding pEX18Tc-For-*bfmS*^{PAO1} plasmid. Subsequently, the resultant plasmid, pEX18Tc-For-*bfmS*^{R393H} (table S1), was constructed by using the primer pair R393H-F/R393H-R and a QuikChange II site-directed mutagenesis kit (Stratagene, Catalog#: 200518). The pEX18Tc-For-*bfmS*^{R393H} was further electroporated into the Δ *bfmS* mutant (with gentamicin resistance cassette) (table S1) in order to generate the *bfmS*^{R393H} allelic exchange mutant as described above.

To construct *bfmS*^{DK2} Δ *bfmR*, pEX18Ap::*bfmRUGD* plasmid (table S1) was electroporated into *bfmS*^{DK2} allelic exchange mutant with selection for gentamicin resistance. To construct *bfmS*^{DK2} Δ *gtrS* and *bfmS*^{R393H} Δ *gtrS* mutants, pEX18Ap::*gtrSUGD* plasmid (table S1) was electroporated into *bfmS*^{DK2} and allelic exchange mutants, respectively, with selection for gentamicin resistance. Colonies were screened for gentamicin sensitivity and loss of sucrose (5%) sensitivity, which typically indicates a double-cross-over event and thus marks the occurrence of gene replacement. PCR and DNA sequencing further confirmed the replacement of the gene allele.

A similar strategy was used to construct the DK2-*bfmS*^{PAO1} and AU15431-*bfmS*^{PAO1} mutants. Briefly, pEX18Tc-For-*bfmS*^{PAO1} plasmid was electroporated into DK2- Δ *bfmS* and AU15431- Δ *bfmS* (table S1), respectively. Colonies were screened

for tetracycline and gentamicin sensitivity and loss of sucrose (5%) sensitivity.

Overexpression of recombinant proteins in *E. coli* and their purifications

The following ten recombinant proteins were expressed in *E. coli*: His₆-GtrSc, the N-terminal His₆-tagged cytosolic segment of GtrS (residues 269-465); BfmSc, the N-terminal His₆- and GST-tagged cytosolic segment of BfmS (residues 175-435); BfmSc^{DK2}, a BfmSc mutant in which the leucine 181 (L181) and glutamic acid 376 (E376) of BfmS were respectively replaced by proline (P) and Q (glutamine); BfmSc^{DK2 H238A}, a BfmSc^{DK2} mutant in which the histidine 238 (H238) of BfmS was replaced by alanine (A); SUMO-BfmSc, the N-terminal His₆-SUMO tagged cytosolic segment of BfmS (residues 175-435); SUMO-BfmSc^{DK2}, a SUMO-BfmSc variant in which the leucine 181 (L181) and glutamic acid 376 (E376) of BfmS were respectively replaced by proline (P) and Q (glutamine); SUMO-BfmSc^{T242R}, a SUMO-BfmSc variant in which the tyrosine 242 (T242) of BfmS was replaced by arginine (R); SUMO-BfmSc^{R393H}, a SUMO-BfmSc variant in which the arginine 393 (R393) of BfmS was replaced by histidine (H); His₆-BfmR, N-terminal His₆-tagged BfmR; His₆-BfmR^{D55A}, a His₆-BfmR variant in which the Aspartic acid 55 (D55) of BfmR was replaced by alanine (A).

For the construction of expression plasmids of the His₆-GtrSc proteins, primers gtrS-KD-F (with *Bam*HI site) and gtrS-KD-R (*Eco*RI) were used. The DNA fragment amplified from *P. aeruginosa* MPAO1 genomic DNA encoding the kinase domain of *gtrS* (residues 269-465) was cloned into pET28a (table S1), yielding pET28a-*GtrSc* plasmid. For the expression of BfmSc proteins, primers bfmS-KD-F (with *Bam*HI site) and bfmS-KD-R (*Xho*I) were used and the corresponding DNA fragment encoding the kinase domain of WT BfmS (residues 175-435) was cloned into the prokaryotic expression vector pGEX-6p-1-6His (table S1), yielding pGEX-6p-1-BfmSc plasmid (the gene cassette was fused in-frame to 3'-terminal of glutathione S-transferase gene of the pGEX-6p-1-6His). For generating pGEX-6p-1-BfmSc^{DK2}, the primer pairs BfmS(L181P)-F/BfmS(L181P)-R and BfmS(E376Q)-F/BfmS(E376Q)-R, and a QuikChange II site-directed mutagenesis kit (Stratagene, Catalog#: 200518) were used. For generating pGEX-6p-1-BfmS^{DK2 H238A-Cter}, the primer pair BfmS(H238A)-F/BfmS(H238A)-R and a QuikChange II site-directed mutagenesis kit were used. For the expression of SUMO-BfmSc proteins, primers bfmS-KD-2F (with *Kpn*I site) and bfmS-KD-2R (*Hind*III) were used and the corresponding DNA fragment encoding the kinase domain of WT BfmS (residues 175-435) was cloned into the prokaryotic expression vector pET28a(+)-sumo, yielding pET28a(+)-sumo-BfmSc plasmid (table S1). For generating pET28a(+)-sumo-*BfmSc*^{DK2}, the primer pairs BfmS(L181P)-F/BfmS(L181P)-R and BfmS(E376Q)-F/BfmS(E376Q)-R, and a QuikChange II site-directed mutagenesis kit were used. For generating pET28a(+)-

sumo-*BfmSc*^{T242R} and pET28a(+)-sumo-*BfmSc*^{R393H}, the primer pairs T242R-F/T242R-R and R393H-F/ R393H-R were used, respectively. All constructs were sequenced to ensure that no unwanted mutations resulted.

The protein was expressed in *E. coli* strain BL21 star (DE3) and purifications were performed as previously described (24, 50, 53, 54). Briefly, bacteria were grown at 37°C overnight in 10 ml of LB medium with shaking (250 rpm). The cultures were transferred into 1 L of LB medium incubated at 37°C with shaking (200 rpm) until the OD₆₀₀ reached 0.6, and then IPTG (isopropyl-1-thio-β-d-galactopyranoside) was added to a final concentration of 1.0 mM. After 4 h incubation at 30°C with shaking (200 rpm), the cells were harvested by centrifugation and stored at - 80°C. The cells were lysed at 4 °C by sonication in lysis buffer [50 mM Tris (pH 7.4), 200 mM NaCl, 1 mM PSMF and 2 mM DTT]. Clarified cell lysate was loaded onto a HisTrap HP column (Code#: 17-5247-01, GE Healthcare), washed with Ni-NTA washing buffer and eluted with Ni-NTA elution buffer. The fractions containing BfmSc proteins were loaded onto the HiTrap Desalting 5 x 5 ml (Sephadex G-25 S) (Code#: 17-1408-01, GE Healthcare) with a running condition of 50 mM Tris (pH 7.4), 200 mM NaCl and 2 mM DTT to remove the imidazole. The purified protein was > 90% pure as estimated by a 12% (wt/vol) SDS/PAGE gel.

***In vitro* phosphorylation assays**

In vitro autophosphorylation were carried out in phosphorylation reaction mixtures (100 μl) contained purified proteins (~20 μg) in phosphorylation reaction buffer [50 mM Tris-HCl, pH 7.5; 50 mM KCl, 1 mM DTT, 5 mM MgCl₂]. The reaction was initiated by addition of 10 μCi of [γ-³²P]ATP (PerkinElmer, BLU002A500UC) and then incubated at room temperature for 5 min (or for the indicated time). 10 μl aliquots were removed following the addition of 2 μl 5 × SDS loading buffer, and the sample was resolved onto a 12% SDS-PAGE, visualized by autoradiography and Coomassie blue staining.

To examine the transphosphorylation of BfmR, the His₆-GtrSc, BfmSc, and BfmSc^{DK2} proteins (20-40 μg) were incubated in phosphorylation reaction buffer [50 mM Tris-HCl, pH 7.5; 50mM KCl, 1 mM DTT, 5 mM MgCl₂] containing 10 μCi [γ-³²P]ATP for 5 min (or for the time indicated) as described above. Either purified His₆-BfmR or His₆-BfmR^{D55A}, as indicated, was added to the reaction mixture in a final volume of 100 μl. After incubation at room temperature for 5 min (or for the time indicated), 10 μl aliquots were removed, in which the transphosphorylation reaction was stopped by adding 2 μl of 5 × SDS loading buffer, and analyzed by SDS-PAGE, visualized by autoradiography and Coomassie blue staining.

In vitro phosphorylation were also monitored by Pro-Q stain according to the protocol of the manufacturer (Invitrogen). For *in vitro* autophosphorylation assays,

either BfmSc (~3 µg), BfmSc^{DK2} (~1.5 µg), or His₆-BfmR (~2 µg) was incubated in phosphorylation reaction mixtures (20 µl) supplemented with 2 mM ATP; For *in vitro* phosphorylation of BfmR by BfmS, SUMO-BfmSc (~2 µg) and SUMO-BfmSc^{DK2} (~2 µg) were respectively incubated with His₆-BfmR (~2 µg) in phosphorylation reaction mixtures (20 µl) supplemented without or with 2 mM ATP, as indicated. After incubation at on ice for the indicated times, 10 µl aliquots were removed and the reaction was stopped by adding 2 µl of 5 × SDS loading buffer, and analyzed by SDS-PAGE. To examine the phosphorylation of BfmR by GtrS, the His₆-GtrSc (~15 µg) was first incubated in phosphorylation reaction buffer containing 5 mM ATP for 10 min and then the purified His₆-BfmR (~15 µg) was added to the reaction mixture in a final volume of 100 µl. After incubation at room temperature for the indicated times, 10 µl aliquots were removed, in which the phosphorylation reaction was stopped by adding 2 µl of 5 × SDS loading buffer, and analyzed by SDS-PAGE. After staining with Pro-Q Diamond, the gels were stained with Coomassie blue to determine total protein content. The proteins stained with Pro-Q Diamond were visualized using a Tanon-5200 multi (Tanon) at an excitation wavelength of 535 nm and a band pass emission filter of 605 nm. Protein phosphorylation level was quantified by determining the ratio of the intensity of phosphoprotein in Pro-Q Diamond image to its intensity of total protein in Coomassie blue image using ImageQuant software (Molecular Dynamics, Sunnyvale, CA) when required.

***In vitro* dephosphorylation assays**

To examine the dephosphorylation of P~BfmR, His₆-BfmR was first transphosphorylated by SUMO-BfmSc (at a SUMO-BfmSc/His₆-BfmR ratio of 1:6) for 10 min and then the excess of radiolabeled ATP was removed by desalting tubes Bio-Spin®6 (BioRad). To examine the dephosphorylation of P~BfmR in the absence of additional BfmS or BfmS^{DK2}, P~His₆-BfmR samples were fractionated by 12% SDS-PAGE, and radiolabeled proteins were visualized by autoradiography. To examine BfmS- or BfmS^{DK2}-mediated dephosphorylation of P~BfmR, SUMO-BfmSc and SUMO-BfmSc^{DK2} was respectively added into the reaction to reach a 4:1 (SUMO-BfmSc/His₆-BfmR or SUMO-BfmSc^{DK2}/His₆-BfmR) ratio, the reactions were initiated by adding 3 mM ADP at a final concentration and then incubated at room temperature for the indicated time. Reactions were stopped by the addition of 5 µl 5 × SDS loading buffer into a 20 µl reaction mixtures, and a 10 µl aliquot was resolved onto a 12% SDS-PAGE, visualized by autoradiography and Coomassie blue staining.

In vitro dephosphorylation were also monitored by Pro-Q stain. To examine the dephosphorylation of BfmR, His₆-BfmR proteins (~ 40 µg) were first transphosphorylated by His₆-GtrSc (at a His₆-GtrSc/His₆-BfmR ratio of 1:1) for 30 min phosphorylation reaction buffer supplemented with 5 mM ATP. The excess of ATP was removed by desalting tubes Bio-Spin®6 (BioRad). SUMO-BfmSc and its

variants (BfmSc^{DK2}, BfmSc^{T242R}, and BfmSc^{R393H}) was respectively added into the reaction to reach a 2:3 (SUMO-BfmSc/His₆-BfmR) ratio. The reactions were initiated by adding 3 mM ADP at a final concentration and then incubated at room temperature for the indicated times, stopped by the addition of 2 μ l 5 \times SDS loading buffer. 10 μ l aliquot was resolved onto a 12% SDS-PAGE. Phosphoproteins were stained with the Pro-Q Diamond.

Localized Surface Plasmon Resonance

An OpenSPR localized surface plasmon resonance (Nicoya Lifesciences) was used to analyze the interaction of BfmS with BfmR. His₆-BfmR protein was fixed on the COOH sensor chip by capture-coupling, then SUMO-BfmSc at concentrations of 12.5 nM, 40 nM, 80nM, 100nM and SUMO-BfmSc^{DK2} at concentrations of 25 nM, 50nM, 80nM, 100nM were injected sequentially into the chamber in PBS running buffer at 25°C. The binding time and disassociation time were both 240 s, the flowrate was 20 μ l/min, the chip was regenerated with 0.02% SDS. A one to one diffusion corrected model was fitted to the wavelength shifts corresponding to the varied drug concentration. The data was retrieved and analyzed with TraceDrawer software (Ridgeview Instruments AB). Kinetic parameters were calculated using a global analysis, and the data was fitted to a one to one model.

Sample preparation and the Phos-tag gel electrophoresis

For the detection of in vivo BfmR phosphorylation, *P. aeruginosa* MPAO1 and its derivatives were grown at 37°C for 24 h on M8-glutamate minimal agar plate supplemented with 0.2 % glucose. To prepare cell lysates for the Phos-tag (APEXBIO, Code#: F4003) gel assay, bacteria cells were scraped from the plate and immediately resuspended in 60 μ l of lysis buffer [50 mM Tris-Cl (pH 7.5), 150 mM NaCl, 1 mM MgCl₂, 0.1% Triton X-100, 15 μ g/ml DNase I, 0.5 mM PMSF, 1 mM DTT] with 0.1% (vol/vol) Lysonase. Sufficient lysis was achieved by repeated pipetting up and down for 10 s followed by addition of 20 μ l of 4 \times SDS loading buffer. 15 μ l aliquots of the resulting cell lysates were immediately loaded onto a Phos-tag gel (10% acrylamide gels containing 25 μ M acrylamide-Phos-tag ligand and 50 μ M MnCl₂) (25).

For the detection of BfmR and BfmS phosphorylation in DK2 and AU15431 strains or in their derivatives, overnight cultures (LB) were washed twice and diluted 100-fold in fresh PB medium. The liquid cultures were grown in a 20-ml tube with a volume-to medium ratio of 5:1, shaken at 250 rpm for 3 h, of aeration. After collection of the cells by centrifugation, the pellet was washed once with 1 ml of 1 \times PBS and suspended in 1 ml of lysis buffer (50 mM Tris-HCl, pH 7.5; 50 mM NaCl, 1

mM DTT ,5% Glycerinum) supplied with 1 µl protease inhibitor cocktail (ThermoFisher, Cat#: 78430). The mixture was homogenized by mechanical disruption (Fast Prep FP2400 instrument; Qbiogene) and then centrifuging at 2, 300 g for 5 min. The supernatant was collected and followed by addition of 5 × SDS loading buffer, and 15 µl aliquots were loaded onto a Phos-tag gel as described above for electrophoresis.

After 3 h of electrophoresis at 30 mA in Tris-Glycine-SDS running buffer (25 mM Tris, 192 mM glycine, 0.1% SDS, pH 8.4) at 4°C, the Phos-tag gel was washed 10 min at room temperature with Transfer Buffer [20%(v/v) methanol, 50 mM Tris, 40 mM glycine] supplied with 1 mM EDTA to remove Mn²⁺ from the gel, then the gel was incubated at room temperature with gentle shaking for another 10 min in Transfer Buffer (20%(v/v) methanol, 50 mM Tris, 40 mM glycine) twice to remove EDTA.

Co-immunoprecipitation

Overnight cultures of *P. aeruginosa* were washed twice and diluted 100-fold in fresh M8-glutamate minimal medium supplemented with glucose. The liquid cultures were grown in a 100 ml flask with a volume-to medium ratio of 3:1, shaking with 250 rpm at 37 °C for 3 h. 30 ml cultures were harvested by centrifugation, washed once and suspended in 1 ml of lysis buffer provided in the CO-IP kit (Pierce) supplied with 1 µl protease inhibitor cocktail (ThermoFisher, Cat#: 78420). The mixture was homogenized by mechanical disruption (Fast Prep FP2400 instrument; Qbiogene) and then the debris was removed by centrifuging and filtrating through 0.44 µm filters. 500 µl clarified lysates were incubated with the resins immobilized with specific antibodies or not for 12 h at 4 °C. The bound materials were washed and eluted following the manufacturer's recommendation (ThermoFisher, Cat#: 26149). Total samples (clarified lysates) and the immunocomplexes eluted from the resins were analyzed by western blot with specific antibodies, as indicated.

Western blot analysis

Samples resolved on gels were transferred to PVDF (Bio-Rad) membranes through semi-dry transfer assembly (Bio-Rad) for 30 min at room temperature. The membrane was incubated with the primary antibody in 10 ml of 5% (wt/vol) skim milk at 4 °C overnight following the blocking step [10 ml of 5% (wt/vol) skim milk] at room temperature for 2 h, and then washed three times at room temperature for 15 min in TBST buffer [10 mM Tris-HCl, pH 7.5, 150 mM NaCl, and 0.1% Tween 20]. Then, membranes were incubated with the secondary antibody for 2 h at room temperature and washed three times for 15 min in TBST. The chemiluminescent detection reaction

was performed and detected by Tanon-5200 multi, according to the manufacturer's recommendation.

BfmR-Flag proteins were detected by Western blot analysis using a mouse anti-Flag monoclonal antibody (Cat#: AGM12165, Aogma) followed by a secondary, sheep anti-mouse IgG antibody conjugated to horseradish peroxidase (HRP) (Code#: NA931, GE Healthcare). GtrS-HA proteins were detected with a mouse anti-HA monoclonal antibody (Cat#: 66006-1-Ig, Proteintech) followed by a secondary, sheep anti-mouse IgG antibody conjugated to horseradish peroxidase (HRP). For detection of BfmS protein, anti-BfmS polyclonal antibody prepared by immunizing a rabbit with an N-terminal 6His-tagged periplasmic segment (residues 34-154) of BfmS (Shanghai Immune Biotech CO., Ltd) and an anti-rabbit IgG antibody conjugated to horseradish peroxidase (HRP) (Code#: NA934, GE Healthcare) were used. For detection of RNAP protein, anti-RNAP (Neoclone, #WP003) antibody and anti-mouse IgG antibody conjugated to horseradish peroxidase (HRP) (Code#: NA931, GE Healthcare). For detection of ClpP, anti-ClpP polyclonal antibody prepared by immunizing a rabbit with a *P. aeruginosa* N-terminal 6His-tagged full-length ClpP protein (Sangon Biotech Co., Ltd.) and an anti-rabbit IgG antibody conjugated to horseradish peroxidase (HRP) (Code#: NA934, GE Healthcare) were used. For detection of PA2480, anti-PA2480 polyclonal antibody prepared by immunizing a rabbit with ploypeptides of *P. aeruginosa* PA2480 (96-112aa) (Wuhan ABclonal Biotechnology Co., Ltd) and an anti-rabbit IgG antibody conjugated to horseradish peroxidase (HRP) (Code#: NA934, GE Healthcare) were used.

Bacterial two-hybrid assays

The Euromedex bacterial two-hybrid system (Cat #: EUK001), consisting of two compatible plasmids, pKT25 and pUT18C, were designed to investigate GtrS-BfmR interactions in vivo. The pKT25 and pUT18C plasmids allow the creation of in-frame fusions of the T25 and T18 catalytic domains of *Bordetella pertussis* adenylate cyclase with GtrS and BfmR.

For generating pKT25 derivative pKT25-*gtrS*, GtrS gene was amplified by PCR from MPAO1 genomic DNA using primer pair T25-*gtrS*-F/T25-*gtrS*-R (*Bam*HI/*Kpn*I sites), and then ligated into the same sites of pKT25. In the resultant plasmid pKT25-*gtrS*, the full length *gtrS* is inserted immediately downstream of the N-terminus of T25 in pKT25, creating a single hybrid gene (*T25-gtrS*) that encodes the target protein at the C-terminus and the T25 domain at the N-terminus. For generating pKT25 derivative pKT25-*gtrS-bfmS*^{DK2}, a ~1.4 kb PCR product covering 20 bp of the *bfmS* upstream region and the *bfmS*^{DK2} was amplified from DK2 genomic DNA using primers *bfmS*-comp-2F (with *Kpn*I site) and *bfmS*-comp-2R (with *Eco*RI site), and the PCR products were cloned into plasmid pKT25-*gtrS*. In the resultant plasmid pKT25-*gtrS-bfmS*^{DK2}, the *bfmS*^{DK2} gene is inserted downstream of the hybrid T25-

gtrS and the direction of its transcription is in the same orientation as the *lac* on pKT25. For generating pUT18C derivative pUT18C-*bfmR*, primer pair T18C-*bfmR*-F/T18C-*bfmR*-R (*Bam*HI/*Eco*RI sites) were used to amplify *bfmR* from MPAO1 genomic DNA, and the PCR products were cloned into pUT18C, creating a single hybrid gene that encodes the BfmR protein at the C-terminus and the T18 domain at the N-terminus. The primers used for PCRs are listed in table S2, and all constructs were sequenced to ensure that no unwanted mutations resulted.

To test the possible interaction between two proteins, a pKT25 derivative and a pUT18C derivative were co-transformed by electroporation into the adenylate cyclase-deficient *E. coli* strain, BTH101. Transformants were selected using kanamycin (50 µg/ml) and ampicillin (100 µg/ml) on LB agar plates, and were subsequently inoculated onto the M63/maltose agar plates supplemented with kanamycin (25 µg/ml), ampicillin (50 µg/ml), X-gal (40 µg/ml), and IPTG (0.5 mM), incubated at 30°C for up to 6 days. The appearance of (blue) colonies indicated positive interactions between the target proteins. Protein-protein interaction was also detected by measuring the β-galactosidase activities in bacteria grown in LB broth containing kanamycin (50 µg/ml), ampicillin (100 µg/ml), and 1 mM IPTG at 37°C for 6 h and 12 h, according to BACTH system procedure.

Isolation of cytoplasmic membrane proteins

Overnight *P. aeruginosa* LB cultures were washed twice and diluted 50-fold in M8-glutamate minimal medium supplemented with 10 mM glucose. The liquid cultures (20 ml) were grown in a 100-ml flask shaking with 250 rpm at 37°C for 6 h ($OD_{600} \approx 0.5$), the cultures were harvested by centrifugation at 5,000 g for 10 min at 4 °C, suspended in lysis buffer (20 mM Tris-Cl, pH 8.0; 50mM NaCl, 1mM DTT) supplied with 1 X protease inhibitor cocktail (ThermoFisher, Cat#: 78430), and lysed by sonication. Unbroken cells were removed by centrifugation at 5,000 g for 20 min at 4 °C and membranes were pelleted by centrifugation at 100,000 g for 1 h at 4 °C. The inner membrane was solubilized by adding sodium N-lauroylsarcosinate to the suspension at a final concentration of 1 % and incubating for 30 min at room temperature and the outer membrane was removed by centrifugation at 40,000 g for 40 min at 4 °C. The whole cell proteins and inner membrane proteins were analysed by 10 % (w/v) SDS-PAGE.

Monitoring gene expression by *lux*-based reporters

The plasmids mini-CTX-*lux* (carrying a promoterless *luxCDABE* reporter gene cluster, table S1) was used to construct promoter-*luxCDABE* reporter fusions *pa4103-lux*. To this end, the *pa4103* promoter region (−659 to +19 of the start codon) was

amplified by PCR using the primers pro-pa4103-F (with *Xho*I site) and pro-pa4103-R (with *Bam*HI site) and cloned into the *Xho*I and *Bam*HI sites of the mini-CTX-lux (table S1) to generate mini-CTX-*pa4103-lux*. The resulting plasmid was conjugated into *P. aeruginosa* strains and the construct was integrated into the *attB* site as described previously through a diparental mating using *E. coli* S17 λ -pir as the donor. In MPAO1 and its derivatives, parts of the mini-CTX-lux vector containing the tetracycline resistance cassette were deleted using a flippase (FLP) recombinase encoded on the pFLP2 plasmid. The plasmid pMS402 was used to construct promoter-*luxCDABE* reporter fusions of the *gltB* as described previously (24). Briefly, the *gltB* promoter region (-740 to +18 of the start codon) was amplified by PCR using the primers pro-pa3190-F (with *Xho*I site) and pro-pa3190-R (with *Bam*HI site). All the promoters are oriented in the same direction as *luxCDABE*, and constructs were sequenced to ensure that no unwanted mutations resulted.

Unless noted otherwise, the expression of promoter fusion genes was measured in M8-glutamate minimal medium supplemented with 2 mM glucose in a 96-well black-wall clear-bottom plate (Corning incorporated, Costar, Code#:3603). Briefly, overnight LB cultures were washed twice and diluted to an OD₆₀₀ of 0.05 in the minimal medium, and then a 100 μ l volume of the sample was added to the wells, and subsequently a 60 μ l volume of filter-sterilized mineral oil was added in order to prevent evaporation during the assay. Promoter activities were measured as counts per second (CPS) of light production with a Synergy 2 Multi-Mode Microplate Reader as described previously (24, 50). Additionally, the expression of promoter fusion genes was also carried out using a tube culture method, as indicated. In the tube culture method, bacteria were grown in a 20 ml tube with a flask volume-to-medium volume ratio of 5:1. After incubation at 37°C with shaking (250 rpm) for the indicated times, a 100 μ l volume of the sample was added to the well of a 96-well black-wall clear-bottom plate (Corning incorporated, Costar, Code#:3603) in order to measure the CPS of light production. Each sample was tested in triplicate. Relative light units were calculated by normalizing CPS to OD₆₀₀.

Analysis of *bfmRS* transcripts by RT-PCR

The total DNase-treated RNA (0.1 μ g) was reversely transcribed to synthesize cDNA using the PrimeScript RT reagent Kit (Takara) with Random 6 mers primer according to the manufacturer's protocol. PCR amplified using primers F (anneals 311 bp upstream of the *bfmR* stop codon) and R (anneals 183 bp downstream of *bfmS* start codon) or primers F and 2R (anneals 741 bp downstream of *bfmS* start codon). The reaction was carried out using an OneStep reverse transcription-PCR (RT-PCR) kit (Qiagen, Code#: 210212) according to the manufacturer's instructions. The RT-PCR products were then analyzed by electrophoresis through 1 % agarose gel.

Analysis of microarray expression data of DK2 isolates

Two microarray expression data sets obtained from the online NCBI Gene Expression Omnibus (GEO) Database with the accession numbers GSE31227 and GSE62970 were used. In data set GSE31227, the transcriptomes of sixteen DK2 isolates, including twelve DK2 late stage isolates (that are, CF30-1979, CF173-1984, CF333-1991, CF66-1992, CF333-1997, CF173-2002, CF243-2002, CF333-2003, CF173-2005, CF333-2005, CF333-2007, and CF66-2008) and four DK2 early stage isolates (CF43-1973, CF66-1973, CF105-1973, and CF114-1973) have been measured at exponential growth phase in LB medium (26, 55). To identify evolved gene expression changes in DK2, we compared the transcriptomes of twelve DK2 late stage isolates (12 triplicate samples) to those of three DK2 early isolates (CF43-1973, CF105-1973, and CF114-1973; 3 triplicate samples), and a fold change ≥ 3 and $P < 0.01$ by paired Student's *t*-test was used as threshold to determine significant differentially expressed genes (DEGs). Meanwhile, we compared the transcriptomes of the twelve DK2 late stage isolates to those of the non-CF-adapted isolate PAO1 strain, respectively. The transcriptome of the early stage isolate CF66-1973 was not used in our analysis, since this isolate may belong to the group of adapted isolates, given that it has two mutations located in the genes *rpoN* and *mucA* and these mutations are common to the adapted isolates and they are associated with an adapted phenotype (9, 26, 37, 55).

We also compared the gene expression profiles of DK2-91 and DK2-07 to that of DK2-WT, based on the data set GSE62970, respectively, and a fold change ≥ 3 and $P < 0.01$ by paired Student's *t*-test was used as threshold to determine significant DEGs as described above. Data set GSE62970 contains gene expression data of triplicate analysis of three DK2 isolates (DK2-WT, DK2-91 and DK2-07) grown *in vitro* in glucose minimal medium. Among them, DK2-91 and DK2-07 are late stage isolates isolated from the same patient in 1991 and 2007, respectively, while DK2-WT resembles a non-adapted isolate.

RNA isolation, RNA-Seq, and RNA-Seq data analysis

Overnight cultures of WT *P. aeruginosa* MPAO1 strain and its derivatives, including $\Delta bfmS$, $\Delta bfmS\Delta gtrS$, $bfmS^{DK2}$, $bfmS^{DK2}\Delta gtrS$, and $\Delta bfmRS$ mutants, were washed and diluted 50-fold in M8-glutamate minimal medium supplemented with 10 mM glucose. 20 ml liquid cultures were grown in a 100 ml flask at 37 °C, shaking with 250 rpm for 6 h. Total RNA was immediately stabilized with RNA protect Bacteria Reagent (Qiagen, CAS#:76506) and then extracted by using a Qiagen RNeasy kit (Cat#:74104) following the manufacturer's instructions. rRNA removal, cDNA library construction, and paired-end sequencing with the Illumina HiSeq™ 2000 were completed by Guangdong Magigene Biotechnology Co., Ltd. The edgeR software package (56) was utilized to detect DEGs. A fold change ≥ 2 and $FDR \leq 0.05$ (edgeR, Benjamini-Hochberg's method) was used as threshold to determine the DEGs. All RNA-seq data (three independent biological replicates for each sample) have been submitted to the NCBI Sequence Read Archive (SRA)

(<https://submit.ncbi.nlm.nih.gov/subs/>) under the BioProject accession PRJNA597232, with the following BioSample accession numbers: SAMN13674998 to SAMN13675015 (RNA-Seq reviewer link: <https://dataview.ncbi.nlm.nih.gov/object/PRJNA597232?reviewer=9s5fsoe8meocidstu02krmtm52>).

Generating *bfmS* natural alleles

The QuickChange site-directed mutagenesis kit (Stratagene, Catalog#:200518) was used to generate mutated versions of *bfmS*. For generating A21G, A281T, A42E, A4T, D295N, E376Q, F31L, G179D, G347D, G399D, I178N, L163V, L164F, L168-d, L168-L, L181P, L181Q, L184P, Q241R, Q92E, R393H, T120K, T242R, V278M, V380A, and Y280H, primer pairs BfmS(A21G)F/BfmS(A21G)R, BfmS(A281T)F/BfmS(A281T)R, BfmS(A42E)F/BfmS(A42E)R, BfmS(A4T)F/BfmS(A4T)R, BfmS(D295N)F/BfmS(D295N)R, BfmS(E376Q)F/BfmS(E376Q)R, BfmS(F31L)F/BfmS(F31L)R, BfmS(G179D)F/BfmS(G179D)R, BfmS(G347D)F/BfmS(G347D)R, BfmS(G399D)F/BfmS(G399D)R, BfmS(I178N)F/BfmS(I178N)R, BfmS(L163V)F/BfmS(L163V)R, BfmS(L164F)F/BfmS(L164F)R, BfmS(L168-d)F/BfmS(L168-d)R, BfmS(L168-L)F/BfmS(L168-L)R, BfmS(L181P)F/BfmS(L181P)R, BfmS(L181Q)F/BfmS(L181Q)R, BfmS(L184P)F/BfmS(L184P)R, BfmS(Q241R)F/BfmS(Q241R)R, BfmS(Q92E)F/BfmS(Q92E)R, BfmS(R393H)F/BfmS(R393H)R, BfmS(T120K)F/BfmS(T120K)R, BfmS(T242R)F/BfmS(T242R)R, BfmS(V278M)F/BfmS(V278M)R, BfmS(V380A)F/BfmS(V380A)R, and BfmS(Y280H)F/BfmS(Y280H)R (Table S1) were used, respectively. When required, iteratively reconstruction is used to generate *bfmS* variants that contains multiple site mutations. The primers used for PCRs are listed in table S2, and all constructs were sequenced to ensure that no unwanted mutations resulted.

Bioassay of C4-HSL activity

The autoinducer of the *rhl* system, C4-HSL, was measured using pDO100 (pKD-*rhlA*), which is an *rhlA* promoter-based *P. aeruginosa* strain. This detection system was developed by fusing the C4-HSL-responsive *rhlA* promoter upstream of *luxCDABE* and introducing the construct into pDO100, an *rhlI* mutant strain (57). For preparation of the sample, *P. aeruginosa* cells were grown in PB medium at 37°C with shaking (250 rpm) in a 20-ml tube (with a flask volume-to-medium volume ratio of 5:1) for indicated time, and then 1 ml bacterial culture was centrifuged and sterilized by using a 0.22 µm pore size filter.

The reporter strain pDO100 (pKD-*rhlA*) was grown in LB medium plus 100

µg/ml kanamycin overnight at 37°C with shaking (250 rpm) and diluted to an OD₆₀₀ of 0.05 in fresh LB plus kanamycin, and subsequently, 90 µl was added to the wells of a 96-well black-wall clear-bottom plate (Corning incorporated, Costar). A 10 µl portion of the samples or medium control was added to the wells than gently blending, at last 60 µl volume of filter-sterilized mineral oil was added in order to prevent evaporation during the assay. The luminescence value was measured in a Synergy 2 Multi-Mode Microplate Reader, and calculated from the luminescence value minus that of the medium control. In this assay, the growth curves of pDO100 (pKD-*rhlA*) are identical, and CPS values became an indirect measure of the supernatant C4-HSL.

Measurement of pyocyanin production.

Pyocyanin was extracted from culture supernatants and measured using previously reported methods (24). *P. aeruginosa* DK2 and its derivatives were grown in PB medium, cultures were diluted down to a final OD₆₀₀ of 0.05 in fresh PB medium and 3 ml of this suspension was added to 18 mm X 200 mm (18 in width and 200 in length) glass tubes at 37 °C with shaking (250 rpm) for 12 h, then 3 ml culture was centrifuged and filtered (pore size, 0.22 µm). 1.5 ml of chloroform was added to 2.5 ml of culture supernatant. After extraction, the chloroform layer was transferred to a fresh tube and mixed with 1 ml of 0.2 N HCl. After centrifugation, the top layer (0.2 M HCl) was removed and its absorption measured at 520 nm. Concentrations, expressed as micrograms of pyocyanin produced per ml of culture supernatant, were determined by multiplying the optical density at 520 nm (OD₅₂₀) by 17.072.

Biofilm formation assays

The biofilm formation by MPAO1 and its derivatives were assayed by determining the ability of the cells to adhere to the wells of polystyrene Stripwell™ Microplate (1 X 8 Flat Bottom; Corning incorporated, Costar, Code#: 42592) as previously described with some modifications (58). Briefly, an overnight PB culture was diluted down to a final OD₆₀₀ of 0.05 in fresh PB medium and dispensed at 100 µl per well. Inoculated plates were incubated under static conditions at 37°C for 72 h. Biofilm formation by DK2 and its derivatives was measured in 20 ml glass tubes (Code#: 95-3, Haimen). The overnight PB culture was diluted down to a final OD₆₀₀ of 0.05 in fresh PB medium and 3 ml of this suspension was added to 18 mm X 200 mm (18 in width and 200 in length) glass tubes, which were incubated statically at 37°C for 72 h. In order to measure the degree of attachment, non-adhered cells were removed and the biofilms rinsed with distilled water. Biofilms were stained by the addition of 150 µl (or 5 ml to the tubes) of 1% crystal violet (Cat#: 3603, Sigma-Aldrich) for 15 min followed by rinsing with distilled water. Photos were taken and the cell-associated

dye was solubilized in 150 μ l (or 4.5 ml to the tubes) of 30% acetic acids in water and quantified by measuring the OD₅₅₀ of the resulting solution.

Lettuce leaf model of infection.

A lettuce leaf virulence assay was performed as described previously (24, 50). *P. aeruginosa* strains were grown overnight at 37°C with shaking (250 rpm) in PB broth, washed, resuspended and diluted in sterile 10 mM MgSO₄ to a bacterial density of 1×10^8 CFU/ml. Lettuce leaves were prepared by washing with sterile distilled H₂O and 0.1% bleach. Samples (10 μ l) were then inoculated into the midribs of Romaine lettuce leaves. Containers containing Whatman paper moistened with 10 mM MgSO₄ and inoculated leaves were kept in a growth chamber at 37°C for five days. Symptoms were monitored daily.

***Drosophila* infection assays**

Drosophila melanogaster (male, aged of 5 ± 1 days) were infected by needle pricking according to the protocol previously described (59) with some modifications. Overnight PB cultures of *P. aeruginosa* were diluted 100-fold in fresh PB medium. The liquid cultures were grown in a 20-ml tube with a volume-to medium ratio of 5:1, shaking with 250 rpm at 37°C for 3 h (OD₆₀₀ \approx 0.7). The cell pellets from 1 ml of culture medium were rinsed once and resuspended in 1 X PBS, at a final OD₆₀₀ of 0.3. The flies were anesthetized using carbon dioxide and prick in the dorsal thorax using a sterilized tungsten needle dipped in the appropriate bacterial suspension. The pricked flies were returned to the fly-food vial, kept at 25°C and 65% humidity. At least twelve control flies were also pricked with a solution of 1 X PBS (survival rates 4 days after wounding were between 92% and 100%). Fly survival was scored and survival curves were processed with GraphPad Prism 5 (GraphPad Software, Inc., San Diego, CA) to perform a statistical log-rank (Mantel-Cox) test.

Statistical analysis.

The log-rank test was used for survival analysis. Student's *t*-tests (two-tailed) and Mann-Whitney U test were used to compare two data sets.

Supplementary Materials

Fig. S1. The promoter activities of *bfmR* in MPAO1 and its derivatives.
Fig. S2. Consequences of either *bfmS* missense mutations or *bfmR* deletion.
Fig. S3. Identification of genes involved in activating BfmR.
Fig. S4. Glucose increases the regulatory activity of GtrS.
Fig. S5. Phosphorylation of BfmR and its variant, and co-immunoprecipitation.
Fig. S6. Bacterial two-hybrid assays showing GtrS-BfmR interactions.
Fig. S7. Sequence alignment of the histidine kinases BfmS, GtrS, EnvZ, and HK853.
Fig. S8. Promoter fusion analysis and the phosphorylation assays.
Fig. S9. Pro-Q Diamond staining and surface plasmon resonance (SPR) assays.
Fig. S10. Role of natural *bfmS* variants in BfmR activation.
Fig. S11. Dephosphorylation of BfmR~P by SUMO-BfmSc and its variants.

Table S1. Plasmids and bacterial strains and used in this study

Table S2. Primers used in this study.

Table S3. *bfmS* variants *P. aeruginosa* CF isolates.

Data file 1. Microarray data analysis of DK2

Data file 2. RNA-seq analysis

References and Notes:

1. C. K. Stover *et al.*, Complete genome sequence of *Pseudomonas aeruginosa* PAO1, an opportunistic pathogen. *Nature* **406**, 959-964 (2000) .
2. M. D. Parkins, R. Somayaji, V. J. Waters, Epidemiology, Biology, and Impact of Clonal *Pseudomonas aeruginosa* Infections in Cystic Fibrosis. *Clin Microbiol Rev* **31**, (2018) .
3. J. W. Costerton, P. S. Stewart, E. P. Greenberg, Bacterial biofilms: a common cause of persistent infections. *Science* **284**, 1318-1322 (1999) .
4. S. C. Langton Hwer, A. R. Smyth, Antibiotic strategies for eradicating *Pseudomonas aeruginosa* in people with cystic fibrosis. *Cochrane Database Syst Rev* **4**, CD004197 (2017) .
5. A. Folkesson *et al.*, Adaptation of *Pseudomonas aeruginosa* to the cystic fibrosis airway: an evolutionary perspective. *Nat Rev Microbiol* **10**, 841-851 (2012) .
6. C. Winstanley, S. O'Brien, M. A. Brockhurst, *Pseudomonas aeruginosa* Evolutionary

- Adaptation and Diversification in Cystic Fibrosis Chronic Lung Infections. *Trends Microbiol* **24**, 327-337 (2016) .
7. X. Didelot, A. S. Walker, T. E. Peto, D. W. Crook, D. J. Wilson, Within-host evolution of bacterial pathogens. *Nat Rev Microbiol* **14**, 150-162 (2016) .
 8. E. E. Smith *et al.*, Genetic adaptation by *Pseudomonas aeruginosa* to the airways of cystic fibrosis patients. *Proc Natl Acad Sci U S A* **103**, 8487-8492 (2006) .
 9. L. Yang *et al.*, Evolutionary dynamics of bacteria in a human host environment. *Proc Natl Acad Sci U S A* **108**, 7481-7486 (2011) .
 10. D. W. Martin *et al.*, Mechanism of conversion to mucoidy in *Pseudomonas aeruginosa* infecting cystic fibrosis patients. *Proc Natl Acad Sci U S A* **90**, 8377-8381 (1993) .
 11. J. Klockgether, N. Cramer, S. Fischer, L. Wiehlmann, B. Tummler, Long-Term Microevolution of *Pseudomonas aeruginosa* Differs between Mildly and Severely Affected Cystic Fibrosis Lungs. *Am J Respir Cell Mol Biol* **59**, 246-256 (2018) .
 12. R. L. Marvig, H. K. Johansen, S. Molin, L. Jelsbak, Genome analysis of a transmissible lineage of *pseudomonas aeruginosa* reveals pathoadaptive mutations and distinct evolutionary paths of hypermutators. *PLoS Genet* **9**, e1003741 (2013) .
 13. T. Markussen *et al.*, Environmental heterogeneity drives within-host diversification and evolution of *Pseudomonas aeruginosa*. *MBio* **5**, e01592-01514 (2014) .
 14. R. L. Marvig, L. M. Sommer, S. Molin, H. K. Johansen, Convergent evolution and adaptation of *Pseudomonas aeruginosa* within patients with cystic fibrosis. *Nat Genet* **47**, 57-64 (2015) .
 15. N. Cramer *et al.*, Microevolution of the major common *Pseudomonas aeruginosa* clones C and PA14 in cystic fibrosis lungs. *Environ Microbiol* **13**, 1690-1704 (2011) .

16. B. A. Wee *et al.*, Whole genome sequencing reveals the emergence of a *Pseudomonas aeruginosa* shared strain sub-lineage among patients treated within a single cystic fibrosis centre. *BMC Genomics* **19**, 644 (2018) .
17. M. T. Laub, M. Goulian, Specificity in two-component signal transduction pathways. *Annu Rev Genet* **41**, 121-145 (2007) .
18. A. M. Stock, V. L. Robinson, P. N. Goudreau, Two-component signal transduction. *Annu Rev Biochem* **69**, 183-215 (2000) .
19. B. L. Wanner, Is cross regulation by phosphorylation of two-component response regulator proteins important in bacteria? *J Bacteriol* **174**, 2053-2058 (1992) .
20. K. R. Guckes *et al.*, Strong cross-system interactions drive the activation of the QseB response regulator in the absence of its cognate sensor. *Proc Natl Acad Sci U S A* **110**, 16592-16597 (2013) .
21. K. R. Guckes *et al.*, Signaling by two-component system noncognate partners promotes intrinsic tolerance to polymyxin B in uropathogenic *Escherichia coli*. *Sci Signal* **10**, (2017) .
22. O. E. Petrova, K. Sauer, A novel signaling network essential for regulating *Pseudomonas aeruginosa* biofilm development. *PLoS Pathog* **5**, e1000668 (2009) .
23. O. E. Petrova, J. R. Schurr, M. J. Schurr, K. Sauer, The novel *Pseudomonas aeruginosa* two-component regulator BfmR controls bacteriophage-mediated lysis and DNA release during biofilm development through PhdA. *Mol Microbiol* **81**, 767-783 (2011) .
24. Q. Cao *et al.*, A novel signal transduction pathway that modulates rhl quorum sensing and bacterial virulence in *Pseudomonas aeruginosa*. *PLoS Pathog* **10**, e1004340 (2014) .
25. E. Kinoshita, E. Kinoshita-Kikuta, K. Takiyama, T. Koike, Phosphate-binding tag, a new tool to

- visualize phosphorylated proteins. *Mol Cell Proteomics* **5**, 749-757 (2006) .
26. L. Yang *et al.*, Bacterial adaptation during chronic infection revealed by independent component analysis of transcriptomic data. *BMC Microbiol* **11**, 184 (2011) .
27. M. H. Rau, R. L. Marvig, G. D. Ehrlich, S. Molin, L. Jelsbak, Deletion and acquisition of genomic content during early stage adaptation of *Pseudomonas aeruginosa* to a human host environment. *Environ Microbiol* **14**, 2200-2211 (2012) .
28. S. M. Cuskey, P. V. Phibbs, Jr., Chromosomal mapping of mutations affecting glycerol and glucose catabolism in *Pseudomonas aeruginosa* PAO. *J Bacteriol* **162**, 872-880 (1985) .
29. A. E. Sage, W. D. Proctor, P. V. Phibbs, Jr., A two-component response regulator, *gltR*, is required for glucose transport activity in *Pseudomonas aeruginosa* PAO1. *J Bacteriol* **178**, 6064-6066 (1996) .
30. A. Daddaoua, C. Molina-Santiago, J. de la Torre, T. Krell, J. L. Ramos, *GtrS* and *GltR* form a two-component system: the central role of 2-ketogluconate in the expression of exotoxin A and glucose catabolic enzymes in *Pseudomonas aeruginosa*. *Nucleic Acids Res* **42**, 7654-7663 (2014) .
31. J. O'Callaghan *et al.*, A novel host-responsive sensor mediates virulence and type III secretion during *Pseudomonas aeruginosa*-host cell interactions. *Microbiology* **158**, 1057-1070 (2012) .
32. S. Tamber, R. E. Hancock, On the mechanism of solute uptake in *Pseudomonas*. *Front Biosci* **8**, s472-483 (2003) .
33. J. M. Skerker *et al.*, Rewiring the specificity of two-component signal transduction systems. *Cell* **133**, 1043-1054 (2008) .

34. P. Casino, V. Rubio, A. Marina, Structural insight into partner specificity and phosphoryl transfer in two-component signal transduction. *Cell* **139**, 325-336 (2009) .
35. T. Spilker, J. J. LiPuma, Draft Genome Sequences of 63 *Pseudomonas aeruginosa* Isolates Recovered from Cystic Fibrosis Sputum. *Genome Announc* **4**, (2016) .
36. J. J. Bijlsma, E. A. Groisman, Making informed decisions: regulatory interactions between two-component systems. *Trends Microbiol* **11**, 359-366 (2003) .
37. S. Damkiaer, L. Yang, S. Molin, L. Jelsbak, Evolutionary remodeling of global regulatory networks during long-term bacterial adaptation to human hosts. *Proc Natl Acad Sci U S A* **110**, 7766-7771 (2013) .
38. Z. D. Blount, J. E. Barrick, C. J. Davidson, R. E. Lenski, Genomic analysis of a key innovation in an experimental *Escherichia coli* population. *Nature* **489**, 513-518 (2012) .
39. E. H. Baker, D. L. Baines, Airway Glucose Homeostasis: A New Target in the Prevention and Treatment of Pulmonary Infection. *Chest* **153**, 507-514 (2018) .
40. J. S. Tregoning, P. Mallia, Modulating airway glucose to reduce respiratory infections. *Expert Rev Respir Med* **13**, 121-124 (2019) .
41. P. Mallia *et al.*, Role of airway glucose in bacterial infections in patients with chronic obstructive pulmonary disease. *J Allergy Clin Immunol* **142**, 815-823 e816 (2018) .
42. P. P. Alva, R. Prasad, T. Venkatesh, P. S. Suresh, R. Premanath, Increased virulence in *Pseudomonas aeruginosa* at pathological glucose levels. *Infect Dis (Lond)* **51**, 153-156 (2019) .
43. P. J. Wittkopp, B. K. Haerum, A. G. Clark, Evolutionary changes in cis and trans gene regulation. *Nature* **430**, 85-88 (2004) .

44. O. Lamrabet *et al.*, Plasticity of Promoter-Core Sequences Allows Bacteria to Compensate for the Loss of a Key Global Regulatory Gene. *Mol Biol Evol* **36**, 1121-1133 (2019) .
45. I. Necedal, A. D. Johnson, How Transcription Networks Evolve and Produce Biological Novelty. *Cold Spring Harb Symp Quant Biol* **80**, 265-274 (2015) .
46. T. Hindre, C. Knibbe, G. Beslon, D. Schneider, New insights into bacterial adaptation through in vivo and in silico experimental evolution. *Nat Rev Microbiol* **10**, 352-365 (2012) .
47. H. D. Kulasekara *et al.*, A novel two-component system controls the expression of *Pseudomonas aeruginosa* fimbrial cup genes. *Molecular microbiology* **55**, 368-380 (2005) .
48. A. Becher, H. P. Schweizer, Integration-proficient *Pseudomonas aeruginosa* vectors for isolation of single-copy chromosomal lacZ and lux gene fusions. *Biotechniques* **29**, 948-950, 952 (2000) .
49. T. T. Hoang, R. R. Karkhoff-Schweizer, A. J. Kutchma, H. P. Schweizer, A broad-host-range Flp-FRT recombination system for site-specific excision of chromosomally-located DNA sequences: application for isolation of unmarked *Pseudomonas aeruginosa* mutants. *Gene* **212**, 77-86 (1998) .
50. N. Yang *et al.*, The Crc protein participates in down-regulation of the Lon gene to promote rhamnolipid production and rhl quorum sensing in *Pseudomonas aeruginosa*. *Mol Microbiol* **96**, 526-547 (2015) .
51. I. Jansons *et al.*, Deletion and transposon mutagenesis and sequence analysis of the pRO1600 OriR region found in the broad-host-range plasmids of the pQF series. *Plasmid* **31**, 265-274 (1994) .
52. N. T. Keen, S. Tamaki, D. Kobayashi, D. Trollinger, Improved broad-host-range plasmids for

- DNA cloning in gram-negative bacteria. *Gene* **70**, 191-197 (1988) .
53. Y. Ding *et al.*, Metabolic sensor governing bacterial virulence in *Staphylococcus aureus*. *Proc Natl Acad Sci U S A* **111**, E4981-4990 (2014) .
54. F. Chen *et al.*, Small-molecule targeting of a diapophytoene desaturase inhibits *S. aureus* virulence. *Nat Chem Biol* **12**, 174-179 (2016) .
55. J. C. Thogersen, M. Morup, S. Damkiaer, S. Molin, L. Jelsbak, Archetypal analysis of diverse *Pseudomonas aeruginosa* transcriptomes reveals adaptation in cystic fibrosis airways. *BMC Bioinformatics* **14**, 279 (2013) .
56. M. D. Robinson, D. J. McCarthy, G. K. Smyth, edgeR: a Bioconductor package for differential expression analysis of digital gene expression data. *Bioinformatics* **26**, 139-140 (2010) .
57. H. Liang, J. Duan, C. D. Sibley, M. G. Surette, K. Duan, Identification of mutants with altered phenazine production in *Pseudomonas aeruginosa*. *J Med Microbiol* **60**, 22-34 (2011) .
58. G. A. O'Toole, Microtiter dish biofilm formation assay. *J Vis Exp*, (2011) .
59. Y. Apidianakis, L. G. Rahme, *Drosophila melanogaster* as a model host for studying *Pseudomonas aeruginosa* infection. *Nat Protoc* **4**, 1285-1294 (2009) .
60. K. Duan, C. Dammel, J. Stein, H. Rabin, M. G. Surette, Modulation of *Pseudomonas aeruginosa* gene expression by host microflora through interspecies communication. *Mol Microbiol* **50**, 1477-1491 (2003) .
61. M. A. Jacobs *et al.*, Comprehensive transposon mutant library of *Pseudomonas aeruginosa*. *Proc Natl Acad Sci U S A* **100**, 14339-14344 (2003) .
62. J. Jeukens *et al.*, Comparative genomics of isolates of a *Pseudomonas aeruginosa* epidemic strain associated with chronic lung infections of cystic fibrosis patients. *PLoS One* **9**, e87611

- (2014) .
63. D. Williams *et al.*, Divergent, coexisting *Pseudomonas aeruginosa* lineages in chronic cystic fibrosis lung infections. *American journal of respiratory and critical care medicine* **191**, 775-785 (2015) .
64. S. Naughton *et al.*, *Pseudomonas aeruginosa* AES-1 exhibits increased virulence gene expression during chronic infection of cystic fibrosis lung. *PLoS One* **6**, e24526 (2011) .
65. K. Mathee *et al.*, Dynamics of *Pseudomonas aeruginosa* genome evolution. *Proc Natl Acad Sci U S A* **105**, 3100-3105 (2008) .
66. R. van Mansfeld *et al.*, Within-Host Evolution of the Dutch High-Prevalent *Pseudomonas aeruginosa* Clone ST406 during Chronic Colonization of a Patient with Cystic Fibrosis. *PLoS One* **11**, e0158106 (2016) .
67. J. R. Dettman, N. Rodrigue, S. D. Aaron, R. Kassen, Evolutionary genomics of epidemic and nonepidemic strains of *Pseudomonas aeruginosa*. *Proc Natl Acad Sci U S A* **110**, 21065-21070 (2013) .
68. V. N. Kos *et al.*, The resistome of *Pseudomonas aeruginosa* in relationship to phenotypic susceptibility. *Antimicrobial agents and chemotherapy* **59**, 427-436 (2015) .
69. I. Bianconi *et al.*, Draft Genome Sequences of 40 *Pseudomonas aeruginosa* Clinical Strains Isolated from the Sputum of a Single Cystic Fibrosis Patient Over an 8-Year Period. *Genome announcements* **4**, (2016) .
70. S. Chugani *et al.*, Strain-dependent diversity in the *Pseudomonas aeruginosa* quorum-sensing regulon. *Proc Natl Acad Sci U S A* **109**, E2823-2831 (2012) .
71. A. van Belkum *et al.*, Phylogenetic Distribution of CRISPR-Cas Systems in Antibiotic-Resistant

- Pseudomonas aeruginosa*. *MBio* **6**, e01796-01715 (2015) .
72. A. Penesyan *et al.*, Genetically and Phenotypically Distinct *Pseudomonas aeruginosa* Cystic Fibrosis Isolates Share a Core Proteomic Signature. *PLoS One* **10**, e0138527 (2015) .
73. Y. Yin, T. R. Withers, S. L. Johnson, H. D. Yu, Draft Genome Sequence of a Mucoïd Isolate of *Pseudomonas aeruginosa* Strain C7447m from a Patient with Cystic Fibrosis. *Genome announcements* **1**, (2013) .
74. J. Jeukens *et al.*, Complete Genome Sequence of Persistent Cystic Fibrosis Isolate *Pseudomonas aeruginosa* Strain RP73. *Genome announcements* **1**, (2013) .
75. I. Bianconi *et al.*, Comparative genomics and biological characterization of sequential *Pseudomonas aeruginosa* isolates from persistent airways infection. *BMC genomics* **16**, 1105 (2015) .
76. J. Dingemans *et al.*, The deletion of TonB-dependent receptor genes is part of the genome reduction process that occurs during adaptation of *Pseudomonas aeruginosa* to the cystic fibrosis lung. *Pathogens and disease* **71**, 26-38 (2014) .

Acknowledgements: We thank Professor Lars Jelsbak of Technical University of Denmark for providing *P. aeruginosa* DK2 strain. We thank Professor of John J. LiPuma of University of Michigan Medical School for providing *P. aeruginosa* AU15431 isolate. We appreciate the technical support for RNA-Seq and initial data analysis from Guangdong Magigene Biotechnology Co., Ltd., and surface plasmon resonance (SPR) assay and initial data analysis from Shanghai CFBiotechnology Co., Ltd.. We also thank S.A. Frank, MA for editing the manuscript. **Funding:** This work was supported by grants from the National Natural Science Foundation (NSFC)(grant nos. 31670136, 31870127, 81861138047 and 81661138004 to L.L) and the Ministry of Science and Technology (MOST) (grant no. 2016YFA0501503 to L.L) of China. This study was also funded by the Science and Technology Commission of Shanghai Municipality (grant no. 19JC1416400 to L.L). **Author contributions:** Q.C. and L.L. conceived the study; Q.C. did most experiments. Y.W and X.Z performed some site

mutagenesis experiments. N.Y, C.X, K.F, F.C, H.L., Y.Z, X.D., Y.F, C-G.Y., and M.W. provided technical assistance. L.L. supervised the study. Q.C., T.B, and L.L. analysed the data. L.L. supervised the study and wrote the manuscript with input from Q.C. and T.B. All authors discussed the results and commented on the manuscript. **Competing interests:** All authors have no competing interests. **Data and Materials Availability:** The RNA-seq data have been deposited to to the NCBI Sequence Read Archive (SRA) (<https://submit.ncbi.nlm.nih.gov/subs/>) under the BioProject accession PRJNA597232, with the following BioSample accession numbers: SAMN13674998 to SAMN13675015. All other data needed to evaluate the conclusions in the paper are present in the paper or the Supplementary Materials.

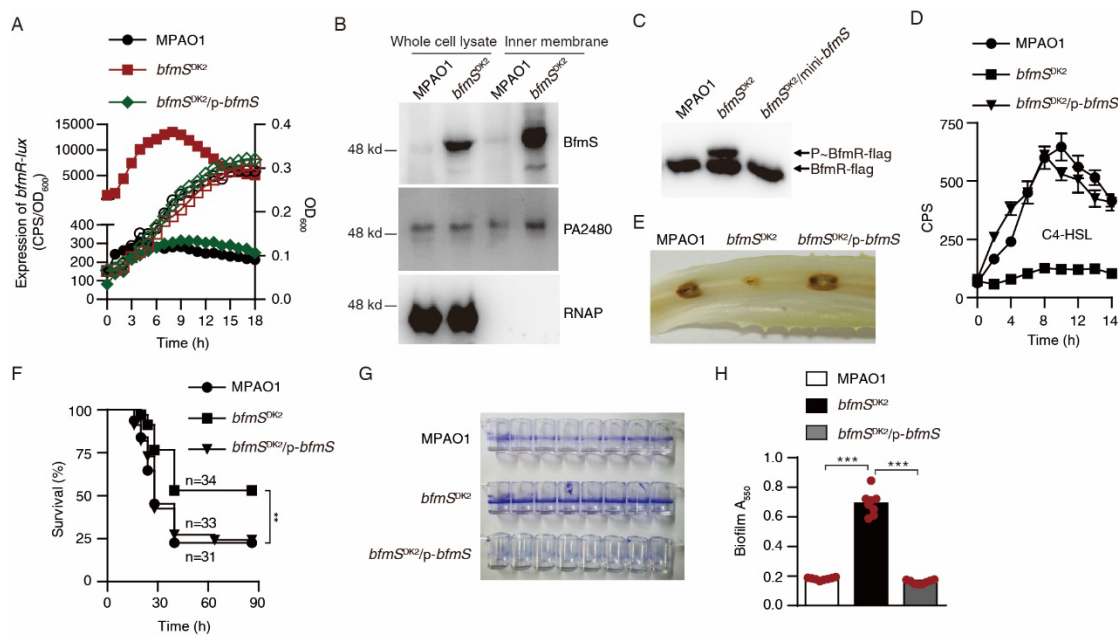


Fig. 1. Consequence of L181P/E376Q missense mutations in *bfmS*. (A) The *bfmR* promoter activity of *P. aeruginosa* strains cultured in 96-well plates containing M8-glutamate minimal medium supplemented with 2 mM glucose. Expression of *bfmR-lux* (CPS, counts per second; closed symbols) were determined at different phases of the cell growth monitored by measuring the optical density at 600 nm (OD₆₀₀; open symbols). Data from n = 6 biological replicates reported as means ± SEM. (B) Western blotting analysis for the production of BfmS and its variant from bacterial whole-cell lysates and purified inner membranes. PA2480 (a predicted membrane-associated histidine kinase of *P. aeruginosa*) and cytoplasmic RNA polymerase (RNAP) alpha subunit are probed as a loading control. Images are representative of two independent experiments. (C) Western blotting analysis for the in vivo

phosphorylation of BfmR analyzed on Phos-tag™ gel. Images are representative of three independent experiments. (D) Relative amounts of C4-HSL produced by *P. aeruginosa* strains grown in pyocyanin production broth (PB medium) at 37°C for 9 h. Data from n = 3 biological replicates reported as means ± SEM. (E) Photograph shows lettuce midrib after 3 days of infection with *P. aeruginosa* cells. Both MPAO1 and *bfmS*^{DK2}/p-*bfmS* strains show necrosis and tissue maceration of infection, and the *bfmS*^{DK2} mutant shows weak signs of infection. Images are representative of three independent experiments. (F) *D. melanogaster* killing by MPAO1 and its derivatives. n indicates the number of flies used. **P < 0.01 (log-rank test; *bfmS*^{DK2} compared with either MPAO1 or *bfmS*^{DK2}/p-*bfmS*). (G and H) Biofilm formation. Photograph in (G) showing ring-shape biofilms (stained by 1% crystal violet) near the air-liquid interface on the inner surface of polystyrene Stripwell™ Microplate with quantification shown in (H), where data from n = 8 biological replicates reported as mean ± SEM (**P < 0.001, Student's two-tailed *t*-test). No statistically significant difference was observed between MPAO1 and *bfmS*^{DK2}/p-*bfmS* strains. In (A, D, E, F, G, and H), MPAO1 and *bfmS*^{DK2} carry an empty pAK1900 vector as control, p-*bfmS* denotes pAK1900-*bfmS* (table S1). In (C), MPAO1 and *bfmS*^{DK2} carry an empty integration-proficient mini-CTX-lacZ vector (table S1) as control.

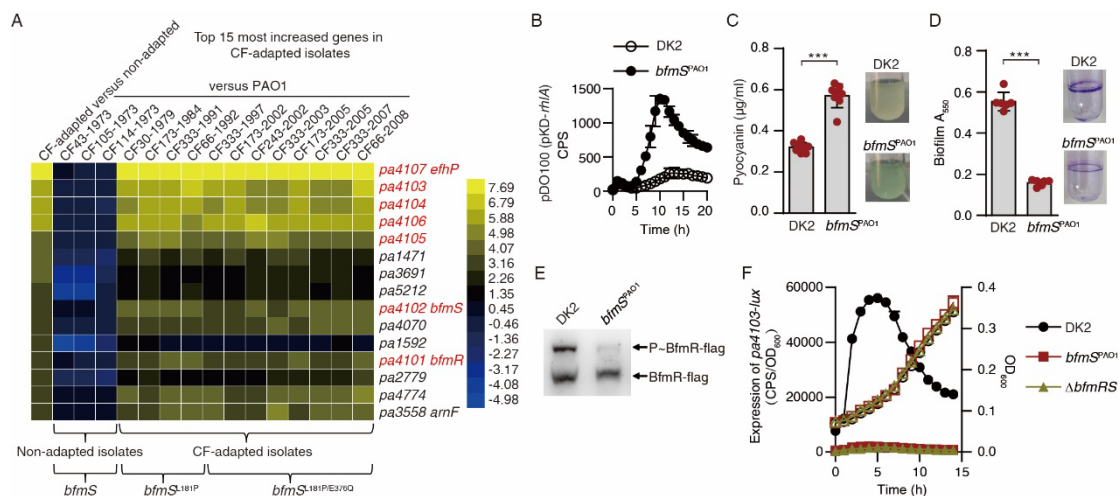


Fig. 2. BfmR is highly activated in the CF-adapted isolates of *P. aeruginosa* DK2 lineage. (A) Heatmaps showing the expression profiles of the top 15 upregulated genes in CF-adapted DK2 isolates with respect to the non-CF-adapted isolates of DK2 lineage. Expression level of gene is represented as log₂ expression ratios (Sheet 1 of Data file 1). (B to F) Effect of L181P/E376Q missense mutations in *bfmS* on the amount of C4-HSL (B), the production of pyocyanin (C), the formation of biofilm (D), the phosphorylation level of BfmR (E), and the expression of *pa4103-lux* (F) of the DK2 strain. In (B), data from n = 3 biological replicates reported as means ± SEM; in (C), data from n = 8 biological replicates reported as mean ± SEM (**P < 0.001, Student's two-tailed *t*-test), and inserted photographs showing the blue-green pigment of *P. aeruginosa* cultures; in (D), data from n = 6 biological replicates

reported as mean \pm SEM (** $P < 0.001$, Student's two-tailed t -test), and inserted photograph showing ring-shape biofilms (stained by 1% crystal violet) near the air-liquid interface on the inner surface of glass tubes. (E) Western blot analysis of in vivo phosphorylation of BfmR-flag analyzed on Phos-tag™ gel. Protein samples are derived from bacteria carrying pRK415-*bfmR*-flag plasmid (table S1). Images are representative of two independent experiments. (F) The promoter activities of *pa4103* (CPS, counts per second; closed symbols) were determined at different phases of the cell growth monitored by measuring the optical density at 600 nm (OD₆₀₀; open symbols). Data represent means \pm SEM of $n = 3$ biological replicates.

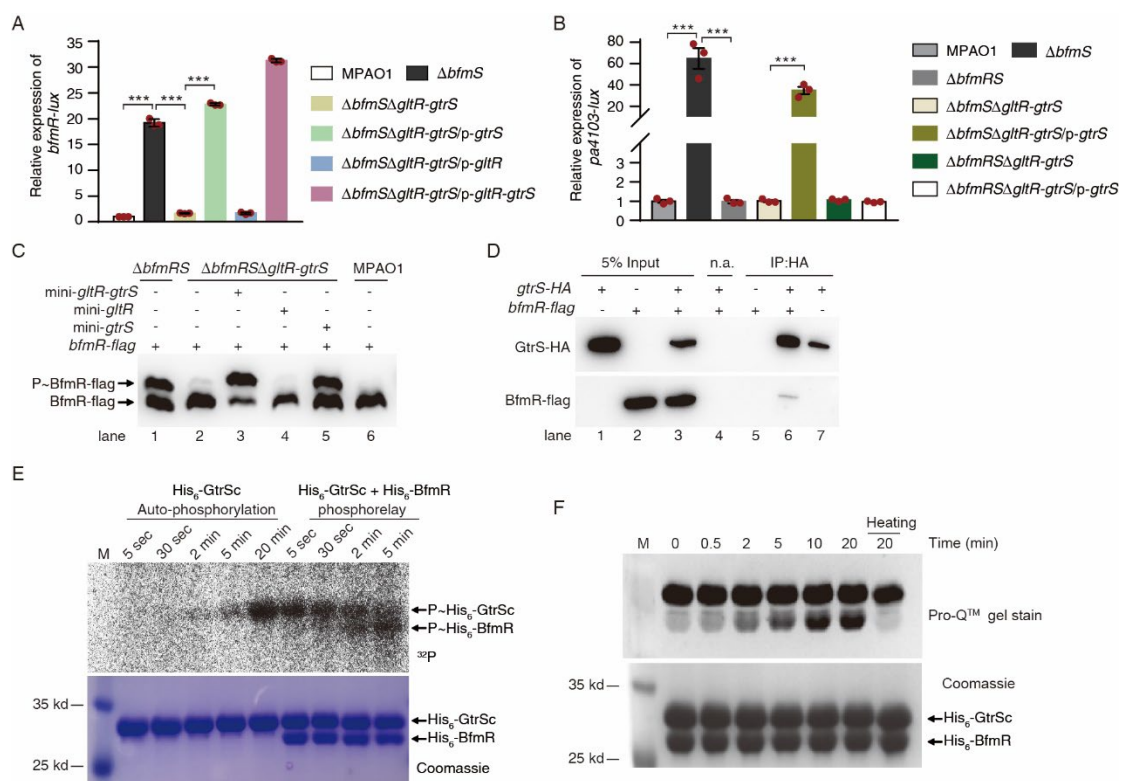


Fig. 3. GtrS forms a TCS with BfmR. (A and B) Relative expression of *bfmR-lux* (A) and *pa4103-lux* (B) when bacteria were grown in tubes containing minimal medium supplemented with 2 mM glucose at 37°C with shaking (250 rpm) for 6 h. The expressions of *bfmR-lux* and *pa4103-lux* in MPAO1 were set to 1, respectively, and the other values were adjusted accordingly, as indicated. In (A) and (B), data represent means \pm SEM of $n = 3$ biological replicates (** $P < 0.001$, Student's two-tailed t -test). In (B), no statistically significant difference was observed between $\Delta bfmRS\Delta gtrR-gtrS$ and $\Delta bfmRS\Delta gtrR-gtrS/p-gtrS$ strains. *P. aeruginosa* strains, MPAO1, $\Delta bfmS$, $\Delta bfmS\Delta gtrR-gtrS$, $\Delta bfmRS$, and $\Delta bfmRS\Delta gtrR-gtrS$ carrying an empty pAK1900 vector as control; *p-gtrS*, *p-gltR*, and *p-gltR-gtrS* denote pAK1900-*gtrS*, pAK1900-*gltR*, and pAK1900-*gltR-gtrS* (table S1), respectively. (C) Western blot analysis of in vivo phosphorylation of BfmR-flag analyzed on Phos-tag™ gel. Images are representative of two independent experiments. (D) Western blot image

showing the Co-immunoprecipitation of GtrS-HA and BfmR-flag. Whole cell extracts from $\Delta bfmS$ mutant expressing *gtrS-HA* (lanes 1, 3, 4, 6, and 7) and/or *bfmR-flag* (lanes 2–6) were immunoprecipitated without (lane 4; n.a.) or with (lanes 5–7) anti-HA antibody. Images are representative of two independent experiments. (E) Autoradiogram showing the auto-phosphorylation and trans-phosphorylation activity of His₆-GtrSc. After auto-phosphorylation of His₆-GtrSc with [γ -³²P]ATP for 20 min, His₆-BfmR was added to the reaction mixtures and samples were taken as indicated time. M, protein marker. Images are representative of two independent experiments. (F) Phosphoprotein detection with Pro-Q Diamond phosphoprotein gel stains showing the phosphorylation of His₆-BfmR by His₆-GtrSc. Aliquots were removed at the indicated time points for analysis by SDS-PAGE, followed by Pro-Q Diamond staining to identify phosphorylation and Coomassie blue staining to detect protein levels. Heating, the sample was exposed to the heating at 100°C for 5 min prior to SDS-PAGE. M, protein markers. Images are representative of three independent experiments.

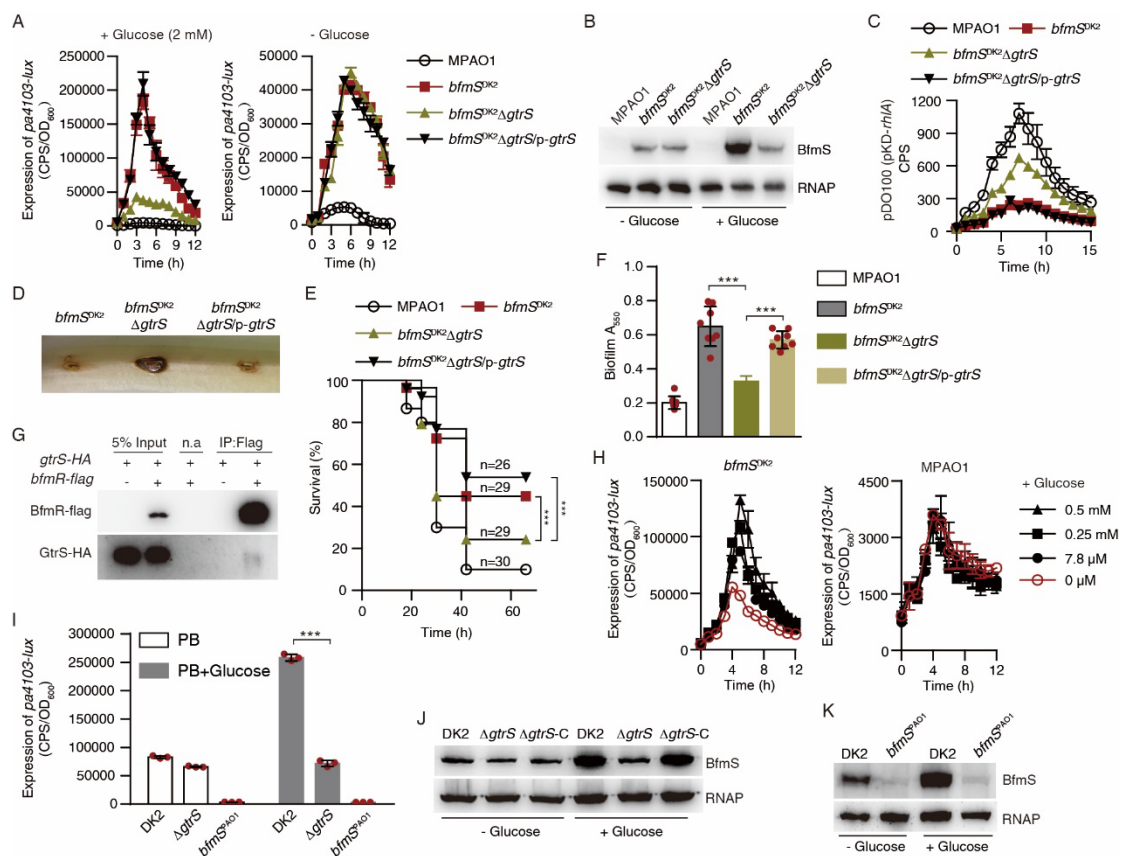


Fig. 4. GtrS activating BfmR when *bfmS* undergoes L181P/E376Q missense mutations. (A) Expression of *pa4103-lux* in MPAO1 and its derivatives cultured in M8-glutamate minimal medium supplemented with or without glucose. Data represent means \pm SEM of $n = 3$ biological replicates. (B) Western blot analysis of the production of BfmS in *P. aeruginosa* strains cultured in tubes containing M8-glutamate minimal medium supplemented with or without glucose at 37°C with

shaking for 6 h. Images are representative of two independent experiments. (C) Relative amounts of C4-HSL. Data represent means \pm SEM of $n = 3$ biological replicates. (D) Photograph shows lettuce midrib after 3 days of infection with *P. aeruginosa* cells. Images are representative of three independent experiments. (E) *D. melanogaster* killing by MPAO1 and its derivatives. n indicates the number of flies used. *** $P < 0.001$ (log-rank test). (F) The adhesion/biofilm formation (A550) by *P. aeruginosa* strains. Data represent means \pm SEM of $n = 8$ biological replicates (*** $P < 0.001$, Student's two-tailed t -test). (G) Western blot images showing the co-immunoprecipitation of GtrS-HA and BfmR-flag. Whole cell extracts from *bfmS*^{DK2} mutant expressing GtrS-HA and/or BfmR-flag were immunoprecipitated without (n.a.) or with (IP: Flag) anti-Flag antibody. Images are representative of two independent experiments. (H) Expression of *pa4103-lux* in *bfmS*^{DK2} and WT MPAO1 cultured in M8-glutamate minimal medium supplemented with or without glucose, as indicated. Data represent means \pm SEM of $n = 3$ biological replicates. (I, J, and K) Expression of *pa4103-lux* (I) and the production of BfmS protein (J and K) in DK2 and its derivatives cultured in PB medium for 6 h. In (I), data represent means \pm SEM of $n = 3$ biological replicates (*** $P < 0.001$, Student's two-tailed t -test). In (J and K), images are representative of two independent experiments. In (A, C, D, E, and F), MPAO1, *bfmS*^{DK2}, and *bfmS*^{DK2} Δ *gtrS* mutants harbor an empty pAK1900 vector as control; p-*gtrS* denotes pAK1900-*gtrS* plasmid (table S1). In (J), DK2 and its isogenic Δ *gtrS* mutant harbor an empty pRK415 plasmid as control. Δ *gtrS*-C denotes Δ *gtrS* mutant carrying a pRK415-*gtrS* plasmid (table S1).

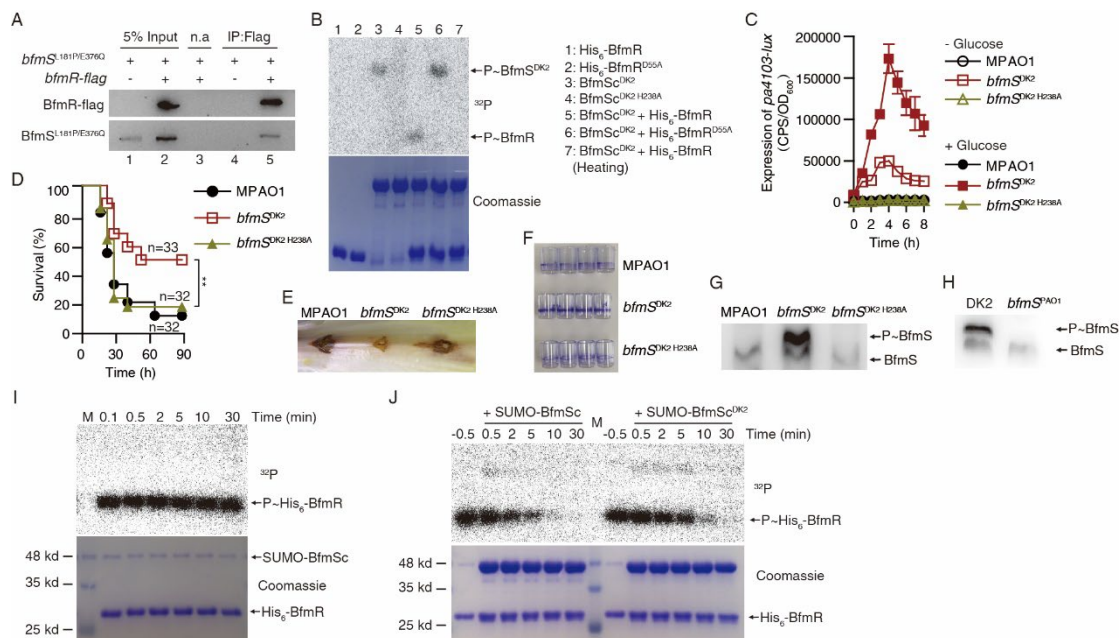


Fig. 5. BfmS^{DK2} activates BfmR in a direct manner. (A) Western blot images showing the Co-immunoprecipitation of BfmR-flag and BfmS^{L181P/E376Q} (BfmS^{DK2}). Whole cell extracts from *bfmS*^{DK2} mutant expressing *bfmR*-flag were

immunoprecipitated without (lane 3, n.a.) or with (IP: Flag) anti-Flag antibody. Images are representative of two independent experiments. (B) Autoradiogram after SDS-PAGE showing the autophosphorylation and transphosphorylation activity of BfmS^{DK2} and BfmS^{DK2 H238A}. Protein bands stained with Coomassie blue (bottom panel) after autoradiography (top panel) were shown. Images are representative of two independent experiments. (C) Expression of *pa4103-lux*. Values represent means \pm SD (n = 3 biological replicates). (D) *D. melanogaster* killing by MPAO1 and its derivatives. n indicates the number of flies used. **P < 0.01 (log-rank test; *bfmS*^{DK2} compared with either MPAO1 or *bfmS*^{DK2 H238A}). (E) Photograph shows lettuce midrib after 3 days of infection with *P. aeruginosa* cells. Images are representative of three independent experiments. (F) Photograph showing ring-shape biofilms (stained by 1% crystal violet) near the air-liquid interface on the inner surface of polystyrene StripwellTM Microplate. Images are representative of three independent experiments. (G, H) Western blot analysis of in vivo phosphorylation of BfmS analyzed on Phos-tagTM gel. Images are representative of two independent experiments. (I, J) Time course of P~BfmR dephosphorylation in the absence (in I) or presence of additional either SUMO-BfmSc or SUMO-BfmSc^{DK2} (in J). Images are representative of two independent experiments. His₆-BfmR was first transphosphorylated by SUMO-BfmSc for 10 min. After removal of ATP, P~His₆-BfmR samples were taken at the indicated time points (in I). In (J), SUMO-BfmSc or SUMO-BfmSc^{DK2} was added to the reaction mixtures after removal of ATP. M, protein markers.

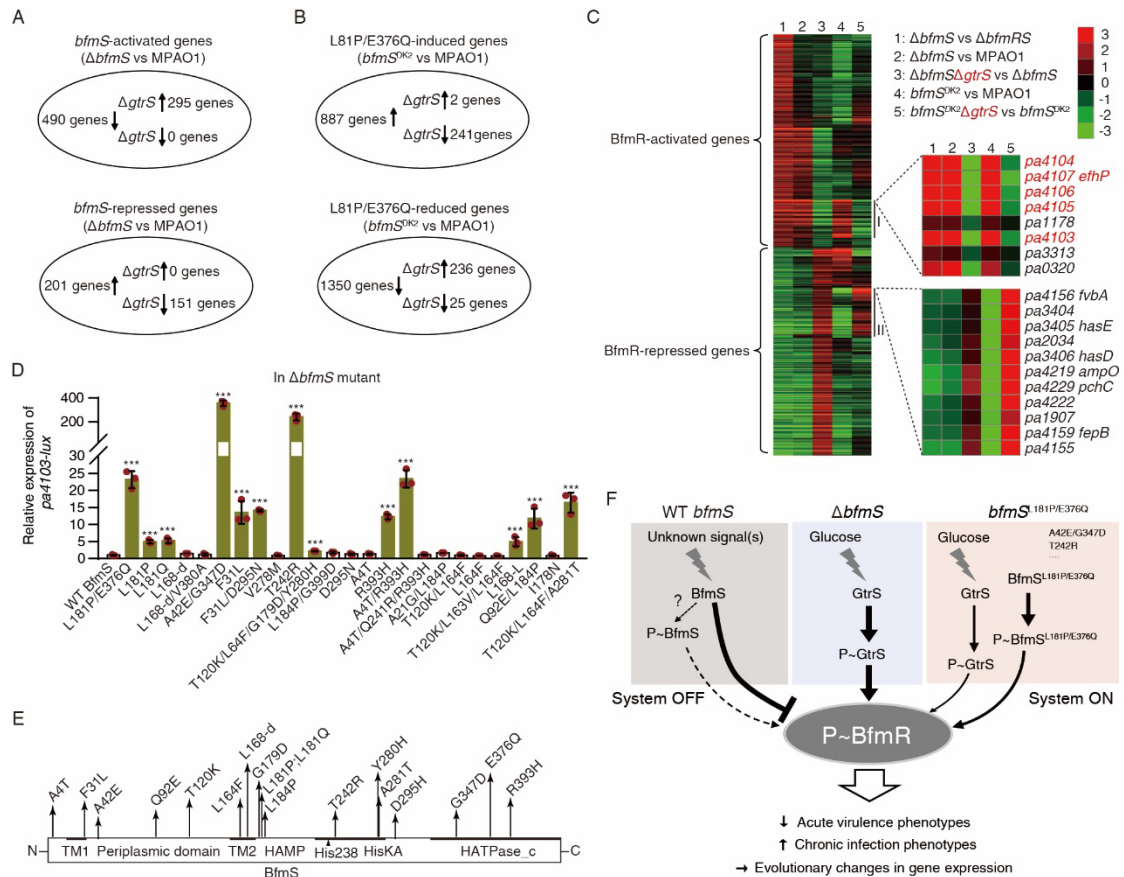


Fig. 6. RNA-seq analysis and role of natural *bfmS* variants in the transcriptional regulatory activity of BfmR. (A) Effect of deletion of *gtrS* in the $\Delta bfmS$ mutant background on the expression of *bfmS*-activated and -repressed genes. (B) Effect of deletion of *gtrS* in the *bfmS*^{DK2} background on the expression of L81P/E376Q mutations-induced and -reduced genes. (C) Heatmaps showing the relative expression of BfmR-activated and -repressed genes in different *P. aeruginosa* strains. Lane 1, BfmR-activated and -repressed genes determined by comparing the transcriptome of $\Delta bfmS$ to that of $\Delta bfmRS$ ($n = 3$ independent experiments, with a $|\log_2$ fold-change $|\geq 1$ and $FDR \leq 0.05$). (D) The relative expression of *pa4103-lux* in *P. aeruginosa* strains cultured in 96-well plates containing minimal medium supplemented with 2 mM glucose for 3 h. Values are relative to $\Delta bfmS$ mutant carrying a WT *bfmS* (set to 1), as indicated. Data represent means \pm SD of $n = 3$ biological replicates (***) $P < 0.001$, Student's two-tailed *t*-test; also with a 2-fold higher level of *pa4103-lux* activity compared to that of WT BfmS). (E) Positions of *bfmS* spontaneous missense mutations involved in the increased transcriptional regulatory activity of BfmR. TM1, aa 10–32; periplasmic domain, aa 33–151; TM2, aa 152–174. HAMP domain, aa 175–227; HisKA, aa 326–434; HisKA with the active site at H238 in BfmS of PAO1. Periplasmic domain was not predicted in SMART but was assumed to be between the TM1 and TM2; aa, amino acid. (F) A proposed mechanism and consequences of mutations in *bfmS*. In wild-type cells, BfmS prevents the phosphorylation of BfmR; however, BfmS may have a role in promoting the accumulation of P~BfmR under certain conditions. In $\Delta bfmS$ mutant, the absence of *bfmS* leads to the phosphorylation

of BfmR by GtrS. When *bfmS* was mutated to either L181P/E376Q or A42E/G347D, accumulation of P~BfmR also occurs, mainly resulting from two effects: i) increased autophosphorylation of BfmS, and ii) cross-phosphorylation between GtrS and BfmR. The lines show the interaction between the players: arrow, activation; hammerheads, repression; solid line, a direct direct connection; dotted line, a putative connection. The question mark (“?”) denotes a yet-unidentified effect.

Figures and Figure legends

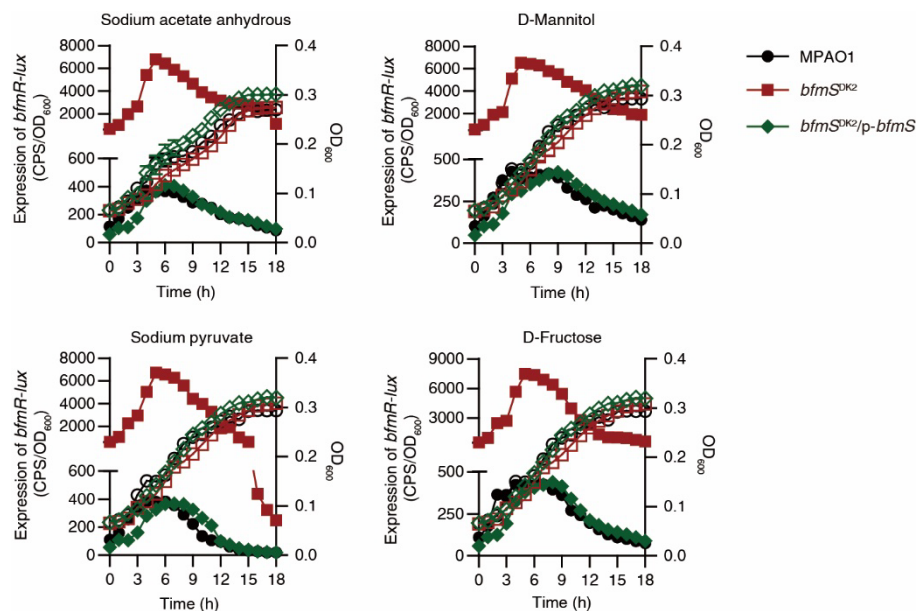


Fig. S1. The promoter activities of *bfmR* in MPAO1 and its derivatives. Expression of *bfmR-lux* (CPS, counts per second; closed symbols) were determined at different phases of the cell growth monitored by measuring the optical density at 600 nm (OD₆₀₀; open symbols). Bacteria were cultured in 96-well plates containing M8-glutamate minimal medium supplemented with either 2 mM sodium acetate anhydrous, D-Mannitol, sodium pyruvate, or D-Fructose at a final concentration of 2 mM, as indicated. MPAO1 and *bfmS*^{DK2} carry an empty pAK1900 vector as control, p-*bfmS* denotes pAK1900-*bfmS* (table S1). Values represent means \pm SD of n = 6 biological replicates.

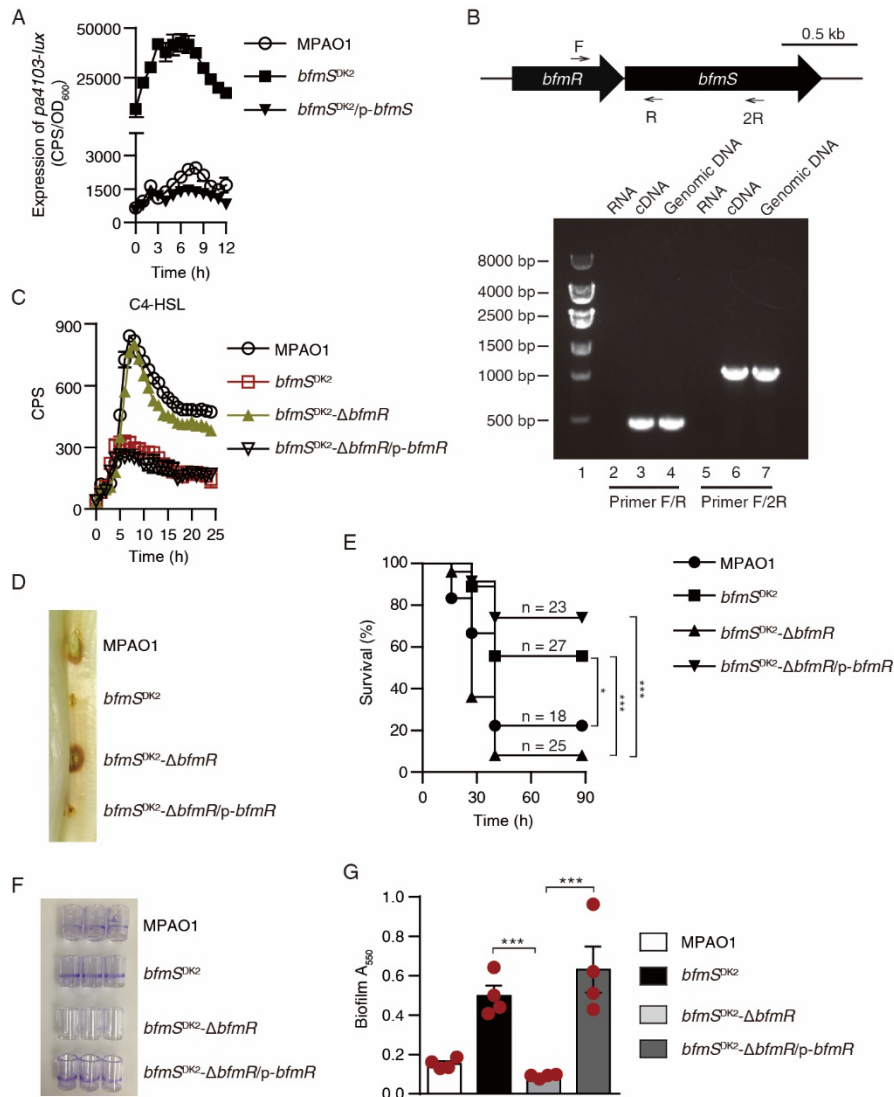


Fig. S2. Consequences of either *bfmS* missense mutations or *bfmR* deletion. (A) The expression of *pa4103-lux* in MPAO1 and its derivatives cultured in 96-well plates containing M8-glutamate minimal medium supplemented with 2 mM glucose. CPS, counts per second; OD₆₀₀, an optical density at 600 nm. Data represent means ± SD (n = 3 biological replicates). (B) Reverse transcription polymerase chain reaction (RT-PCR) analysis. *Upper panel*, scheme showing the position and orientation of the primers (black arrows) in respect to *bfmR* and *bfmS*. *Lower panel*, ethidium bromide-stained agarose gel (1%) of whole-cell RNA-based RT-PCR (lanes 2, 3, 5, and 6) and genome-based PCR (lanes 4 and 7) products amplified with the following primers: F and R (lanes 2-4) and F and 2R (lanes 5-7); controls without reverse transcriptase (RT) added were included (lanes 2 and 5); DNA size standards (in base pairs) are indicated. Images are representative of two independent experiments. (C) Relative amounts of C4-HSL measured by the pDO100 (pKD-*rhlA*) system. MPAO1 and its derivatives were grown in tubes containing pyocyanin production broth (PB medium) at 37°C for 12 h with shaking (250 rpm), the supernatants were subsequently prepared and measured for their ability to promote the luminescence values of the C4-HSL

reporter strain pDO100 (pKD-*rhlA*). CPS values became an indirect measure of supernatant C4-HSL. Data represent means \pm SD (n = 3 biological replicates). (D) Photograph shows lettuce midrib after 3 days of infection with *P. aeruginosa* cells. Both WT MPAO1 and *bfmS*^{DK2}- Δ *bfmR* mutant show necrosis and tissue maceration of infection, while the *bfmS*^{DK2} mutant and the complementary strain of *bfmS*^{DK2}- Δ *bfmR* mutant (*bfmS*^{DK2}- Δ *bfmR*/p-*bfmR*) show weak signs of infection. Images are representative of two independent experiments. (E) *D. melanogaster* killing by MPAO1 and its derivatives. n indicates the number of flies used. *P < 0.05, ***P < 0.001, log-rank test. (F) Photograph showing ring-shape biofilms (stained by 1% crystal violet) near the air-liquid interface on the inner surface of polystyrene Stripwell™ Microplate. Images are representative of three independent experiments. (G) The adhesion/biofilm formation (A550) by *P. aeruginosa*. Data represent means \pm SD of n = 4 independent experiments (***P < 0.001, Student's two-tailed *t*-test). MPAO1, *bfmS*^{DK2}, and *bfmS*^{DK2}- Δ *bfmR* carry an empty pAK1900 as control; p-*bfmR* denotes pAK1900-*bfmR* (table S2).

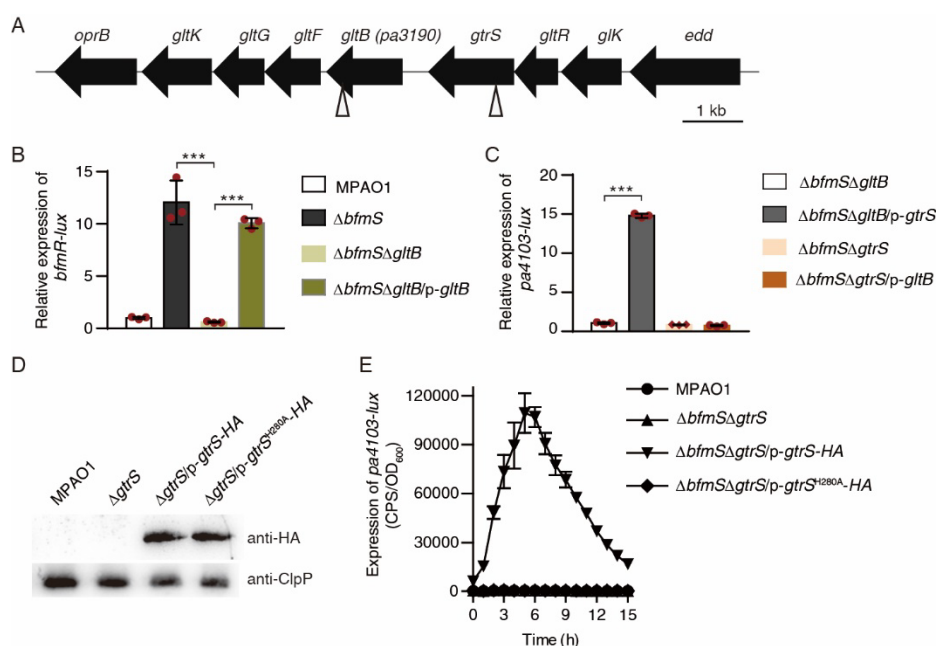


Fig. S3. Identification of genes involved in activating BfmR. (A) Schematic representation of genes involved in glucose uptake and metabolism in *P. aeruginosa* PAO1 (<http://www.pseudomonas.com>). The transposon insertion site is indicated by triangle. (B) Relative expression of *bfmR-lux* in MPAO1 and its derivatives. The expression of *bfmR-lux* in MPAO1 was set to 1, and the other values were adjusted accordingly. Data are from n = 3 biological replicates and reported as means \pm SD (***P < 0.001, Student's two-tailed *t*-test). MPAO1, Δ *bfmS*, and Δ *bfmS* Δ *gltB* carry an empty pAK1900 plasmid as control; p-*gltB* denote pAK1900-*gltB* (table S1). (C) Relative expression of *pa4103-lux*. The expression of *pa4103-lux* in Δ *bfmS* Δ *gltB* was set to 1, and the other values were adjusted accordingly. Data from n = 3 biological

replicates reported as means \pm SD (***) $P < 0.001$, Student's two-tailed t-test). No statistically significant difference was observed between $\Delta bfmS\Delta gtrS$ and $\Delta bfmS\Delta gtrS/p-gltB$ strains. $\Delta bfmS\Delta gtrS$ and $\Delta bfmS\Delta gtrS$ carry an empty pAK1900 plasmid as control, while p-*gtrS* and p-*gltB* respectively denote pAK1900-*gtrS* and pAK1900-*gltB* (table S1). (D and E) Effect of H280A mutation on the production of GtrS (D) and on the regulatory activity of GtrS against the expression of *pa4103-lux* (E). MPAO1, $\Delta gtrS$, or $\Delta bfmS\Delta gtrS$ carrying an empty pAK1900 plasmid as control; p-*gtrS*-HA and p-*gtrS*^{H280A}-HA denote pAK1900-*gtrS*-HA and pAK1900-*gtrS*^{H280A}-HA (table S1), respectively. In (D), images are representative of two independent experiments; in (E), data from n = 3 biological replicates reported as means \pm SD. In (B-D), bacteria were grown in tubes containing M8-glutamate minimal medium supplemented with 2 mM glucose with shaking (250 rpm) at 37 °C for 5 h. In (E), bacteria were cultured in 96-well plates containing M8-glutamate minimal medium supplemented with 2 mM glucose; CPS, counts per second; OD₆₀₀, an optical density at 600 nm.

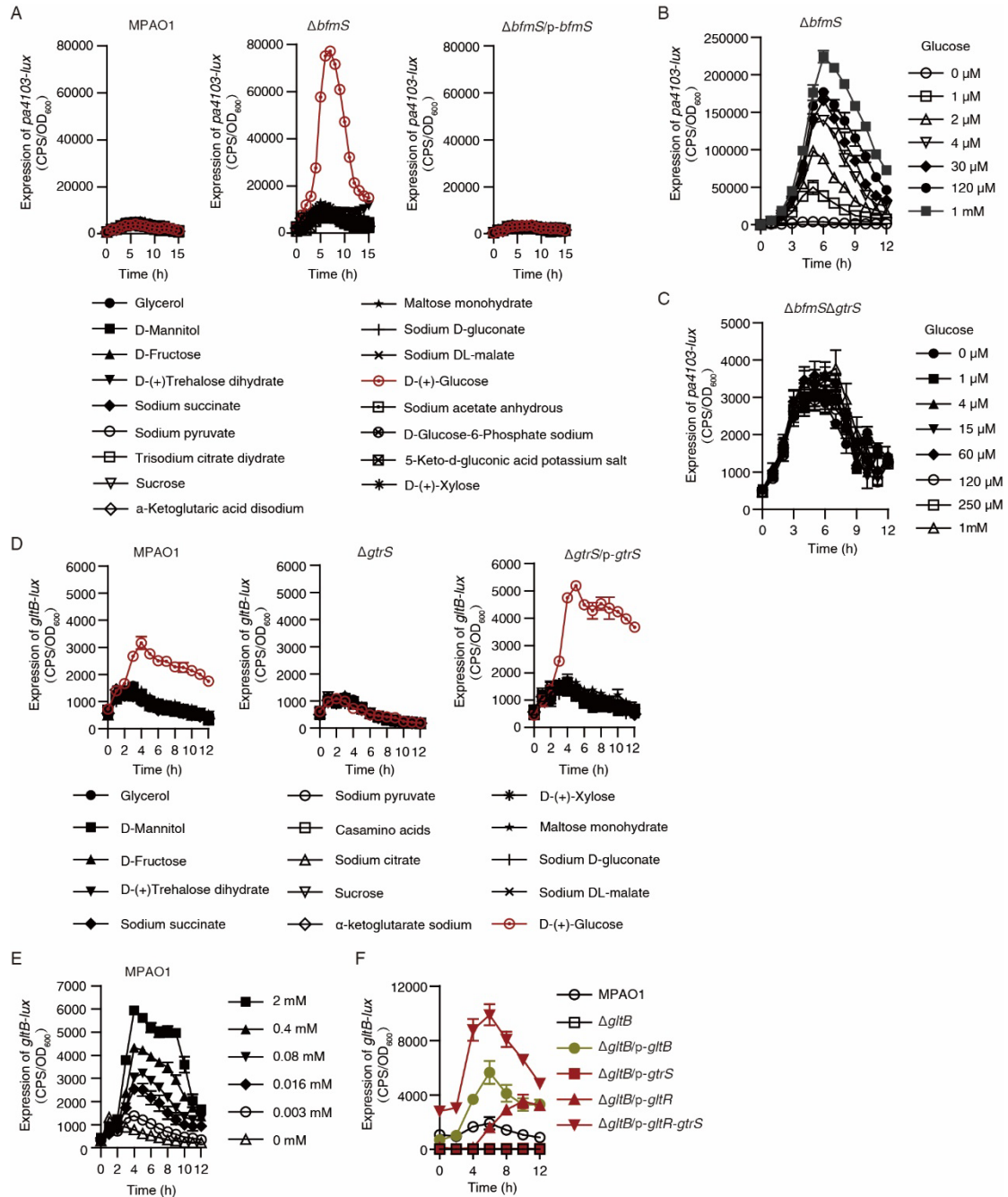


Fig. S4. Glucose increases the regulatory activity of GtrS. (A) The expression of *pa4103-lux* in *P. aeruginosa* strains grown in 96-well plates containing M8-glutamate minimal medium supplemented without or with 20 μ M of the indicated carbohydrates. Data represent means \pm SD (n = 3 biological replicates). MPAO1 and $\Delta bfmS$ harbor an empty pAK1900 plasmid as control; p-*bfmS* denotes pAK1900-*bfmS* (table S1). (B and C) The expression of *pa4103-lux* in $\Delta bfmS$ (B) and $\Delta bfmS\Delta gtrS$ (C) mutants cultured in 96-well plates containing M8-glutamate minimal medium supplemented with indicated concentrations of glucose. Data represent means \pm SD (n = 3 biological replicates). (D) The expression of *gltB-lux* in MPAO1 and its derivatives cultured in 96-well plates containing M8-glutamate minimal medium supplemented with 20 μ M

of indicated carbohydrate. Data represent means \pm SD ($n = 3$ biological replicates). MPAO1 and $\Delta gtrS$ harbor an empty pAK1900 plasmid as control; p-*gtrS* denotes pAK1900-*gtrS* plasmids (table S1). (E) Expression of *gltB-lux* in MPAO1 cultured in 96-well plates containing minimal medium supplemented with indicated concentrations of glucose. Data represent means \pm SD ($n = 3$ biological replicates). (F) Expression of *gltB-lux* in MPAO1 and its derivatives grown in M8-glutamate minimal medium supplemented with 20 μ M of glucose. Data represent means \pm SD ($n = 3$ biological replicates). In (F), MPAO1 and $\Delta gltB$ harbor an empty pAK1900 plasmid as control; p-*gltB*, p-*gtrS*, p-*gltR*, and p-*gltR-gtrS* respectively denote pAK1900-*gltB*, pAK1900-*gtrS*, pAK1900-*gltR*, and pAK1900-*gltR-gtrS* plasmids (table S1).

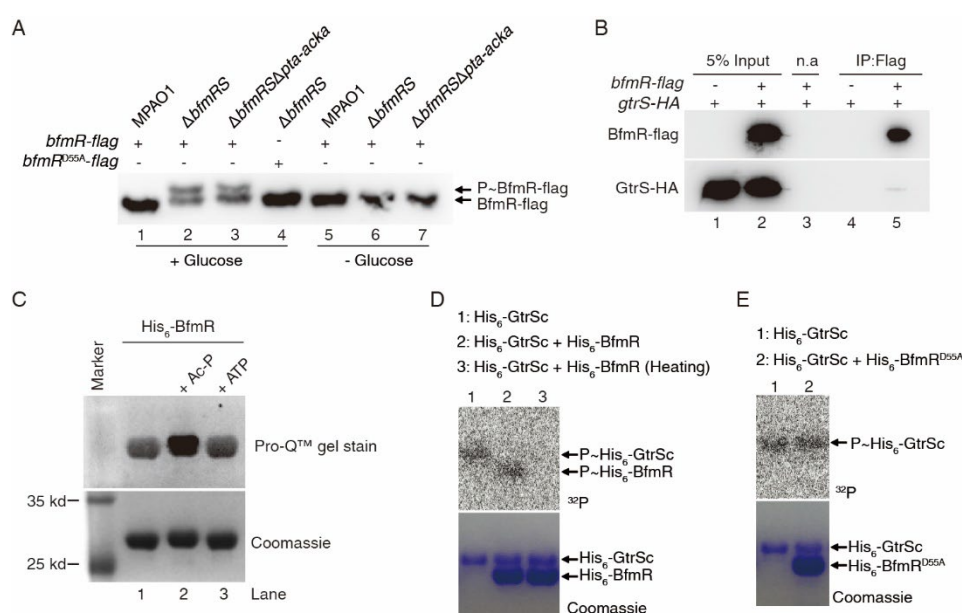


Fig. S5. Phosphorylation of BfmR and its variant, and co-immunoprecipitation.

(A) Western blot analysis of in vivo phosphorylation of BfmR-flag analyzed on Phos-tag™ gel. Bacteria carrying either pAK1900-*bfmR-flag* or pAK1900-*bfmR^{D55A}-flag* plasmid (table S1), as indicated; P~BfmR-flag denotes the phosphorylated BfmR-flag proteins. Images are representative of two independent experiments. (B) Western blot image showing the Co-immunoprecipitation of GtrS-HA and BfmR-flag. Whole cell extracts from $\Delta bfmS$ mutant expressing *gtrS-HA* and/or *bfmR-flag* (lanes 2, 3, and 5) were immunoprecipitated without (lane 3; n.a.) or with (lanes 4-5, IP: Flag) anti-Flag antibody. Images are representative of two independent experiments. (C) SDS-PAGE and phosphoprotein staining with Pro-Q Diamond showing the effect of ATP (2 mM) on the phosphorylation of His₆-BfmR. Phosphorylation of BfmR by acetyl phosphate (Ac-P) (22) was used as a positive control. The intensities of Pro-Q Diamond stained bands of purified proteins were standardized against the intensities of the same bands after gels were restained with Coomassie blue. Images are representative of three independent experiments. (D) Effect of heating on the phosphorylation of His₆-BfmR by His₆-GtrSc. His₆-GtrSc was first auto-phosphorylation with [γ -³²P]ATP for 5 min,

then His₆-BfmR was added to the reaction mixtures and samples were taken after 10 min, with or without heating at 100°C for 5 min prior to SDS-PAGE. Protein bands stained with Coomassie blue after autoradiography were shown. “P~” denotes the phosphorylated proteins. Images are representative of two independent experiments. (E) Autoradiogram after SDS-PAGE showing the transphosphorylation activity of His₆-GtrSc against the His₆-BfmR^{D55A} proteins. Images are representative of two independent experiments. Protein bands stained with Coomassie blue after autoradiography were shown, and “P~” denotes the phosphorylated proteins.

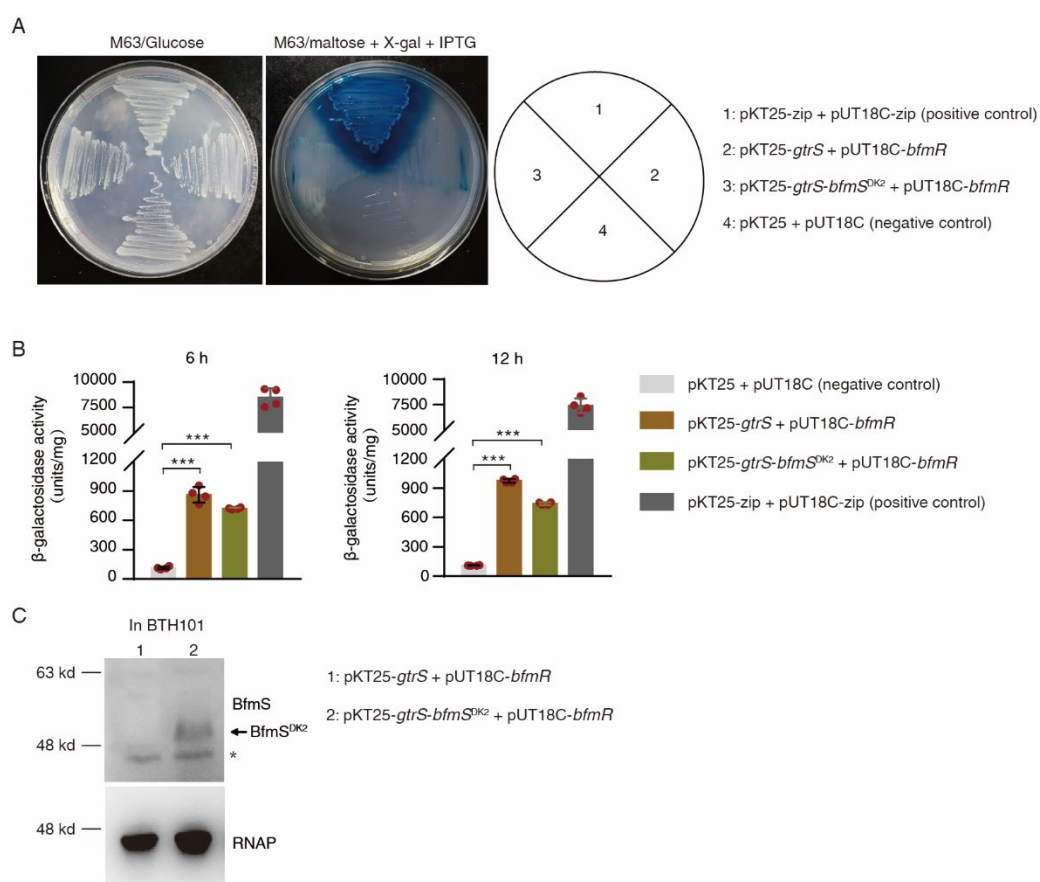


Fig. S6. Bacterial two-hybrid assays showing GtrS-BfmR interactions. (A) *E. coli* BTH101 recombinants bearing indicated combinations of plasmids were plated on either M63/glucose agar or M63/maltose agar containing 40 μg/ml X-gal and 0.5 mM IPTG as indicated, and incubated at 30°C for 6 days. *E. coli* BTH101 bearing vectors encoding the zip fragment (pUT18C-*zip* and pKT25-*zip*) were used as the positive control, while *E. coli* BTH101 co-expressing T18 and T25 tags on vectors (pUT18C and pKT25) were used as negative control. Images are representative of two independent experiments. (B) Expression of β-galactosidase activity cultured in LB broth containing 1mM IPTG for 6 and 12 h. Data from n = 4 biological replicates reported as means ± SD (**P < 0.01, Student's two-tailed t-test). (C) Western blotting analysis for the production of BfmS^{DK2} protein in *E. coli* BTH101 bearing

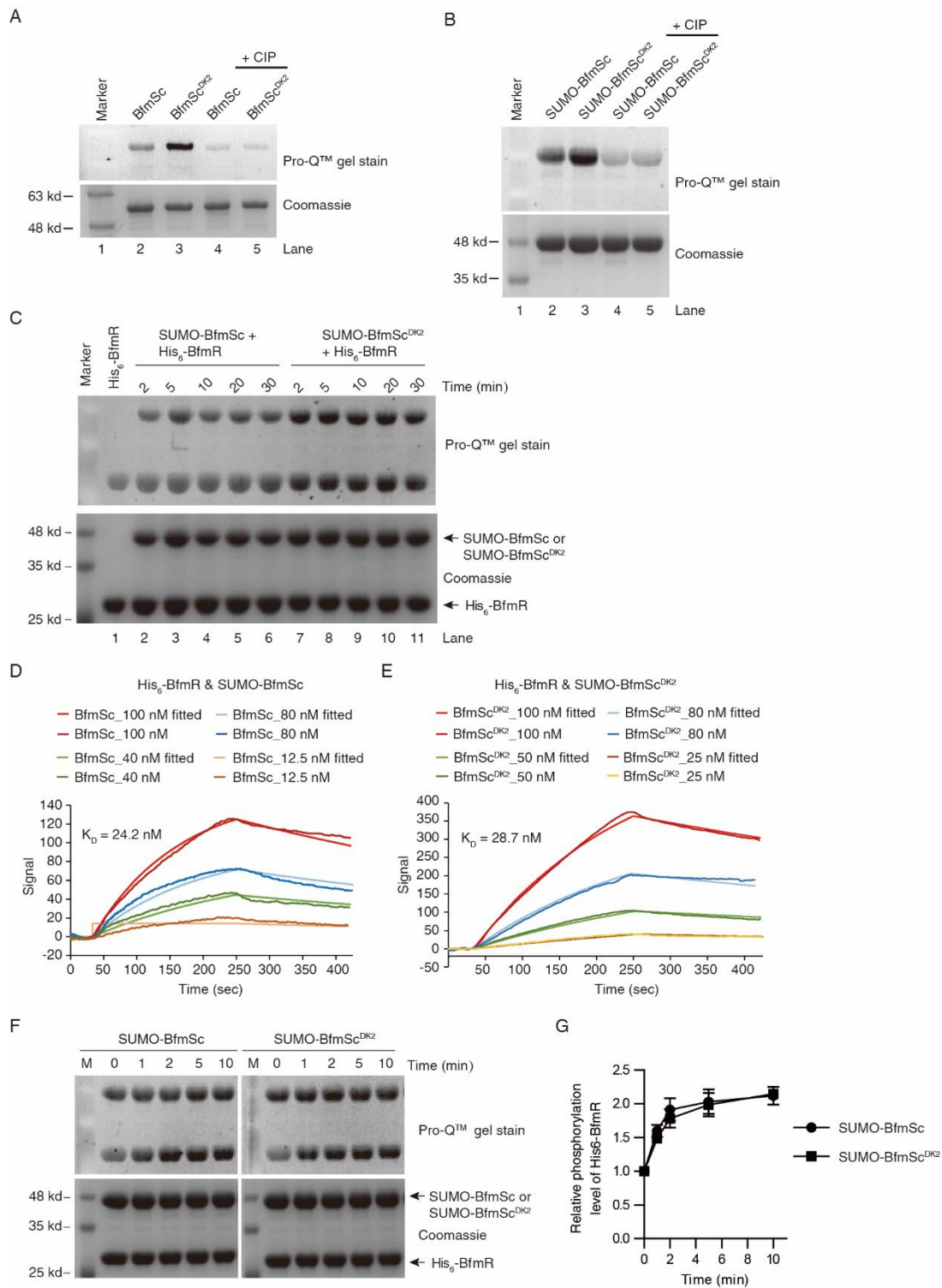


Fig. S9. Pro-Q Diamond staining and surface plasmon resonance (SPR) assays.

(A) Phosphoprotein detection with Pro-Q Diamond phosphoprotein gel stains showing the phosphorylation level of the purified BfmSc proteins and its variant. Lane 1, standard protein molecular sizes, in kilodaltons (kd); lane 2, the recombinant protein BfmSc; Lane 3, the recombinant protein BfmSc^{DK2}; lane 4 and 5, proteins were dephosphorylated by treatment with 0.5U calf intestinal alkaline phosphatase (CIP) for 1 h. Images are representative of two independent experiments. (B) The

level of phosphorylation of purified SUMO-BfmSc proteins and its variant. Lane 1, standard protein molecular sizes, in kilodaltons (kd); lane 2, the recombinant protein SUMO-BfmSc; Lane 3, the recombinant protein SUMO-BfmSc^{DK2}; lane 4 and 5, proteins were dephosphorylated by treatment with 30U calf intestinal alkaline phosphatase (CIP) for 1 h. Images are representative of two independent experiments. (C) *In vitro* transphosphorylation of His₆-BfmR by either purified SUMO-BfmSc (lane 3-7) or SUMO-BfmSc^{DK2} (lane 8-11) in the absence of exogenous ATP. Aliquots were removed at the indicated time points for analysis by SDS-PAGE, followed by Pro-Q Diamond staining to identify phosphorylation and Coomassie blue staining to detect protein levels. Images are representative of three independent experiments. (D, E) Analysis of protein interactions by OpenSPR showing the effect of L181P/E376Q mutations on the binding affinity of BfmS to BfmR. Analysis performed in TraceDrawer using a 1:1 binding interaction model. K_D, affinity constant. (F and G) Representative images (F) and analysis (G) of the phosphorylation of BfmR by SUMO-BfmSc and its variant SUMO-BfmSc^{DK2} in the presence of exogenous ATP (2 mM). The intensities of Pro-Q Diamond stained bands of His₆-BfmR proteins were standardized against the intensities of the same bands after gels were restained with Coomassie blue and was further normalized to the vehicle group within each experiment. Data from n = 3 independent experiments reported as means ± SEM. No statistically significant difference (by Mann-Whitney U test) was observed between BfmSc and BfmS^{DK2} groups at the same time point.

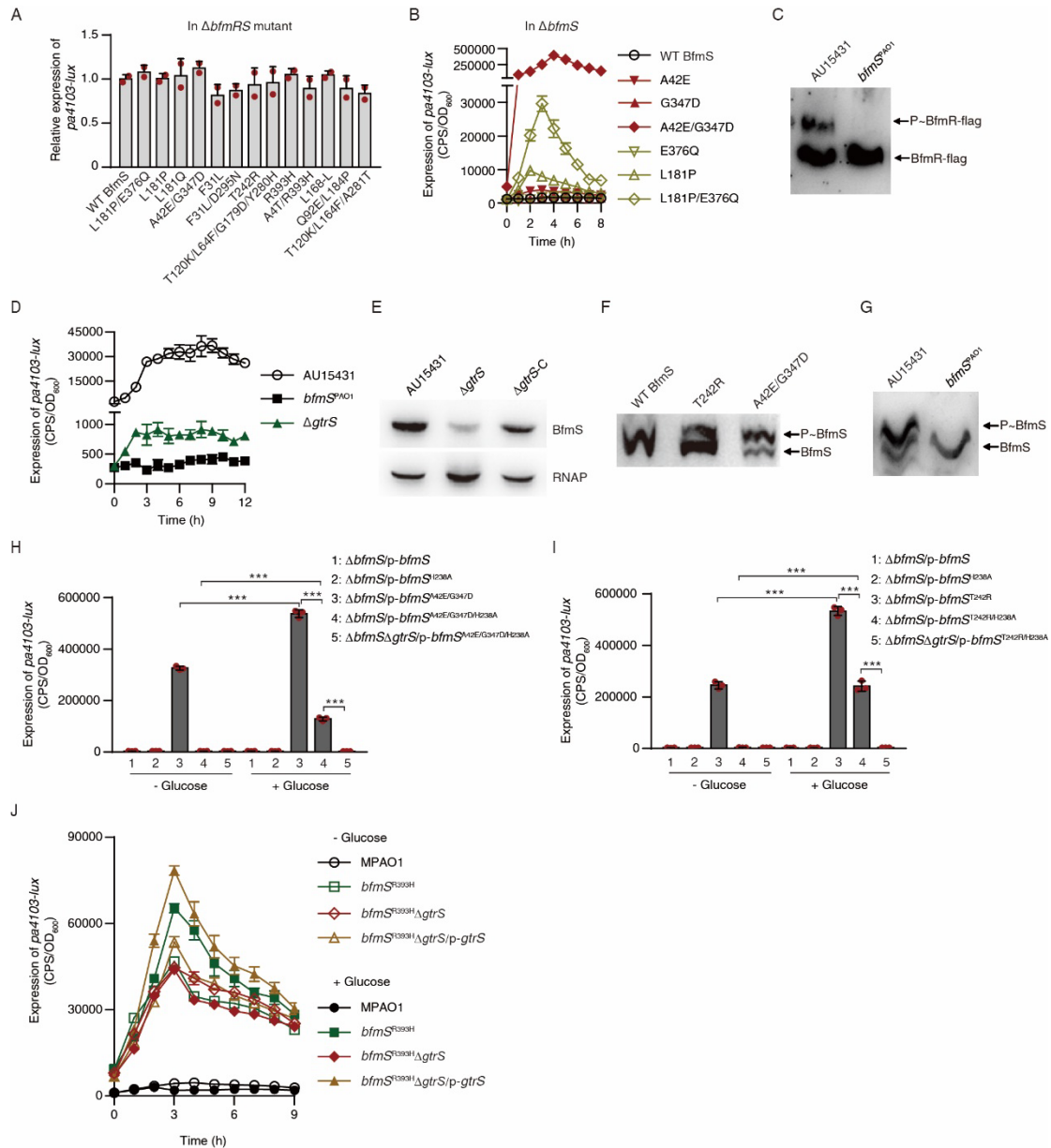


Fig. S10. Role of natural *bfmS* variants in BfmR activation. (A) The relative expression of *pa4103-lux* when bacteria were grown in 96-well plates containing minimal medium supplemented with 2 mM glucose for 3 h. Values are relative to $\Delta bf mRS$ mutant carrying a wild-type *bfmS* (set to 1). Data represent means \pm SD of $n = 3$ biological replicates. (B) Expression of *pa4103-lux* in MPAO1 $\Delta bf mS$ mutant carrying a plasmid-borne WT *bfmS* or its variants. Data from $n = 3$ biological replicates reported as means \pm SD. (C) Western blot analysis of in vivo phosphorylation of BfmR-flag analyzed on Phos-tag™ gel. Images are representative of two independent experiments. (D) Expression of *pa4103-lux* in AU15431 isolate and its derivatives cultured in cultured in 96-well plates containing PB medium. Data from $n = 3$ biological replicates reported as means \pm SD. (E) Western blot images showing the effect of *gtrS* deletion on the production of BfmS in AU15431 isolate. Protein samples derived from bacteria grown in tubes containing PB medium

supplemented with 2 mM glucose at 37°C for 6 h with shaking (250 rpm). RNA polymerase (RNAP) alpha subunit is probed as a loading control. Images are representative of two independent experiments. (F) Western blot analysis of *in vivo* phosphorylation of BfmS and its variants analyzed on Phos-tag™ gel. Protein samples derived from $\Delta bfmS$ mutant carrying p-*bfmS*, p-*bfmS*^{T242R}, or p-*bfmS*^{A42E/G347D} plasmid (table S1), as indicated. Images are representative of two independent experiments. (G) Western blot analysis of *in vivo* phosphorylation of BfmS and its variants analyzed on Phos-tag™ gel. Images are representative of three independent experiments. (H and I) Effect of *bfmS* missense mutations on the *pa4103-lux* when bacteria grown in 96-well plates containing minimal medium supplemented without or with glucose (2 mM) for 4 h. Data from n = 3 biological replicates reported as means \pm SD (**P < 0.001, Student's two-tailed *t*-test). (J) Expression of *pa4103-lux* in MPAO1 and its derivatives cultured in 96-well plates containing M8-glutamate minimal medium supplemented without (-) or with (+) 2 mM glucose. Data represent means \pm SEM of three biological replicates. MPAO1, *bfmS*^{R393H}, *bfmS*^{R393H} $\Delta gtrS$ harbor an empty pAK1900 plasmid as control (table S1).

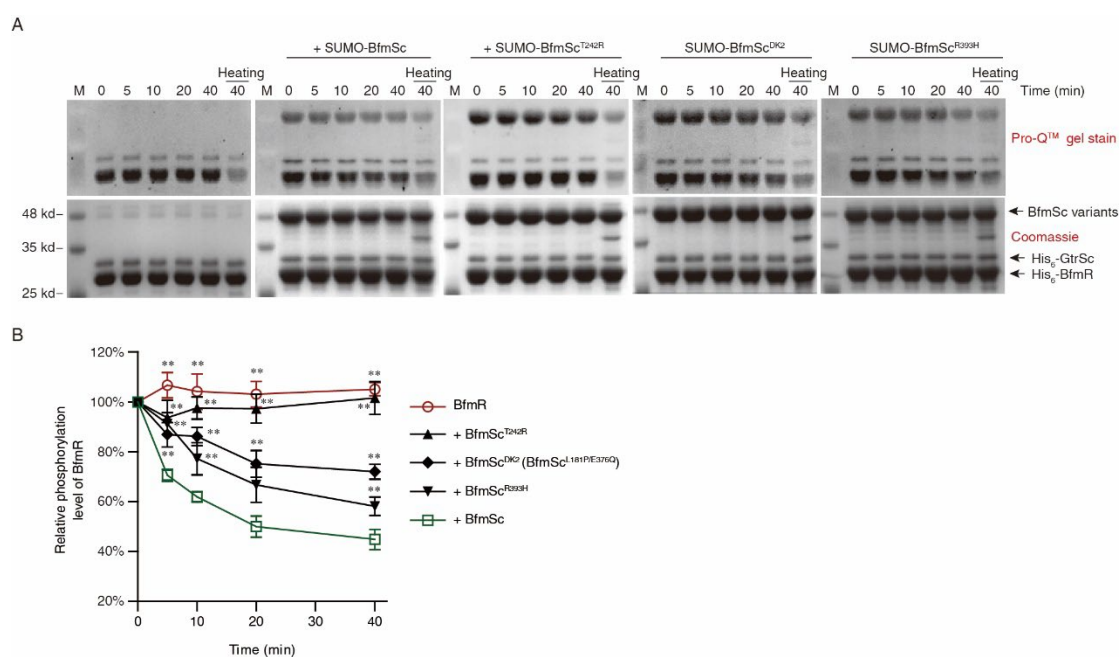


Fig. S11. Dephosphorylation of BfmR~P by BfmSc and its variants. (A) Representative images of Pro-Q Diamond phosphoprotein gel stains showing the dephosphorylation of BfmR~P by purified BfmSc and its indicated variants. His₆-BfmR was first phosphorylated by His₆-GtrSc for 30 min. After removal of ATP, the P~His₆-BfmR sample was treated without (*left panel*) or with purified SUMO-BfmSc and its variants, as indicated. Aliquots were removed at the indicated time points for analysis by SDS-PAGE, followed by Pro-Q Diamond staining to identify

phosphorylation and Coomassie blue staining to detect protein levels. M, protein markers. Heating, the sample was exposed to the heating at 100°C for 5 min prior to SDS-PAGE. (B) Graphic data showing the dephosphorylation of BfmR~P by purified BfmSc and its variants. Data from n = 4 independent experiments reported as means ± SEM. The significant differences were indicated by marks: **P < 0.01 (Mann-Whitney U test) when compared to the same time point of the BfmSc group. No statistically significant difference was observed between BfmSc^{R393H} and BfmSc at the time point of 20 min. The intensities of Pro-Q Diamond stained bands of His₆-BfmR proteins were standardized against the intensities of the same bands after gels were restained with Coomassie blue, and the normalized data were further corrected by subtracting the background signal detected from the heated samples. The results are reported as percentage relative to the control sample (at the time point of 0 min), respectively.

Table S1. Plasmids and bacterial strains and used in this study

Plasmids or strains	Relevant characteristics ^a	Source
Plasmids		
mini-CTX-lacZ	Gene delivery vector for inserting genes at the CTX phage <i>att</i> site on <i>P. aeruginosa</i> chromosome, Tc ^r ; <i>lacZ</i> -based promoter reporter	(48)
mini-CTX-lux	Gene delivery vector for inserting genes at the CTX phage <i>att</i> site on <i>P. aeruginosa</i> chromosome, Tc ^r ; <i>lux</i> -based promoter reporter	(48)
pAK1900	<i>E. coli</i> - <i>P. aeruginosa</i> shuttle cloning vector, Ap ^r Cb ^r	(51)
pBT20	Mini-TnM delivery vector; Ap ^r Gm ^r	(47)
pET28a	T7 <i>lac</i> promoter-operator, N-terminal His tag, kan ^r	Novagen
pET28a(+)-sumo	SUMO fusion protein expression vector; Kan ^r	Novagen
pEX18Ap	Gene replacement vector, mob ⁺ <i>sacB</i> , Ap ^r	(49)
pEX18Tc	Gene replacement vector, mob ⁺ <i>sacB</i> , Tc ^r	(49)
pFLP2	Source of Flp recombinase; Ap ^r /Cb ^r	(49)

pGEX-6p-1-6His	pGEX-6p-1 derivative carry insertion of a DNA sequence (ATGCATCATCATCATCAT) immediately before the start codon of the GST gene in pGEX-6P-1. Ap ^r ; <i>E. coli</i> expression vector.	Lab stock
pKT25	BACTH vector designed to express a given polypeptide fused in-frame at its N-terminal end with the T25 fragment; p15 ori; Km ^r	Euromedex
pMS402	<i>lux</i> -based promoter reporter plasmid, Kan ^r Tp ^r	(60)
pPS858	pBR322 derivative carrying a FRT-Gm cassette, Ap ^r	(49)
pRK415	Broad-host-range cloning vector; <i>plac</i> MCS Tc ^r	(52)
pUT18C	BACTH vector designed to express a given polypeptide fused in-frame at its N-terminal end with the T18 fragment; ColE1 ori; Ap ^r	Euromedex
pUT18C-zip, pKT25-zip	Derivatives of pUT18C and pKT25 with a 114 bp DNA fragment encoding a leucine zipper (positive control for two-hybrid assays)	Euromedex
<i>bfmR-lux</i>	pMS402 containing <i>bfmR</i> promoter region	(24)
<i>gltB-lux</i>	mini-CTX-lux containing <i>gltB</i> promoter region (-740 to +18 of the start codon of <i>gltB</i>)	This study
mini- <i>bfmR-lacZ</i>	mini-CTX-lacZ derivative carrying <i>bfmR-lacZ</i> reporter fusion	This study
mini- <i>bfmS</i>	mini-CTX-lacZ derivative carrying <i>bfmS</i> controlled by the <i>lac</i> promoter of the	This study

	pAK1900	
mini-ctx-BfmR-Flag	mini-CTX-lacZ derivative carrying <i>bfmR-Flag</i>	(24)
mini- <i>gltR</i>	mini-CTX-lacZ derivative carrying <i>gltR</i> controlled by the <i>lac</i> promoter of the pAK1900	This study
mini- <i>gltR-gtrS</i>	mini-CTX-lacZ derivative carrying <i>gltR-gtrS</i> controlled by the <i>lac</i> promoter of the pAK1900	This study
mini- <i>gtrS</i>	mini-CTX-lacZ derivative carrying <i>gtrS</i> controlled by the <i>lac</i> promoter of the pAK1900	This study
<i>pa4103-lux</i>	mini-CTX-lux containing <i>pa4103</i> promoter region (-659 to +19 of the start codon of <i>pa4103</i>)	This study
p- <i>bfmR</i>	PAK1900 derivative carrying <i>bfmR</i> (<i>PA4101</i>) on a <i>c.</i> 0.8 kb <i>HindIII/BamHI</i> fragment in same orientation as <i>plac</i>	(24)
p- <i>bfmR</i> ^{D55A} - <i>flag</i>	p- <i>bfmR-flag</i> carrying <i>bfmR</i> (<i>pa4101</i>) which has alanine substitution mutant at the site of aspartate residue 55	This study
p- <i>bfmR-flag</i>	pAK1900 derivative carrying a <i>bfmR-flag</i> fusion gene for the expression of C-terminal Flag-tagged BfmR proteins	This study
p- <i>bfmS</i>	pAK1900 derivative carrying <i>bfmS</i> (<i>pa4102</i>) on a ~1.4 kb <i>HindIII/BamHI</i> fragment in same orientation as <i>plac</i>	(24)
p- <i>bfmS</i> ^{A21G/L184P}	p- <i>bfmS</i> derivative carrying A21G and L184P substitutions	This study
p- <i>bfmS</i> ^{A42E/G347D}	p- <i>bfmS</i> derivative carrying A42E and G347D substitutions	This study
p- <i>bfmS</i> ^{A42E/G347D/H238A}	p- <i>bfmS</i> derivative carrying A42E, G347D and H238A substitutions	This study

$p\text{-}bfmS^{A4T}$	$p\text{-}bfmS$ derivative carrying threonine substitution mutant at the site alanine 4	This study
$p\text{-}bfmS^{A4T/Q241R/R393H}$	$p\text{-}bfmS$ derivative carrying A4T, Q241R, and R393H substitutions	This study
$p\text{-}bfmS^{A4T/R393H}$	$p\text{-}bfmS$ derivative carrying A4T and R393H substitutions	This study
$p\text{-}bfmS^{D295N}$	$p\text{-}bfmS$ derivative carrying asparagine substitution mutant at the site aspartic acid 295	This study
$p\text{-}bfmS^{E376Q}$	$p\text{-}bfmS$ derivative carrying glutamine substitution mutant at the site glutamic acid 376	(24)
$p\text{-}bfmS^{F31L}$	$p\text{-}bfmS$ derivative carrying leucine substitution mutant at the site phenylalanine 31	This study
$p\text{-}bfmS^{F31L/D295N}$	$p\text{-}bfmS$ derivative carrying F31L and D295N substitutions	This study
$p\text{-}bfmS^{H238A}$	$p\text{-}bfmS$ derivative carrying H238A substitution	This study
$p\text{-}bfmS^{I178N}$	$p\text{-}bfmS$ derivative carrying asparagine substitution mutant at the site isoleucine 178	This study
$p\text{-}bfmS^{L164F}$	$p\text{-}bfmS$ derivative carrying phenylalanine substitution mutant at the site leucine 164	This study
$p\text{-}bfmS^{L168-d}$	$p\text{-}bfmS$ derivative carrying deletion mutant at the site leucine 168	This study
$p\text{-}bfmS^{L168-d/V380A}$	$p\text{-}bfmS$ derivative carrying L168-d and V380A substitution	This study
$p\text{-}bfmS^{L168-L}$	$p\text{-}bfmS$ derivative carrying L168-L (Leu insertion after Leu-168)	This study
$p\text{-}bfmS^{L181P}$	$p\text{-}bfmS$ derivative carrying proline substitution mutant at the site leucine 181	(24)
$p\text{-}bfmS^{L181P/E376Q}$	$p\text{-}bfmS$ derivative carrying both L181P	(24)

	and E376Q substitutions	
p- <i>bfmS</i> ^{L181Q}	p- <i>bfmS</i> derivative carrying glutamine substitution mutant at the site leucine 181	This study
p- <i>bfmS</i> ^{L184P/G399D}	p- <i>bfmS</i> derivative carrying L184P and G399D substitutions	This study
p- <i>bfmS</i> ^{Q92E/L184P}	p- <i>bfmS</i> derivative carrying Q92E and L184P substitutions	This study
p- <i>bfmS</i> ^{R393H}	p- <i>bfmS</i> derivative carrying histidine substitution mutant at the site arginine 393	(24)
p- <i>bfmS</i> ^{T120K/L163V/L164F}	p- <i>bfmS</i> derivative carrying T120K, L163V, and L164F substitutions	This study
p- <i>bfmS</i> ^{T120K/L164F}	p- <i>bfmS</i> derivative carrying T120K and L164F substitutions	This study
p- <i>bfmS</i> ^{T120K/L164F/A281T}	p- <i>bfmS</i> derivative carrying T120K, L164F, and A281T substitutions	This study
p- <i>bfmS</i> ^{T120K/L164F/G179D/Y280H}	p- <i>bfmS</i> derivative carrying T120K, L164F, G179D, and Y280H substitutions	This study
p- <i>bfmS</i> ^{T242R}	p- <i>bfmS</i> derivative carrying arginine substitution mutant at the site threonine 242	This study
p- <i>bfmS</i> ^{T242R/H238A}	p- <i>bfmS</i> derivative carrying T242R and H238A substitutions	This study
p- <i>bfmS</i> ^{V278M}	p- <i>bfmS</i> derivative carrying methionine substitution mutant at the site valine 278	This study
pET28a(+)-sumo- <i>BfmSc</i>	pET28a(+)-sumo derivative carrying <i>BfmSc</i> for the expression of an N-terminal 6His-SUMO tagged cytosolic segment of BfmS (residues 175-435)	This study
pET28a(+)-sumo- <i>BfmSc</i> ^{DK2}	pET28a(+)-sumo- <i>BfmSc</i> derivative, with missense mutations (L181P and E376Q) in <i>bfmS</i>	This study
pET28a(+)-sumo- <i>BfmSc</i> ^{R393H}	pET28a(+)-sumo- <i>BfmSc</i> derivative, with	This study

	R393H missense mutation in <i>bfmS</i>	
pET28a(+)-sumo- <i>BfmSc</i> ^{T242R}	pET28a(+)-sumo- <i>BfmSc</i> derivative, with T242R missense mutation in <i>bfmS</i>	This study
pET28a-6His-BfmR	pET28a derivative carrying <i>bfmR</i> (<i>pa4101</i>)	(24)
pET28a-6His-BfmR ^{D55A}	pET28a derivative carrying <i>bfmR</i> (<i>pa4101</i>) which has alanine substitution mutant at the site of aspartate residue 55	(24)
pET28a- <i>GtrSc</i>	pET28a derivative carrying <i>GtrSc</i> for the expression of an N-terminal His-tagged cytosolic segment of GtrS (residues 269-465)	This study
pEX18Ap:: <i>acka-pta</i> UTD	pEX18Ap derivative, for replacing <i>acka-pta</i> loci with a tetracycline resistance cassette from plasmid mini-CTX-lacZ	(24)
pEX18Ap:: <i>bfmRSUGD</i>	pEX18Ap derivative, for replacing <i>bfmRS</i> loci with a gentamicin resistance cassette from plasmid pPS858	(24)
pEX18Ap:: <i>bfmRUGD</i>	pEX18Ap derivative, for replacing <i>bfmR</i> with a gentamicin resistance cassette from plasmid pPS858	This study
pEX18Ap:: <i>bfmSUGD</i>	pEX18Ap derivative, for replacing <i>bfmS</i> gene with a gentamicin resistance cassette from plasmid pPS858	(24)
pEX18Ap:: <i>gltR-gtrSUGD</i>	pEX18Ap derivative, for replacing <i>gltR-gtrS</i> loci with a gentamicin resistance cassette from plasmid pPS858	This study
pEX18Ap:: <i>gtrSUGD</i>	pEX18Ap derivative, for replacing <i>gtrS</i> with a gentamicin resistance cassette from plasmid pPS858	This study
pEX18Ap:: <i>pa3190UGD</i>	pEX18Ap derivative, for replacing <i>gltB</i> with a gentamicin resistance cassette from plasmid pPS858	This study

pEX18Tc-For- <i>bfmS</i> ^{DK2}	pEX18Tc derivative, for replacing WT <i>bfmS</i> with <i>bfmS</i> ^{DK2} (<i>bfmS</i> ^{L181P/E376Q})	This study
pEX18Tc-For- <i>bfmS</i> ^{DK2 H238A}	pEX18Tc derivative, for replacing WT <i>bfmS</i> with <i>bfmS</i> ^{DK2 H238A} (<i>bfmS</i> ^{L181P/E376Q/H238A})	This study
pEX18Tc-For- <i>bfmS</i> ^{PAO1}	pEX18Tc derivative, for replacing mutated <i>bfmS</i> allele with WT <i>bfmS</i>	This study
pEX18Tc-For- <i>bfmS</i> ^{R393H}	pEX18Tc derivative, for replacing WT <i>bfmS</i> with <i>bfmS</i> ^{R393H}	This study
pGEX-6p-1- <i>BfmSc</i>	pGEX-6p-1-6His derivative carrying <i>BfmSc</i> for the expression of an N-terminal 6His- and GST-tagged cytosolic segment of BfmS (residues 175-435)	This study
pGEX-6p-1- <i>BfmSc</i> ^{DK2}	pGEX-6p-1- <i>BfmSc</i> derivative carrying both L181P and E376Q substitutions	This study
pGEX-6p-1- <i>BfmS</i> ^{DK2 H238A} - <i>Cter</i>	pGEX-6p-1- <i>BfmSc</i> ^{DK2} derivative carrying H238A substitution	This study
p- <i>gltB</i>	pAK1900 derivative carrying <i>gltB</i> on a ~1.3 kb HindIII/ <i>KpnI</i> fragment in same orientation as <i>plac</i>	This study
p- <i>gltR</i>	pAK1900 derivative carrying <i>gltR</i> on a ~0.77 kb HindIII/ <i>KpnI</i> fragment in same orientation as <i>plac</i>	This study
p- <i>gltR-gtrS</i>	pAK1900 derivative carrying <i>gltR-gtrS</i> on a ~2.3 kb HindIII/ <i>BamHI</i> fragment in same orientation as <i>plac</i>	This study
p- <i>gtrS</i>	pAK1900 derivative carrying <i>gtrS</i> on a ~1.5 kb HindIII/ <i>BamHI</i> fragment in same orientation as <i>plac</i>	This study
p- <i>gtrS</i> ^{H280A} - <i>HA</i>	p- <i>gtrS-HA</i> carrying <i>gtrS</i> which has alanine substitution mutant at the site of histidine 280	This study
p- <i>gtrS-HA</i>	pAK1900 derivative carrying a <i>gtrS-HA</i>	This study

	fusion gene for the expression of C-terminal HA-tagged GtrS proteins	
pKT25- <i>gtrS</i>	<i>gtrS</i> cloned into pKT25	Euromedex
pKT25- <i>gtrS</i> - <i>bfmS</i> ^{DK2}	<i>gtrS</i> and <i>bfmS</i> ^{DK2} cloned into pKT25	Euromedex
pRK415- <i>bfmR</i> - <i>flag</i>	pAK415 derivative carrying a <i>bfmR</i> - <i>flag</i> fusion gene for the expression of C-terminal Flag-tagged BfmR proteins	This study
pRK415- <i>bfmS</i>	pAK415 derivative carrying <i>bfmS</i> (<i>pa4102</i>) on a ~1.4 kb <i>HindIII</i> / <i>Bam</i> HI fragment in same orientation as <i>plac</i>	This study
pRK415- <i>gtrS</i>	pAK415 derivative carrying <i>gtrS</i> (<i>pa3191</i>) on a ~1.5 kb <i>HindIII</i> / <i>Bam</i> HI fragment in same orientation as <i>plac</i>	This study
pUT18C- <i>bfmR</i>	<i>bfmR</i> cloned into pUT18C	Euromedex
<i>P. aeruginosa</i> strains		
AU15431	CF isolate, <i>bfmS</i> ^{A42E/G347D}	(35)
DK2	CF isolate, <i>bfmS</i> ^{L181P/E376Q}	(27)
MPAO1	Wild type, WT <i>bfmS</i>	(61)
pDO100 (pKD- <i>rhlA</i>)	<i>rhlI</i> mutant of PAO1 harboring plasmid pKD- <i>rhlA</i>	(57)
AU15431- <i>bfmS</i> ^{PAO1}	AU15431 derivative with a WT <i>bfmS</i> allele replaced the mutated <i>bfmS</i> (<i>bfmS</i> ^{A42E/G347D})	This study
<i>bfmS</i> ^{DK2}	MPAO1 derivative with a mutated <i>bfmS</i> allele (<i>bfmS</i> ^{L181P/E376Q}) replaced the WT <i>bfmS</i>	This study
<i>bfmS</i> ^{DK2 H238A}	MPAO1- <i>bfmS</i> ^{DK2} derivative carrying H238A mutation in the <i>bfmS</i> ^{DK2} allele	This study
<i>bfmS</i> ^{DK2} Δ <i>bfmR</i> (MPAO1)	MPAO1- <i>bfmS</i> ^{DK2} derivative with a gentamicin resistance cassette replaced the <i>bfmR</i>	This study
<i>bfmS</i> ^{DK2} Δ <i>gtrS</i> (MPAO1)	MPAO1- <i>bfmS</i> ^{DK2} derivative with a gentamicin resistance cassette replaced	This study

	the <i>gtrS</i>	
<i>bfmS</i> ^{R393H}	MPAO1 derivative with a mutated <i>bfmS</i> allele (<i>bfmS</i> ^{R393H}) replaced the WT <i>bfmS</i>	This study
<i>bfmS</i> ^{R393H} Δ <i>gtrS</i>	<i>bfmS</i> ^{R393H} derivative with a gentamicin resistance cassette replaced the <i>gtrS</i>	This study
DK2- <i>bfmS</i> ^{PAO1}	DK2 derivative with a WT <i>bfmS</i> allele replaced the mutated <i>bfmS</i> (<i>bfmS</i> ^{L181P/E376Q})	This study
Δ <i>bfmR</i>	MPAO1 derivative with a gentamicin resistance cassette replaced the <i>bfmR</i> gene	This study
Δ <i>bfmRS</i>	MPAO1 derivative with a gentamicin resistance cassette replaced the <i>bfmRS</i> locus	(24)
Δ <i>bfmRS</i> (DK2)	DK2 derivative with a gentamicin resistance cassette replaced the <i>bfmRS</i> locus, by using the pEX18Ap:: <i>bfmRSUGD</i> plasmid	This study
Δ <i>bfmRS</i> Δ <i>pta-ackA</i>	MPAO1 derivative with a gentamicin resistance cassette replaced the <i>bfmRS</i> locus, and a tetracycline resistance cassette replaced the <i>pta-ackA</i> locus	This study
Δ <i>bfmRS</i> Δ <i>gltR-gtrS</i>	MPAO1 derivative with a gentamicin resistance cassette replaced the <i>bfmRS</i> locus, and a deletion of <i>gltR-gtrS</i> locus	This study
Δ <i>bfmS</i>	MPAO1 derivative with a gentamicin resistance cassette replaced the <i>bfmS</i> gene	(24)
Δ <i>bfmS</i> (AU15431)	AU15431 derivative with a gentamicin resistance cassette replaced the <i>bfmS</i> , by using the pEX18Ap:: <i>bfmSUGD</i> plasmid	This study
Δ <i>bfmS</i> (DK2)	DK2 derivative with a gentamicin resistance cassette replaced the <i>bfmS</i> , by	This study

	using the pEX18Ap:: <i>bfmSUGD</i> plasmid	
$\Delta bfmS::bfmR-lacZ$	$\Delta bfmS$ mutant carrying <i>bfmR-lacZ</i> reporter fusion at the CTX phage <i>att</i> site on <i>P. aeruginosa</i> chromosome	This study
$\Delta bfmS\Delta gltB$	MPAO1 derivative with a gentamicin resistance cassette replaced the <i>bfmS</i> , and a deletion of <i>gltB</i>	This study
$\Delta bfmS\Delta gltR-gtrS$	MPAO1 derivative with a gentamicin resistance cassette replaced the <i>bfmS</i> , and a deletion of <i>gltR-gtrS</i> locus	This study
$\Delta bfmS\Delta gtrS$	MPAO1 derivative with a gentamicin resistance cassette replaced the <i>bfmS</i> , and a deletion of <i>gtrS</i>	This study
$\Delta gltB$	MPAO1 derivative with a gentamicin resistance cassette replaced the <i>gltB</i> gene	This study
$\Delta gltR-gtrS$	MPAO1 derivative with a gentamicin resistance cassette replaced the <i>gltR-gtrS</i> locus	This study
$\Delta gtrS$	MPAO1 derivative with a gentamicin resistance cassette replaced the <i>gtrS</i> gene	This study
$\Delta gtrS$ (AU15431)	AU15431 derivative with a gentamicin resistance cassette replaced the <i>gtrS</i> , by using the pEX18Ap:: <i>gtrSUGD</i> plasmid	This study
$\Delta gtrS$ (DK2)	DK2 derivative with a gentamicin resistance cassette replaced the <i>gtrS</i> , by using the pEX18Ap:: <i>gtrSUGD</i> plasmid	This study
<i>E. coli</i> strains		
BL21	F ⁻ <i>ompT hsdS_B (r_B⁻ m_B⁻) gal dcm met</i> (DE3)	Lab stock
DH5a	<i>endA hsdR17 supE44 thi-1 recA1 gyrA relA1Δ(lacZYA-argF)U169 deoR (φ80dlacΔ(lacZ)M15)</i>	Lab stock
<i>E. coli</i> BTH101	Cya-BACTH expression strain; F ⁻ <i>cya-99</i>	Euromedex

	<i>araD139 galE15 galK16 rpsL1 (Str^r) hsdR2 mcrA1 mcrB1</i>	
S17 λ -pir	<i>recA thi pro hsdR⁻M⁺ RP4-2-Tc::Mu Km::Tn7 λpir (Tp^r Str^r)</i>	Lab stock
S17 λ -pir (pFLP2)	S17 λ -pir containing pFLP2	This study
SM10- λ <i>pir</i> (pBT20)	<i>E. coli</i> SM10- λ <i>pir</i> containing pBT20	(47)

^aAp^r, ampicillin resistance; Cb^r, carbenicillin resistance; Kan^r, kanamycin resistance; Tc^r, tetracycline resistance; Tp^r, trimethoprim resistance; Str^r, Streptomycin resistance; Gm^r, gentamycin resistance.

1 **Table S2. Primers used in this study.**

Primer	Sequence	Purpose
pro-bfmR-F	5'-TTTCTCGAGCAACCTGGGCACCGTGTT-3'	Construction the plasmid of mini- <i>bfmR-lacZ</i>
pro-bfmR-R	5'-TTTGGATCCAGGATGTGATCGACATGCTC-3'	Construction the plasmid of mini- <i>bfmR-lacZ</i>
AD2	5'-CANGCTWSGTNTSCAA-3'	For localization of the transposon
Gm447	5'-GTGCAAGCAGATTACGGTGACGAT-3'	For localization of the transposon
Gm464	5'-TGACGATCCCGCAGTGGCTCTC-3'	For localization of the transposon
Gm487	5'-ATACAAAGTTGGGCATACG-3'	For localization of the transposon
gtrS-comp-F	5'-CCCAAGCTTCAGTGGCTACCTGCTGG-3'	Construction of plasmids p- <i>gtrS</i> , pRK415- <i>gtrS</i> , and p-gtrS-HA
gtrS-comp-R	5'-TTTGGATCCGCCAGCCATCACTCCA-3'	Construction of plasmids p- <i>gtrS</i> , pRK415- <i>gtrS</i> , and p-gtrS-HA
gltR-comp-F	5'-CCCAAGCTTCTGAGTCGGCGTCGAGCA-3'	Construction of p- <i>gltR</i> plasmid
gltR-comp-R	5'-TTTGGTACCCGTTTCGCTCATGGCTGCA-3'	Construction of p- <i>gltR</i> plasmid
pa3190-comp-F	5'-GGGAAGCTTGCGCAGACTTGCTCCGAA-3'	Construction of plasmid p- <i>gltB</i>
pa3190-comp-R	5'-TTTGGTACCATCCGCGCCAGGGACTTA-3'	Construction of plasmid p- <i>gltB</i>
bfmS-comp-F	5'-TGGAAGCTTCGACTGGTCG AGGCCATCC-3'	Construction of plasmids pRK415- <i>bfmS</i>
bfmS-comp-R	5'-TTTGGATCCCTCTGTACGG GCGCCTCAGG-3'	Construction of plasmids pRK415- <i>bfmS</i>
D-gtrS-up-F	5'-CCGGAATTCGCGCTTACCTGCAGGACGTA-3'	Deletion of <i>gtrS</i>
D-gtrS-up-R	5'-CGCGGATCCTAGCTGACGCTGGCCGCAT-3'	Deletion of <i>gtrS</i>
D-gtrS-down-F	5'-CGCGGATCCTGGCGGCGAA GTCAGTTTGC-3'	Deletion of <i>gtrS</i>
D-gtrS-down-R	5'-CCCAAGCTTGAGCCAGTTCACCCGGTGT-3'	Deletion of <i>gtrS</i>
D-gltR-up-F	5'-GGTGAATTCATGGGGTGAACGGCGAGTT-3'	For deletion of <i>gltR-gtrS</i>
D-gltR-up-R	5'-TTTGGATCCCTCACGAGGCTCCTCCTTAT-3'	For deletion of <i>gltR-gtrS</i>
D-pa3190-up-F	5'-GGTGAATTCCTTCAACACCATGCATG-3'	Deletion of <i>gltB</i>
D-pa3190-up-R	5'-TTTGGTACCGCGACGGATCGCATTTCAT-3'	Deletion of <i>gltB</i>
D-pa3190-down-F	5'-GTTGGTACCCCAACTTCTT CAACGACC-3'	Deletion of <i>gltB</i>
D-pa3190-down-R	5'-TTTAAGCTTGACGCTGTCCCAGGCCTT-3'	Deletion of <i>gltB</i>

D-bfmR-up-F	5'-TTTGAATTCACCTGGGCAC CGTGTTCAT-3'	Deletion of <i>bfmR</i>
D-bfmR-up-R	5'-TTTGGATCCGTCACCGTGTGGCTTCGA-3'	Deletion of <i>bfmR</i>
D-bfmR-down-R	5'-TTGAAGCTTTTGTCCAGCACCTGGATTTCG-3'	Deletion of <i>bfmR</i>
D-bfmR-down-F	5'-TTTGGATCCGAACCGGAGT ACATCAAGAC-3'	Deletion of <i>bfmR</i>
pAK1900-mini-F	5'-TTTCTCGAGTATCACGAGGCCCTT-3'	For generating mini- <i>bfmS</i> , <i>-gltR-gtrS</i> , <i>-gltR</i> , and <i>-gtrS</i>
pAK1900-mini-R	5'-TGGTCTAGAACGGCCAGTGAATTG-3'	For generating mini- <i>bfmS</i> , <i>-gltR-gtrS</i> , <i>-gltR</i> , and <i>-gtrS</i>
bfmS-allelic-DK2-F	5'-TTTGAATTCCTGGAATGCC CGATTTCGTC-3'	Generating <i>bfmS</i> allelic exchange mutants
bfmS-allelic-DK2-R	5'-TTTAAGCTTCGACTGGATATCGCCGAACC-3'	Generating <i>bfmS</i> allelic exchange mutants
gtrS-KD-F	5'-TTTGGATCCCATTGGCAGAGCCGTCC-3'	Construction of pET28a- <i>GtrSc</i> plasmid
gtrS-KD-R	5'-TTTGAATTCTCACTCCAGCCCCAGG-3'	Construction of pET28a- <i>GtrSc</i> plasmid
gtrS-HA-R	5'- TTTGGTACCTCAAGCGTAGTCTGGGACGTCGTA T GGGTACTCCAGCCCCAGGCGTG-3'	Construction of p- <i>gtrS-HA</i> plasmid
bfmR-comp-F	5'-TTTAAGCTTCACGGGAGCCAGGCAATGGA-3'	Construction of p- <i>bfmR-flag</i> and pRK415- <i>bfmR-flag</i>
bfmR-flag-R	5'- TTTGGATCCTTACTTATCGTCGTCATCCTTGTA ATCTGGATGGGCCTCGACCAG-3'	Construction of p- <i>bfmR-flag</i> and pRK415- <i>bfmR-flag</i>
bfmS-KD-F	5'-TTTGGATCCCGCACCCGCCATCGGTC-3'	Construction of pGEX-6p-1-BfmSc
bfmS-KD-R	5'-CACACTCGAGTCAGGGGTCCAGCTCGATG-3'	Construction of pGEX-6p-1-BfmSc
bfmS-KD-2F	5'-TTTGGTACCCGCACCCGCCATCGGTC-3'	Construction of pET28a(+)-sumo-BfmSc
bfmS-KD-2R	5'-TGGAAGCTTTCAGGGGTCCAGCTCGA-3'	Construction of pET28a(+)-sumo-BfmSc
BfmR(D55A)-F	5'-GTGGACCTGATCGTCCTCGCCATCATGATGC CCGGCGAC-3'	Generation of <i>bfmR</i> ^{D55A}
BfmR(D55A)-R	5'-GTCGCCGGGCATCATGATGGCGAGGACGAT CAGGTCCAC-3'	Generation of <i>bfmR</i> ^{D55A}
GtrS (H280A)-F	5'-TGTTCAAGCGCCATCTCCGCC GACCTGCGCA-	Generation of <i>gtrS</i> ^{H280A}

GtrS (H280A)-R	3' 5'- TGCGCAGGTCGGCGGAGATGGCGCTGAACA-3'	Generation of <i>gtrS</i> ^{H280A}
D-pa3190-up-F	5'-GGTGAATTCCTTCAACACCATGCATG-3'	Deletion of <i>gltB</i>
D-pa3190-up-R	5'-TTTGGTACCGCGACGGATCGCATTCAT-3'	Deletion of <i>gltB</i>
D-pa3190-down-F	5'-GTTGGTACCCCAACTTCTT CAACGACC-3'	Deletion of <i>gltB</i>
D-pa3190-down-R	5'-TTTAAGCTTGACGCTGTCCCAGGCCTT-3'	Deletion of <i>gltB</i>
pro-pa4103-F	5'-TTTCTCGAGACAGGGACAAGCTGTGGAAC- 3'	Construction of mini- <i>pa4103-lux</i>
pro-pa4103-R	5'-TTTGGATCCGAGAGGTTGGGACGGTCAT-3'	Construction of mini- <i>pa4103-lux</i>
pro-pa3190-F	5'-TTTCTCGAGCACGTCGACGACGAC-3'	Construction of pMS402- <i>gltB-lux</i>
pro-pa3190-R	5'-TTTGGATCCAGGCGACGGATCGCA-3'	Construction of pMS402- <i>gltB-lux</i>
F	5'-AGTGGCAACTGGACACCAGC-3'	For analysis of <i>bfmRS</i> transcripts
R	5'-GAGCATGGCTACCGAGATCG-3'	For analysis of <i>bfmRS</i> transcripts
2R	5'-TGATCGGGCTCTGCAGGTCG-3'	For analysis of <i>bfmRS</i> transcripts
T242R-F	5'-TCCCACGACCTGCAGCGGCCGATCA-3'	Generation of <i>bfmS</i> ^{T242R}
T242R-R	5'-TGATCGGCCGCTGCAGGTCGTGGGA-3'	Generation of <i>bfmS</i> ^{T242R}
L184P-F	5'-CTGACCCGGCCGGTGAAGGCCGT-3'	Generation of <i>bfmS</i> ^{L184P}
L184P-R	5'-ACGGCCTTACCCGGCCGGGTCAG-3'	Generation of <i>bfmS</i> ^{L184P}
Q92E-F	5'-AGCCCGGCGAGCCGC TGGCGCT-3'	Generation of <i>bfmS</i> ^{Q92E}
Q92E-R	5'-AGCGCCAGCGGCTCGCCGGGCT-3'	Generation of <i>bfmS</i> ^{Q92E}
D295N-F	5'-AGTTGCCGGG TGAACCTCGA CGCCT-3'	Generation of <i>bfmS</i> ^{D295N}
D295N-R	5'-AGGCGTCGAGGTTACCCGGCAACT-3'	Generation of <i>bfmS</i> ^{D295N}
F31L-F	5'-CGGGCTGTCC CTCGCCTCGC AGTTC-3'	Generation of <i>bfmS</i> ^{F31L}
F31L-R	5'-GAACTGCGAGGCGAGGGACAGCCCG-3'	Generation of <i>bfmS</i> ^{F31L}
R393H-F	5'-AACTCGCGCAATCACGACACCGGTGGCA-3'	Generation of <i>bfmS</i> ^{R393H}
R393H-R	5'-TGCCACCGGTGTCTGATTGCGCGAGTT-3'	Generation of <i>bfmS</i> ^{R393H}
H238A-F	5'-TCGCGGCGATTTCCGCCGACCTGCA-3'	Generation of <i>bfmS</i> ^{H238A}

H238A-R	5'-TGCAGGTCGGCGGAAATCGCCGCGA-3'	Generation of <i>bfmS</i> ^{H238A}
BfmS(I178N)-F	5'-TGCGCACCGCCAACGGTCCGCTGAC-3'	Generation of <i>bfmS</i> ^{I178N}
BfmS(I178N)-R	5'-GTCAGCGGACCGTTGGCGGTGCGCA-3'	Generation of <i>bfmS</i> ^{I178N}
BfmS(L181Q)-F	5'-CATCGGTCCGCAGACCCGGCTGGTG-3'	Generation of <i>bfmS</i> ^{L181Q}
BfmS(L181Q)-R	5'-CACCAGCCGGGTCTGCGGACCGATG-3'	Generation of <i>bfmS</i> ^{L181Q}
BfmS(V287M)-F	5'- TGGTCCGCGAAGG CATGGCCTAT-3'	Generation of <i>bfmS</i> ^{V287M}
BfmS(V287M)-R	5'-ATAGGCCATGCCTTCGCGGACCA-3'	Generation of <i>bfmS</i> ^{V287M}
BfmS(Q241R)-F	5'-TCCCACGACCTGCGGACGCCGATCA-3'	Generation of <i>bfmS</i> ^{Q241R}
BfmS(Q241R)-R	5'-TGATCGGCGTCCGCAGGTCTGGGA-3'	Generation of <i>bfmS</i> ^{Q241R}
BfmS(A21G)-F	5'-GATCCTCTTCGGCGGGCTGGTGCTG-3'	Generation of <i>bfmS</i> ^{A21G}
BfmS(A21G)-R	5'-CAGCACCAGCCCGCCGAAGAGGATC-3'	Generation of <i>bfmS</i> ^{A21G}
BfmS(G179D)-F	5'-CACCGCCATCGACCCGCTGACCCGGCT-3'	Generation of <i>bfmS</i> ^{G179D}
BfmS(G179D)-R	5'-AGCCGGGTCAGCGGGTTCGATGGCGGTG-3'	Generation of <i>bfmS</i> ^{G179D}
BfmS(L164F)-F	5'-CTGCTGGTGCAGTTGTTCTGCTGCT-3'	Generation of <i>bfmS</i> ^{L164F}
BfmS(L164F)-R	5'-GTGCAGAGCAGCAGCAGGAACAAC-3'	Generation of <i>bfmS</i> ^{L164F}
BfmS(A42E)-F	5'-AGCGCTACCAGACCGAGAAGCACATGA-3'	Generation of <i>bfmS</i> ^{A42E}
BfmS(A42E)-R	5'-TCGAGCATCATGTGCTTCTCGGTCTGG-3'	Generation of <i>bfmS</i> ^{A42E}
BfmS(G347D)-F	5'-CGCTGAAGTTCGCCGACGCCGCGCG-3'	Generation of <i>bfmS</i> ^{G347D}
BfmS(G347D)-R	5'-CCAGGCGCGCGGCGTCGGCGAACTT-3'	Generation of <i>bfmS</i> ^{G347D}
BfmS(A4T)-F	5'-ATGAAGCTCACCGTGCCGCGCCCG-3'	Generation of <i>bfmS</i> ^{A4T}
BfmS(A4T)-R	5'-GCGCGGGCGCGGCACGGTGAGCTT-3'	Generation of <i>bfmS</i> ^{A4T}
BfmS(L168-L)-F	5'-GTGCAGTTGCTCCTGCTGCTGCTGC-3'	Generation of <i>bfmS</i> ^{L168-L}
BfmS(L168-L)-R	5'-GCAGCAGCAGCAGGAGCAACTGCAC-3'	Generation of <i>bfmS</i> ^{L168-L}
BfmS(L168-D)-F	5'-GTGCAGTTGCTCCTGCTGCTCT-3'	Generation of <i>bfmS</i> ^{L168-d}
BfmS(L168-D)-R	5'-CCGGTGCAGAGCAGCAGGAGCA-3'	Generation of <i>bfmS</i> ^{L168-d}

BfmS(V380A)-F	5'-CTCGACGAGGCGCTCAAGCCCTTC-3'	Generation of <i>bfmS</i> ^{V380A}
BfmS(V380A)-R	5'-GGCTTGAGCGCCTCGTCGAGTTCC-3'	Generation of <i>bfmS</i> ^{V380A}
BfmS(A281T)-F	5'-AAGGCGTGGCCTATAACCCGCAGCATG-3'	Generation of p- <i>bfmS</i> ^{T120K L168F A281T}
BfmS(A281T)-R	5'-CCGTGCATGCTGCGGGTATAGGCCAC-3'	Generation of p- <i>bfmS</i> ^{T120K L168F A281T}
T25-grS-F	5'-TTTGGATCCATGAGCGAACGGCGGCGCT-3'	For bacterial two-hybrid assays
T25-grS-R	5'-TTTGGTACCTCACTCCAGCCCCAGGCGT-3'	For bacterial two-hybrid assays
T18C-bfmR-F	5'-TTTGGATCCATGGAGCATG TCGATCACAT-3'	For bacterial two-hybrid assays
T18C-bfmR-R	5'-GGTGAATTCTCATGGATGGGCCTCGACCA-3'	For bacterial two-hybrid assays
bfmS-comp-2F	5'-TTTGGTACCCGACTGGTTCG AGGCCCAT-3'	For bacterial two-hybrid assays
bfmS-comp-2R	5'-GGTGAATTCTCAGGGGTCCAGCTCGATGC-3'	For bacterial two-hybrid assays

2
3
4

5 **Table S3. *bfmS* variants in *P. aeruginosa* CF isolates**

Isolate or Strain	Accession ^a	Amino acid change ^b	Geographic location	Source or Reference ^c
Prevalent or epidemic clones				
<i>DK2 lineage (50 isolates)</i>				
39 DK2 isolates	NA	L181P	Denmark: Copenhagen	(9, 12, 27)
11 DK2 isolates	WP_014833884	L181P E376Q	Denmark: Copenhagen	(9, 12, 27)

DK1 lineage (4 isolates)

DK1-NH57388A	WP_003159306	T120K L164F	Denmark: Copenhagen	Direct submission
DK1-P30M0-2006	NA	V278M	Denmark: Copenhagen	(13)
DK1-P30M0-2011	NA	V278M	Denmark: Copenhagen	(13)
DK1-P30M0-2012a	NA	V278M	Denmark: Copenhagen	(13)

M3L7 sub-lineage (26 isolates)

AUS934	WP_034054432	L181Q	Australia	(16)
AUS950	WP_034054432	L181Q	Australia	(16)
AUS952	WP_034054432	L181Q	Australia	(16)
AUS941	WP_034054432	L181Q	Australia	(16)
AUS935	WP_034054432	L181Q	Australia	(16)
AUS936	WP_034054432	L181Q	Australia	(16)
AUS958	WP_034054432	L181Q	Australia	(16)
AUS944	WP_034054432	L181Q	Australia	(16)
AUS945	WP_034054432	L181Q	Australia	(16)
AUS953	WP_034054432	L181Q	Australia	(16)
AUS954	WP_034054432	L181Q	Australia	(16)
AUS22	WP_034054432	L181Q	Australia	(16)
AUS943	WP_034054432	L181Q	Australia	(16)
AUS942	WP_034054432	L181Q	Australia	(16)
AUS940	WP_034054432	L181Q	Australia	(16)
AUS955	WP_034054432	L181Q	Australia	(16)
AUS948	WP_034054432	L181Q	Australia	(16)
AUS937	WP_034054432	L181Q	Australia	(16)
AUS951	WP_034054432	L181Q	Australia	(16)
AUS938	WP_034054432	L181Q	Australia	(16)
AUS946	WP_034054432	L181Q	Australia	(16)
AUS947	WP_034054432	L181Q	Australia	(16)

AUS949	WP_034054432	L181Q	Australia	(16)
AUS956	WP_034054432	L181Q	Australia	(16)
AUS957	WP_034054432	L181Q	Australia	(16)
AUS939	WP_034054432	L181Q	Australia	(16)

Liverpool epidemic strain (LES) and LES-like strain (48 isolates)

LES400	WP_012613595	A21P T120K L164F	U.K.	(62)
LES431	WP_012613595	A21P T120K L164F	U.K.	(62)
LESB58	WP_012613595	A21P T120K L164F	U.K.	(62)
LESB65	WP_012613595	A21P T120K L164F	U.K.	(62)
LESlike1	WP_012613595	A21P T120K L164F	Canada	(62)
LESlike4	WP_012613595	A21P T120K L164F	Canada	(62)
LESlike5	WP_012613595	A21P T120K L164F	Canada	(62)
LESlike7	WP_012613595	A21P T120K L164F	Canada	(62)
31 CF03 isolates	WP_012613595	A21P T120K L164F	Canada	(62)
			U.K.	(63)
9 CF03 isolates	WP_040184288	A21P T120K L164F T326P	U.K.	(63)

Australia epidemic strain-1 (AUS-1) (1 isolate)

AES-1R	WP_019681168	L164F	Australia	(64)
--------	--------------	-------	-----------	------

Manchester epidemic strain (MES) (1 isolate)

C3719	WP_004345952	T120K L163V L164F	U.K.	(65)
-------	--------------	-------------------	------	------

ST406 clone in the Netherlands (1 isolate)

S1 isolate	NA	I178N	Netherlands	(66)
------------	----	-------	-------------	------

33 out of 63 CF isolates from a single CF care center in USA in a study by Spilker et al.

AU15431	WP_061190965	A42E G347D	USA	(35)
AU7032	WP_061190965	A42E G347D	USA	(35)
AU10409	WP_061199510	A4T Q241R R393H	USA	(35)
AU10272	WP_034008880	A4T R393H	USA	(35)
AU10410	WP_034008880	A4T R393H	USA	(35)
AU10836	WP_034008880	A4T R393H	USA	(35)
AU16821	WP_034008880	A4T R393H	USA	(35)
AU7198	WP_034008880	A4T R393H	USA	(35)
AU10502	WP_061195279	T120K L164F Y280H V323A	USA	(35)
AU11990	WP_061195279	T120K L164F Y280H V323A	USA	(35)
AU11991	WP_061195279	T120K L164F Y280H V323A	USA	(35)
AU12424	WP_061195279	T120K L164F Y280H V323A	USA	(35)
AU18274	WP_061195279	T120K L164F Y280H V323A	USA	(35)
AU25116	WP_061195279	T120K L164F Y280H V323A	USA	(35)
AU1215	WP_061180971	L168-d (deletion of Leu-168)	USA	(35)
AU22632	WP_061180971	L168-d	USA	(35)
AU24787	WP_061180971	L168-d	USA	(35)
AU7511	WP_061180971	L168-d	USA	(35)
AU13626	WP_061180971	L168-d	USA	(35)
AU10658	WP_061181593	L168-d V380A	USA	(35)
AU17091	WP_061181593	L168-d V380A	USA	(35)
AU21076	WP_061181593	L168-d V380A	USA	(35)
AU25210	WP_061181593	L168-d V380A	USA	(35)
AU13210	WP_034041871	L168-L (Leu insertion after Leu-	USA	(35)
AU19803	WP_034041871	168)	USA	(35)
AU19804	WP_034041871	L168-L	USA	(35)

AU9899	WP_034041871	L168-L L168-L	USA	(35)
AU10713	WP_060961570	T120K L164F A281T	USA	(35)
AU17550	WP_060961570	T120K L164F A281T	USA	(35)
AU18132	WP_060961570	T120K L164F A281T	USA	(35)
AU19319	WP_060961570	T120K L164F A281T	USA	(35)
AU24526	WP_060961570	T120K L164F A281T	USA	(35)
AU9017	WP_061200633	T120K L164F G179D Y280H	USA	(35)

14 out of 24 isolates from Ontario, Canada in a study by Dettman et al.

JD323	WP_033886257 ^d	A122V L164F	Canada: Hamilton	(67)
JD304	WP_031803682 ^d	A21P T120K L164F	Canada: Ottawa	(67)
JD310	WP_012613595	A21P T120K L164F	Canada: Ottawa	(67)
JD315	WP_012613595	A21P T120K L164F	Canada: Hamilton	(67)
JD322	WP_012613595	A21P T120K L164F	Canada: Toronto	(67)
JD324	WP_012613595	A21P T120K L164F	Canada: Toronto	(67)
JD326	WP_012613595	A21P T120K L164F	Canada: Toronto	(67)
JD329	WP_012613595	A21P T120K L164F	Canada: Hamilton	(67)
JD335	WP_012613595	A21P T120K L164F	Canada: London	(67)
			Canada: Toronto	(67)
JD312	WP_023123707	F31L	Canada: Kitchener	(67)
JD316	WP_033876756	F31L D295N	Canada: Sudbury	(67)
JD328	WP_033876756	F31L D295N	Canada: London	(67)
JD333	WP_033881853 ^d	F31L D295N	Canada: Toronto	(67)
JD317	WP_019681168	L164F	Canada: Toronto	(67)

20 out of 35 CF isolates in a study by Kos VN et al.

AZPAE12152	WP_034046584	A281T	USA: New York	(68)
AZPAE12138	WP_034008880	A4T R393H	USA: New York	(68)
AZPAE12409	WP_004365749	D295N	USA: Cleveland	(68)
AZPAE12422	WP_023123707	F31L	USA: Cleveland	(68)
AZPAE12149	WP_033876756	F31L D295N	USA: New York	(68)
<i>AZPAE12413</i>	WP_034043645	L163-d H272Y D340N	USA: Cleveland	(68)
AZPAE12414	WP_034043645	L163-d H272Y D340N	USA: Cleveland	(68)
<i>AZPAE12415</i>	WP_034043645	L163-d H272Y D340N	USA: Cleveland	(68)
<i>AZPAE12417</i>	WP_034041871	L168-L	USA: Cleveland	(68)
AZPAE12156	WP_034054432	L181Q	USA: New York	(68)
AZPAE12416	WP_033970808	P383S	USA: Cleveland	(68)
AZPAE12418	WP_033970808	P383S	USA: Cleveland	(68)
AZPAE12423	WP_033970808	P383S	USA: Cleveland	(68)
<i>AZPAE12154</i>	WP_034056531	P6S G112D L164F	USA: New York	(68)
AZPAE12145	WP_034052127	Q40E V149A	USA: New York	(68)
AZPAE12421	WP_043108044	R78Q T120K L164F	USA: Cleveland	(68)
AZPAE12151	WP_034031409	T120K K262R S302R S310N R355S	USA: New York	(68)
AZPAE12142	WP_033987210	T242R	USA: New York	(68)
AZPAE12153	WP_034032702	V149A V161A D433A	USA: New York	(68)
AZPAE12140	WP_034065491	Y27H D340N	USA: New York	(68)

24 out of 40 isolates from Trentino Regional Support Cystic Fibrosis Centre (Italy) in a study by Bianconi et al.

TNCF_3	WP_070329877	L184P	Italy	(69)
TNCF_101	WP_070329877	L184P	Italy	(69)
TNCF_105	WP_070329877	L184P	Italy	(69)

TNCF_106	WP_070329877	L184P	Italy	(69)
TNCF_109	WP_070329877	L184P	Italy	(69)
TNCF_130	WP_070329877	L184P	Italy	(69)
TNCF_133	WP_070329877	L184P	Italy	(69)
TNCF_14	WP_070329877	L184P	Italy	(69)
TNCF_151	WP_070329877	L184P	Italy	(69)
TNCF_154	WP_070329877	L184P	Italy	(69)
TNCF_155	WP_070329877	L184P	Italy	(69)
TNCF_155_1	WP_070329877	L184P	Italy	(69)
TNCF_165	WP_070329877	L184P	Italy	(69)
TNCF_167	WP_070329877	L184P	Italy	(69)
TNCF_167_1	WP_070329877	L184P	Italy	(69)
TNCF_174	WP_070329877	L184P	Italy	(69)
TNCF_175	WP_070329877	L184P	Italy	(69)
TNCF_6	WP_070329877	L184P	Italy	(69)
TNCF_68	WP_070329877	L184P	Italy	(69)
TNCF_69	WP_070329877	L184P	Italy	(69)
			Italy	(69)
			Italy	(69)
TNCF_176	WP_070332227	L184P G399D	Italy	(69)
TNCF_12	WP_070341526	Q92E L184P	Italy	(69)
TNCF_10M	WP_070336931	E77D P150L	Italy	(69)
TNCF_76	WP_070335766	A21G L184P	Italy	(69)

141 out of 474 CF isolates from Denmark in a study by Marvig et al.

36 isolates (76, 77, 78, 79, 80, 81, 82, 83, 84, 85, 86, 87, 88, 89, 90, 91, 123,	WP_019681168	L164F	Denmark	(14)
--	--------------	-------	---------	------

124, 125, 126, 127,
128, 129, 130, 131,
132, 133, 324, 328,
124.1, 126.1, 127.1,
81.1, 82.1, LRJ14,
LRJ14)

28 isolates (A, B, C,
D, E, F, G, H, I, J,
K, L, M, N, O, P, Q,
R, S, T, U, V, X, Y,
Z, NA10, NA31,
NA11)

WP_033957058

A122V L164F

Denmark

(14)

21 isolates (95, 96,
97, 98, 99, 100, 101,
102, 103, 104, 105,
106, 107, 108, 109,
193, 194, 195,
LRJ18, LRJ19,
LRJ20)

WP_003159306

T120K L164F

Denmark

(14)

15 isolates (196,
197, 198, 199, 206,
207, 208, 209, 210,
211, 212, 213, 215,
293, 340)

WP_034001102

K262R S310N R355S

Denmark

(14)

11 isolates (418,
422, 423.1, 426, 428,
430, 431, 434, 437,
437.1, 439)

WP_060961570

T120K L164F A281T

Denmark

(14)

<i>10 isolates (134, 135, 148, 423, 427, 436, 138.1, 439.1, LRJ16, LRJ17)</i>	WP_073649900	Q113R K186E V294L A422P	Denmark	(14)
<i>9 isolates (419, 420, 421, 425, 429, 432, 433, 435, 438)</i>	WP_073670735	T120K L164F L233F	Denmark	(14)
<i>8 isolates (201, 203, 204, 205, 214, 223, 201.1, 203.1)</i>	WP_004365749	D295N	Denmark	(14)
<i>1 isolate (245)</i>	WP_073653557	Deletion of H210, A211, A212, and A213	Denmark	(14)
<i>1 isolate (349)</i>	WP_034054976	A422T	Denmark	(14)
<i>1 isolate (427.1)</i>	WP_074227112	T120K L164F L233F G425E	Denmark	(14)

Other strains

SCH_ABX18	WP_034046584	A281T	USA: Seattle	PRJNA369567
CIG1	WP_003119101	A4T	NA	(70)
SCH_ABX01	WP_003119101	A4T	USA: Seattle	PRJNA369567
SCH_ABX02	WP_003119101	A4T	USA: Seattle	PRJNA369567
CF5	WP_004365749	D295N	USA	Direct submission
C1913C	WP_023518026	D340N	Canada: Vancouver, BC	Direct submission
WH-SGI-V-07282	WP_034001102	K262R S310N R355S	Portugal	(71)
PASS4	WP_019681168	L164F	Australia: Sydney	(72)
C7447m	WP_019681168	L164F	Canada	(73)
CF614	WP_023081578	P6S L164F	USA	Direct submission
RP73	WP_016562269	R393H	Germany: Hannover	(74)

0C4A	WP_016562269	R393H	Germany: Hannover	(75)
<i>CF_PA39</i>	WP_024915544	T65N T290A L412I	Belgium	(76)

6 ^a NCBI Reference Sequence.

7 ^b Amino acid of BfmS variants different from that in the laboratory strains PAO1.

8 ^c NCBI BioProject accession number for the Source of some BfmS variants.

9 ^d Partial BfmS sequence.

10 NA, not available; L168-L, Leu insertion after Leu-168; L163-d, deletion of L163; L168-d, deletion of L168.

11 Direct submission, direct submission of sequence data to GenBank.

12 The BfmS variants were identified by using BLASTP analysis against the NCBI protein database and literature searchin

Data file 1. Microarray data analysis of DK2

Data file 2. RNA-seq analysis